

University of Southern Queensland  
Faculty of Health, Engineering and Sciences

# FEA Analysis Of Tractor Axle Modification

---

A dissertation submitted by

**Richard Sambamo**

In fulfilment of the requirements of

**ENG4112 Research Project**

towards the degree of

**Bachelor of Engineering (Mechanical)**

Submitted: October 2014

## ABSTRACT

Agricultural tractor is one of the major and important agriculture implements and the modern heavy agricultural tractors have sophisticated front axles and suspensions. They are also now capable of travelling at speeds of more than 40 km/h. These agricultural tractors are playing an even more important role in the modern Controlled Traffic Farming (CTF) which is being embraced by many Australian farmers. Implementation of CTF however needs the tractors' front axle to be modified to suit its different and unique farming configuration. The large United States based tractor manufacturers have not been able to satisfy this emerging unique market most likely because of its size and local Australian engineering firms have come up with different front axle modifications custom made to fit particular tractors currently on the market.

The purpose of this research project was to determine the safe loading levels for a modified tractor front axle. The modified tractor axle was for John Deere 8530. Creo 2.0 Parametric and Simulate a modern Finite Element Analysis package was used to complete some robust analysis of the existing product under a wider range of load conditions than are feasible through normal field testing. Manufacturer's CAD data was imported into Creo 2.0 Parametric which was then used to create the 3D model of components and axle. Using the loads calculated from the working weight of the JD8530 and the dynamic loads outlined in Vehicle Standards Bulletin 14 (VSB14), the model was committed to Creo 2.0 Simulate for analysis.

Results of the analysis were processed using the same platform and they indicated a potential problem with component 12 which consistently showed stresses above 300 MPa. These results though were based on worst cases of loadings which are unlikely to occur on the field. It was therefore concluded that the modified axle is safe from stress induced failure if the loadings levels are kept within the capacity of JD8530 tractor.

*Keywords: Tractor axle, Finite Element Analysis, Agriculture-controlled Traffic Farming.*

**University of Southern Queensland**  
**Faculty of Health, Engineering and Sciences**  
**ENG4111 AND ENG4112 Research Project**

**Limitations of Use**

The Council of the University of Southern Queensland, its Faculty of Health, Engineering & Sciences, and the staff of the University of Southern Queensland, do not accept any responsibility for the truth, accuracy or completeness of material contained within or associated with this dissertation.

Persons using all or any part of this material do so at their own risk, and not at the risk of the Council of the University of Southern Queensland, its Faculty of Health, Engineering & Sciences or the staff of the University of Southern Queensland.

This dissertation reports an educational exercise and has no purpose or validity beyond this exercise. The sole purpose of the course pair entitled “Research Project” is to contribute to the overall education within the student’s chosen degree program. This document, the associated hardware, software, drawings, and other material set out in the associated appendices should not be used for any other purpose: if they are so used, it is entirely at the risk of the user.

University of Southern Queensland

Faculty of Health, Engineering and Sciences

ENG 4111 AND ENG4112 Research Project

## **Certification of Dissertation**

I certify that the ideas, designs and experimental work, results, analyses and conclusions set out in this dissertation are entirely my own effort, except where otherwise indicated and acknowledged.

I further certify that the work is original and has not been previously submitted for assessment in any other course or institution, except where specifically stated.

Richard Sambamo

Student Number: 0050074894

## Acknowledgements

I would like to thank the project supervisor Chris Snook for his help and guidance on this research project. His support and facilitation of site visit to the farm is greatly appreciated.

I would also like to thank John Foley for taking his time to drive me down to Denny's Engineering and the farm in Allora. Denny's Engineering are contracted to manufacture the axles. The visit gave me an appreciation of the scope and benefits of the project. He gave me a lot of invaluable information including background of his innovations and this project.

Finally I would like to thank my family for all the understanding and support rendered during the course of this research project.

# Table of Contents

	Page
Abstract	i
Limitations of Use Disclaimer	ii
Certification of Dissertation	iii
Acknowledgements	iv
Table of contents	v
List of Figures	vi
List of Tables	vii
I.0 Introduction	1
2.0 Background	3
2.1 Interpreting Client Brief	6
2.2 Project Scope	6
3.0 Literature Review	8
3.1 Finite Element Analysis	8
3.1.1 Why use Finite Element Analysis	9
3.1.2 Types of FEA software	10
3.1.3 Why use Finite Element Analysis	11
3.2 FEA Validation and Verification	12
3.3 Tractor front axle designs and modifications	13
3.4 Types of modified tractor axles	14

4.0	Tractor Specifications	17
4.1	General dimensions and weight.	18
4.2	Original front axle configuration	19
4.3	Modified Axle overview and configuration	19
4.3.1	Difference between MK I and MK II Axles designs	20
4.3.2	Material Properties	21
4.3.2.1	Material failure modes	22
4.3.2.2	Factor of Safety Calculations	23
4.4	Related Standards	24
4.4.1	Drop Test	25
4.4.2	VSB 14 Tests	26
5.0	Review of the e-drawings of the modified axle	28
5.1	Make 2D drawings of the axle components	28
5.2	Issues with drawings and software.	29
6.0	Parametric model of the modified axle	30
7.0	FEA Analysis-Structural and Dynamic	32
7.1	Pre-processing	32
7.1.1	Geometry	32
7.1.2	Element/Model type	32
7.1.3	Material properties of the model	33
7.1.4	Element connectivity/Mesh the model	34

7.1.5	Boundary conditions	34
7.1.6	Overview of Tests and Loading conditions	35
7.2	Processing	39
7.3	Post Processing/Results	40
8.0	Discussions and Results	42
8.1	Loading case 1	42
8.2	Loading case 2	45
8.3	Loading case 3	48
8.4	Loading case 4	51
8.5	Worst case loading-case 5	53
8.6	Convergence of results	57
9.0	Conclusions and suggestions for future work	58
9.1	Conclusions	59
9.2	Recommendations	60
9.3	Future Work	61
10.0	References	63
APPENDIX A: Project Specification		67
APPENDIX B: Project Timelines		68
APPENDIX C: 2D drawings, part and assembly models		69
APPENDIX D: John Deere Tractor Dimensions and Specifications		71

APPENDIX E: Loadings and Constraints	72
APPENDIX F: Risk Assessment	73
APPENDIX G: Factor of Safety Calculations	76
APPENDIX H: Loading Scenarios	78
APPENDIX I: AISI 1020 Steel Mechanical Properties	80
APPENDIX J: Analysis Summary	81
APPENDIX K: Bill of Materials	88
Appendix L: Finite Element Analysis Software Comparison.	90

## LIST OF FIGURES

	Page
Figure 2.1: Controlled traffic farming in practice.	3
Figure 2.2: John Deere 8530 axle extension.	6
Figure 3.1: Mesh refinements.	10
Figure 3.2: John Deere round bail cotton picker extension.	15
Figure 3.3: Axle extensions.	16
Figure 4.1: JD8530 tractor	17
Figure 4.2: Independent-Link Suspension	17
Figure 4.3: Tractor dimension and weight	18
Figure 4.4: Original John Deere 8350 Tractor axle.	19
Figure 4.5: John Deere 8530 with front modified axle.	19
Figure 4.6: Modified John Deere 8350 Tractor axle at close range.	20
Figure 4.7: Generation I (MK I) and MK II Axles	21
Figure 4.8: Stress-Strain graph	23

Figure 4.9: Drop Test Graphical Representation	20
Figure 5.1: Part of Original drawings in e-drawing model viewer.	28
Figure 6.1: Solid Model of Modified Axle sub assembly	30
Figure 6.2: Exploded view of Modified Axle components	31
Figure 6.3: Solid Model of Modified Axle	31
Figure 7.1: Material definition in Creo 2.0	33
Figure 7.2: Finite Element Model of modified Axle	34
Figure 7.3: FE Model of Modified tractor Axle showing constraints and Loadings	35
Figure 7.4: Weight distribution on front axle	36
Figure 7.5: Loading Conditions and boundary constraints	37
Figure 7.6: Loading case 1: Equal reaction loads	38
Figure 7.7: Coordinate System	39
Figure 7.8: Components Contact issues	40
Figure 7.9: Deformed modified axle model	41
Figure 8.1: Loading case 1 Von Mises Stress plot.	42
Figure 8.2: Identified area of high stress	43
Figure 8.3: Displacement plot for loading case 1.	44
Figure 8.4: Displacement graph for loading case 1.	44
Figure 8.5: Loading case 2 Von Mises Stress plot.	46
Figure 8.6: Identified area of high stress	46
Figure 8.7: Displacement plot for loading case 2.	47
Figure 8.8: Displacement graph for loading case 1.	48
Figure 8.9: Loading case 3 Von Mises Stress plot	49

Figure 8.10: Identified area of high stress	49
Figure 8.11: Displacement plot for loading case.	50
Figure 8.12: Displacement plot for loading case 3.	50
Figure 8.13: Loading case 4 Von Mises Stress plot.	51
Figure 8.14: Identified area of high stress	52
Figure 8.15: Displacement plot for loading case 4.	53
Figure 8.16: Displacement graph for loading case 4.	53
Figure 8.17: Loading case 5 Von Mises Stress plot.	54
Figure 8.18: Identified area of high stress	55
Figure 8.19: Displacement plot for loading case 5.	56
Figure 8.20: Displacement graph for loading case 5.	56
Figure 8.21: Convergence of FEA result.	57
Figure B1: Project Timelines.	68
Figure C1: Some examples of modified Axle's components.	70
Figure C2: Wireframe model of the modified Axle.	70
Figure D.1: John Deere 8530 Tractor information	71
Figure E1: Loadings and constraints on model.	72
Figure H1: Loading Case 1- Normal Reaction loads	78
Figure H2: Loading Case 2 - Bump loads: 4g vertical	78
Figure H3: Loading Case 3 – Overturning loads: 4g vertical with 2.5 g side load	79
Figure H4: Loading Case 4 - Skid loads: 2g vertical and 1.2g longitudinal	79
Figure L1: Model exploded view	88

## LIST OF TABLES

	Page
Table 2.1 Savings realised by adoption of Controlled Traffic Farming	5
Table 3.1: Comparison of FEA software results	12
Table 4.1: SAE 1020 steel Mechanical Properties of Steel	22
Table 4.2: Factor of Safety Contributions	24
Table 7.1: SAE1020 steel Mechanical Properties of Steel	33
Table 7.2: Tractor axle weight distribution	35
Table 7.3: Loading Scenarios.	38
Table 8.1: Loading case 1.	42
Table 8.2: Computer Memory and Disk Usage	45
Table 8.3: Loading case 2.	45
Table 8.4: Loading case 3.	48
Table 8.5: Loading case 4.	51
Table 8.6: Loading case 5.	54
Table 9.1: Summary of Von Mises stress, displacements and factor of safety	58
Table F1: Risk Matrix	73
Table F2: Project Risk Assessment	75
Table L1: Bill of Materials	89

## NOMENCLATURE

Symbol	Unit	Description
WD		Wheel Drive
FW		Front Wheel Drive
MFWD		Mechanical Front Wheel Drive
g	m/s <sup>2</sup>	Acceleration due to gravity



## I.0 Introduction

An off road tractor is one of the major and important agriculture implements. It is used in most of the agricultural sectors. It is versatile in its uses because of the power built into it and the wide variety of attachments and implements the tractor is able to tow or push. Tractors are playing a more important role in the modern Controlled Traffic Farming (CTF) which is being embraced by some Australian farmers. By the end of 2011, 21 percent of the farmers in Australia had embraced the Controlled Traffic Farming which accounted for six percentage points increase in adoption up from 15 percent in 2008. Adoption of CTF was first done in the early and mid-nineties. These adoption figures were highlighted in the study done by the Grains Research and Development Corporation and released in July 2013.

The Australian Controlled Traffic Association which is responsible for helping and sharing controlled traffic farming techniques at their 2009 annual conference held in Canberra suggested that CTF fifty percent adoption across the farming sector is achievable within ten years with targeted funding. The initial high costs involved in setting up are slowing the take up of CTF and tractor axle modification is certainly one of the costs. The Fact sheet published in July 2013 by the Grains Research and Development Corporation cited that the CTF can improve profitability and sustainability. It also claimed that CTF can improve grain quality and increase the yields by between two to sixteen percent. The uptake of Controlled Traffic Farming can be increased by building confidence in farmers. Farmers have to be convinced that modifications to their expensive farm implements are of high standard and can withstand the structural and dynamic forces involved when farming due to varied field terrain. Modifications to the implements should also be cost competitive. The cost of conversion can be lowered by moving away from the traditional way of design, build prototype and field test. Modern computer technologies are a more cost effective way of designing, perform component behavioural and structural analysis and validation.

For the tractors to be adaptable to the CTF, the normally short span front axle has to be modified to the required suitable span. And to ensure the sustainable availability and reliability of the tractor in order to achieve the projected yields, any modification to the

farm implements including tractors should be done to high standard and in accordance with relevant standards. This ensures the modifications do not suffer premature failure. This research project seeks to analyse the structural and dynamic implications on a modified front axle for a JD 8530 tractors using Finite Element Analysis. Creo 2.0 Simulate will be mainly used for this analysis. This structural and dynamic analysis will also be done in other available software such ANSYS and Solidworks to compare and validate the results obtained in Creo 2.0 Simulate with time permitting and if such a comparison is necessary.

To simulate the changing terrain of the field, the model of the axle will be subjected to different loading cases and constraints. The Certification load cases as defined for the project will include drop test, Torture Test, The Impact Test, Pit test, Worst load testing and one side impact test. These tests are discussed in more detail under section 4.4 Relevant Standards and Certification Tests.

The above mentioned test cases will be used as loading and boundary constraints conditions for the finite element analysis of the modified tractor front axle. These testing cases will be used to fulfil the main objective of the project which is to determine maximum safe loading capacities of the axle. Recommendations including any further modifications to the axle will be made depending on the outcome of the comprehensive analyses involving the different loading and constraining conditions. Outcome of the analyses will also determine whether there is need to create a parametric model of the axle. A parametric model has critical controlling parameters which can be altered. Alterations to these controlling parameters ultimately change any dependent parameters. A parametric model will be crucial if the initial analyses indicate high stress levels in some components. It is easier and much faster to alter the components dimension in a parametric model than in a standard 3D model where individual components geometry has to be edited.

## 2.0 Project Background



Figure 2.1: Controlled traffic farming in practice.

Controlled Traffic Farming (CTF) is an agricultural system that seeks to minimize the damaging effects of compaction by concentrating wheel traffic to a small area of the field. This is achieved by bringing the front wheels in line with the rear wheels there reducing the overall width of the field area that is being affected by the wheels. The impacted area reduction can be range from 30 to 50 percent depending on the relative sizes of the wheels. The photo in Figure 2.1 shows a narrow distinctive road that has been created due to practice of controlled traffic farming. This ensures that the farm implements use the same tracks all the time. Precision on use of these defined roads have now been improved by incorporation of Global Positioning Systems into the farming system. Farm implements including the tractors are modified to suit different span variations of CTF. Variations in span are 3m, 6m, 9m and 12 metres.

C & C Machining & Engineering, a local engineering company in Toowoomba, Queensland have been involved with widening a great variety of tractors to enable farmers to practice the very effective and increasingly popular controlled traffic farming methods. They claim that they have been modifying the tractors for past 15 years. Controlled farming has certainly been in practice for considerably long time, two decades to be precise and major tractor suppliers such as John Deere and Massey

Ferguson have not embraced the growing need of this agricultural changing and growing market. Controlled farming seeks to separate the field into farm cropping sections and permanent roads which can be used by all agricultural implements such as combine harvesters and tractors. Extending the front axle brings the front wheels in line with the rear wheels and ensures that they are always on the same track thereby creating some permanent roads on the field. The figure 2.1 above shows the tractor with extended front axle performing controlled traffic farming.

Precision Agriculture (2011) noted that the common spacing or the span of the wheels is normally 3metres and there are other spacing variations such as 9m and 12metres. This effectively means that a 9 and 12 metre span machine can utilise the existing 3 metre roads if the intermediate spacing matches. They also claimed that CTF farming improves the agricultural output. Some studies have been done on the impact of converting to controlled traffic farming on the field yields. Studies carried out by various researchers including Botta, et al (2007), Braunack (2008) and Jensen and Neale (2001) cited in Neale, T (2010) showed that yields are reduced by compaction due to harvest traffic in uncontrolled traffic farming. The yield reductions were considered to range from 15 percent to 30 percent. This translated to losses to the farmers of between \$150 to \$300 per hectare. The cost of adopting or converting to controlled traffic farming can be recouped within a few years if the losses due to compaction are eradicated by reducing the area in the field exposed to traffic. This ultimately improves the yield and the profit margins.

Improvements in paddock of field efficiencies and reduced input costs are realised due to controlled traffic farming. Other advantages of CTF include reduction in fuel usage claimed to be in the 50% margins, enables greater accuracy of placing inputs, improves water infiltration and storage, improves timeliness of operations, and reduces operator fatigue. A study by Jensen et al (2012) in Denmark on the socio-impacts of controlled farming in Denmark concluded that the Danish Gross Domestic Product (GDP) increased by 34 million euros due to the implementation of Precision farming (PF) and CTF on larger farms in Denmark. The results also clearly showed that adoption of PF and CTF farming systems will benefit the environment. They were able to verify reduction of environmentally harmful agricultural inputs such as reduced pesticides and fuel. A case study by Bowman, K (2008) on a group of farms owned by Clifton Allora Top Crop concluded that there are indeed cost and environmental benefits. The table shows how the group benefitted by the adoption of controlled traffic farming.

Details	Zero Till	CTF (15% saving)	Savings Per Ha	Savings CATC Group
Seed (\$/ha)	34	30	4	\$16,528
Fertiliser (\$/ha) *	124	108	16	\$66,112
Chemical (\$/ha) **	89	77	12	\$49,584
<b>Total</b>	<b>247</b>	<b>215</b>	<b>32</b>	<b>\$132,224</b>

The CATC group \$ savings relate to 4,132 ha of land being converted to CTF.

Fertiliser based on applying 120 kg/ha of urea @ \$900/ton.

\*\* Chemical based on applying 5 l/ha roundup @ \$12.5/l & \$15/ha for an in-crop spray.

Table 2.1: Savings realised by adoption of CTF Source: (Bowman, K, 2008)

Although uptake of Controlled Farming is on the rise, it is however being slowed down by the fact that modified axles have an unknown risk which the farmers are wary of. Farm implements including the tractor are quite expensive to buy and it is a huge investment for farmers. Any modifications to massive investments such as the tractor have to be therefore done to a high standard that allays any fears the farmers might have. And according to the precision agriculture website, there are obviously some engineering risks with modifying tractors and machinery to wider wheel spacing. The modifications are not normally covered by the original manufacturer's warranty. Any resultant damage to modified parts including rotating parts such as bearings and drive shaft will have to be repaired at the farmer's expense. It is for this reason that any modification to the axle has to be done to a high standard and at a reasonable cost which can convince the farmers into taking up the CTF. The modified axle's susceptibility to breakdowns should therefore be minimised.

There are other advantages of modifying the front axle which may include increase in load that can ultimately be supported in the front. This enables use of other farm front mounted implements. These implements include air seeders, fertiliser spreaders and spray tanks. The modified front axle on a John Deere 8530 is shown in Figure 2.2 below. This is first generation (MK I) axle design that was manufactured about 7 years ago. The axle has its shortcomings including that it is a long single piece and mounting onto tractor is a huge task. It is quite difficult to handle according to John Foley, the designer of the axle. Second generation axle has been designed by the same designer which is basically an improvement on the first generation. Analysis of this second generation axle is the basis of this project to determine the safe loading levels of the axle.



Figure 2.2: John Deere 8530 modified axle extension. (Photo: R Sambamo)

## 2.1 Interpreting Client Brief

The main objective or emphasis of this research project is to determine the safe loading capacities for the second generation modified axle. The analysis has to be done using modern day computer technology known as Finite Element Analysis (FEA) which has the capacity to simulate designs as in real life situations. The supplied manufacturer's CAD data will be used to build the 3D model of the modified axle. A complete robust analysis of the 3D model of the axle will have to be performed and these tests should cover a wide range of load conditions than are feasible through normal field testing.

## 2.2 Project Scope

The following is an outline of the scope of this project.

- Relevant literature on axles and different analyses that have been performed using FEA packages will be reviewed. It will also be noted how these cases relate to the analysis of the axle under consideration.
- A literature review on finite element analysis will also be completed to

determine the best practices of analysis used in the industry. This will ensure that best and more reliable results are attained.

- Discussion of different loading situations or cases which include:  
Drop test, Torture Test, The Impact Test, Pit test, Worst load testing and one side impact test.
- Review of literature related to different loading conditions and testing standards that might have been used in previous similar studies.
  
- Review modified axle Cad files.
- Create the 3D models of the axle components and assembly of the components.
- Perform static and structural analysis.
- Review the results of the FEA, structural and dynamic analysis.
- Recommendations, conclusions and any further work to be undertaken.

## 3.0 Literature Review

The first section of this chapter reviews some literature on various types of finite element analysis software and their underlying theory. This will seek to establish if there is any FEA software that is better than the other one. This of course is in relation to accuracy of the results, ease of use, interface, processing times, computer requirements and the overall cost of setting up.

The second part will review any available literature on tractor or some other heavy duty both on field and off field vehicle axle analysis. This review will give an insight into how other analyses have been done and any flaws in the reports. These will also enable to evaluate the benchmarks against which the tests were performed and any relevant engineering standards applied. Different types of axles will also be reviewed.

### 3.1 Finite Element Analysis

Finite element analysis (FEA) is defined as a numerical method of solving engineering problems that would otherwise be difficult to solve using analytical methods. Its main uses are quite varied and include calculation of stresses, deflections and displacements in both simple and complex structures. The application of FEA has also been extended to thermal, structural and fluid flow analysis. Despite its application to many different engineering fields the underlying theory is the same.

The structure or component under analysis is basically divided into sections which are more manageable and easy to manipulate. This process is called discretization and according to Logan, the finite element method involves modelling the structure using small interconnected elements called finite elements and a displacement function is associated with each finite element. These elements are then linked either directly or indirectly, to every other element through common or shared interfaces, including nodes and/or boundary lines and/or surfaces. The material's known stress and strain properties making up the structure are then used to determine the behaviour of a given node in terms of the properties of every other element in the structure. These are formulated into equations for every node and the total set of equations obtained can be solved using matrices to get the overall behaviour in the structure. Matrices are easier to evaluate than the complicated differential equations which result from analytical analysis. The

numerical method gives an estimate result which can be improved by increasing the number of nodes and this obviously results in an even larger set of equations. Computational power of the computer can be utilised to solve these sorts of equations and that is the underlying theory of the FEA software.

### 3.1.1 Why use Finite Element Analysis

1. It is used as a cost effective way of verifying that a new design or a modification to an existing structure or component will meet the required structural, modal or thermal specifications. The traditional way of manufacturing which involves designing, building a prototype and field testing is expensive because the structural behaviour is not known until the new design has been subjected to field testing. Any subsequent problems that may arise with the new design would mean the prototype will have to be redesigned and modified at a cost. Use of Finite Element Analysis removes the need to build a prototype for testing purposes. The new model is tested and modified accordingly before the component is manufactured or fabricated. FEA analysis is effectively a cost cutting exercise. Behaviour of a component is determined before manufacture and saves on building a prototype which may not be able to meet the specifications.
2. The component or components are loaded and constrained as in real situation. Finite element analysis allows loads simulating the real situation to be applied to the model. Constraints such as displacements, planar and pin can also be applied to mimic actual situations where components can be fixed in various translations or may be joined used a pin joint which allows rotation.
3. The results as to how the component will behave under the suggested loadings and constraints can be processed within short time depending on the complexity of the component and the computer capabilities. A model's geometry can be easily altered if the results of an analysis are not satisfactory.
4. The results outcomes from a finite element analysis can be relied on. This depends on the skill level of the analyst. Proper application of the software can produce results that are quite reasonable. León, O, N, Martínez, P, Orta C, P, Adaya (2000) did an experiment to verify the validity of results obtained from a finite element analysis. They concluded that the results of the experiment had a

5.17% variation from the finite element analysis results. The challenge though is in the interpretation of the FEA results provided that the loadings and constraints have been appropriately applied to a well prepared model. According to Toogood, R, (2012) the results obtained from an FEA modelling depends on the quality of the input data. He says the principles of garbage in garbage out (GIGO) apply when using an FEA package. Results could be improved by either adjusting the model's meshing or redefining the convergence of the result. The number of elements and nodes in the model can be increased by changing the convergence of the analysis. An example of refinements is shown in the Figure 3.1.

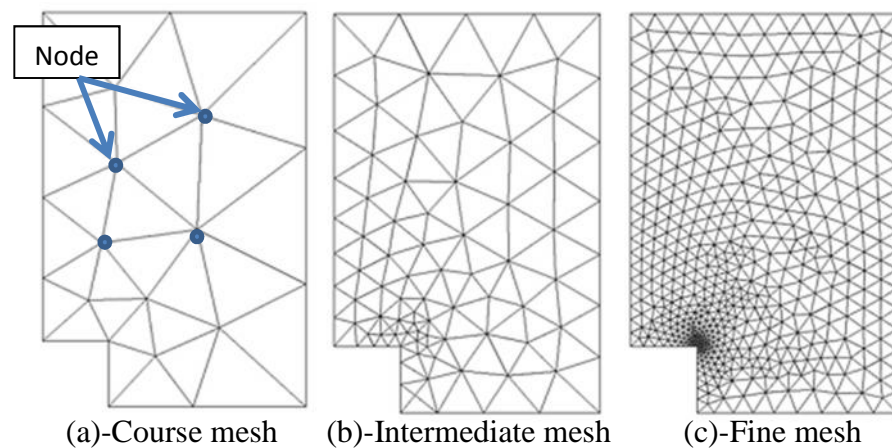


Figure 3.1: Mesh refinements. Source: (COSMOL Blog)

The component on the far left in the figure above has a coarse mesh which has been refined in (b) and (c) by increasing the elements and nodes. The nodes are represented by a few dots in (a) and the line connecting the nodes is known as the element.

5. One other advantage in making 3D parametric model and use them for FEA is that it allows fast variations in the model geometry. If the results of FEA are deemed unsatisfactory the analyst can quickly change the geometry in the 3D model by altering the controlling parameters.

### 3.1.2 Types of FEA software

There is a wide variety of FEA packages on the market and they also vary in their capabilities, pricing and ease of use. A list of FEA packages is shown in Appendix 12. There are 68 FEA software packages that have been compared in the list. They have been compared mainly on their pricing, capabilities, ability to import CAD drawings and types of elements that can be handled. Some of the free software are limited in their capabilities for example FELIPE is only capable of performing four functionalities out of a possible twenty three. There are packages that have extensive capabilities despite being freeware. A package like Elmer is capable of performing around 15 functions out of the possible twenty three. The fact that a package is paid software does not necessarily give it more capabilities than some of the freeware.

Packages are designed for specific applications and it is the ability to perform that particular application that should be considered when deciding which FEA package to use. The applications include the static and structural analysis, Thermal, Computational Fluid dynamics and many more. It is no uncommon to find high cost packages that are quite limited in their applications. These are designed for special applications such as in fluid flow analysis and civil and structural designs. The industry most common packages with a lot of capabilities are ADINA, ANSYS Mechanical NEi/Nastran, Pro/MECHANICA Wildfire 2, COSMOSWorks, COMSOL and Strand 7.

### 3.1.3 FEA software results comparison

Literature sought on comparison of results from different Finite Element Analysis suggests that if the same model is analysed under different platform, the results should be approximately the same. The results would be the same or close if the loads and constraints are applied correctly in each platform used. Adams, V of Impact Engineering Solutions did an experiment to check if the results of an FEA on different platforms were the same. In the experiment four widely used packages were used namely COSMOSWorks Version 2005, ANSYS Version 8.1, NEi/Nastran Version 8.3 and Pro/MECHANICA Wildfire 2. Some of the results from the comparison are shown in Table 3.1 below.

Displacement (in)				
	COSMOSWorks	ANSYS	Nei/Nastran	Pro/MECHANICA
Hinge - No Contact	0.0675	0.0674	0.0686	0.0570
Hinge - Contact	0.0889	0.0708	0.0833	0.0788
Hub-Spoke	0.0042	0.0042	0.0034	0.0039
Plastic Toy	0.0426	0.0425	0.0426	0.0424
Brass Chuck	0.0058	0.0059	0.0052	0.0057
Plastic Tub	2.0670	2.0910	2.1090	
Zinc Ratchet	0.0078	0.0078	0.0079	
Plastic Cover	0.1363	0.1360	0.1360	0.1344
Aluminum Housing	0.0276	0.0274	0.0274	0.0270
Plastic Pole Restraint	0.0282	0.0262	0.0234	0.0208

Table 3.1: Comparison of FEA software results Source: (Adams, V)

It was concluded that the results had variations of up to 10% and thus the results from all platforms were reasonably consistent.

### 3.2 FEA Validation and Verification

The discussion in the above section revolved around how use of different FEA platform influenced the results but the big question is how those results compare to the actual experimental results. The FEA results have to be validated to build some confidence in the outcomes of FEA analysis. An experiment was carried out by Koyuncu, A, Gökler, M, Balkan, T, (2011) to verify the results of FEA on a front axle support for a tractor. Strain gauges were placed on the axle support to measure and calculate the stress under the same loading condition as in the FE Analysis. Results of the experiment were found to have a variance of 7.7% form the FEA results. This basically confirmed that the FEA results can be relied on. MSC/Nastran and Patran finite element analysis packages were used to perform an analysis on the axle support.

Another experiment by N. León, O, Martínez, P, Orta C, P. Adaya, 2000 on front axle beam of a truck sought to validate the results of an FE Analysis. MSC Patran/MS Nastran V. 8 was used to perform the finite element analysis. PhotoStressO which they claim to be a widely used technique for accurately measuring surface strains was used to

measure the stress. They found some that the results of the experiment and the finite element analysis were close and there was a variation of 5.17% in the overall results.

It can therefore be safely concluded that Finite Element Analysis is a reliable and a cost effective way of checking the integrity of designs or modifications. The FEA results correlates favourably with the experimental outcomes. Any platform or the type of software used for an analysis as long as it has the necessary capabilities to perform the particular analysis and the user is competent in its use. Creo 2.0 Parametric and Creo 2.0 Simulate were chosen for the analysis of the modified axle in this project. Creo 2.0 Parametric was used to create the 3D models of the axle components and the complete or assembled model of the axle. The Simulation arm of Creo 2.0 was then used for the finite element analysis of the model. Creo 2.0 Parametric and Simulate although not as popular as the other packages previously discussed was chosen for this project because of its capabilities to perform the required static structural analysis of the modified axle. Other reasons for selecting this particular package include costs and user competency. The package was already on my computer because it had been used in previous courses such computational mechanics so there was no cost involved.

### 3.3 Tractor front axle designs and modifications

Literature on FEA analysis on tractor axle designs and modifications available is not very extensive and this most probably because of business and property protection issues. The few that are available mainly deal with optimisation of axle designs. An optimisation study was done by Mahanty, D et al and mainly designed an axle with the aim of reducing the weight of the current designs. They managed to reduce the weight of the axle while maintaining the structural and dynamic integrity. ANSYS software was used in this particular analysis and the new designs with reduced weight showed some 15% increase in stresses and displacements which was deemed significantly low. They also managed to reduce the weight by 40 %. This study shows that FEA can be a very effective tool in design and component modification which can ultimately cut costs. 40% reduction is quite significant and depending on the production quantities the savings can also be huge.

León, N (2000) seems to confirm the theory that costs are really reduced by optimising axle design through implementing FEA. In their study they managed to validate and

back the results from the FEA analysis by performing series of experimental test. In their research León, N concluded that the proposed engineering development process at their DIRONA site proved to be useful in reducing the development time and costs, while maintaining highest product quality and reliability. The software used in this study is SC Patran / MSC Nastran V. 8.0 was used. The axle design or modification can be improved by changing the variables or parameter which includes the materials and the component dimensions which show high levels of stress and strain. Changing some features such as the holes, undercut, radius and their location on a component can also improve the general stress and displacement results. León, N managed to reduce the weight of the axle by 6.8% by changing the design parameters. The stress only increased by 2% which is negligible. According to Aloni, S, Khedkar, S in their comparative analysis of an axle, they also managed to reduce the weight by 10 percent by changing the material from Steel SAE 1020 – Hot Rolled to ASTM A536 (65-45-12) Ductile Iron – Castings. Factor of Safety was improved from 0.7 to 2.4. From these studies it can concluded that modifications and optimisation can be done without compromising the integrity of the component.

Up to this point the literature reviewed did not include the effects of the dynamic forces which are considered significant at high speed. In addition to normal reaction forces on the axle due to the rugged terrain of the field, dynamic forces also have to be considered in the analysis of the behaviour of the axle. Koyuncu, A, Gökler, M, Balkan, T, (2011) outlined the importance of this dynamic feature of the analysis and put it as equivalent to 3g force. The loadings due to dynamic forces are discussed in detail under section 4.4.

### 3.4 Types of modified tractor axles.

Research into types of axle extensions has shown that there is a wide variety of extensions on the market. The extensions are manufactured to suit particular types of tractor. The tractors have different types of front axle configuration and suspensions and the extension have to be designed accordingly to suit the particular designs. Some examples of modified extensions are shown in Figure 3.1 below.

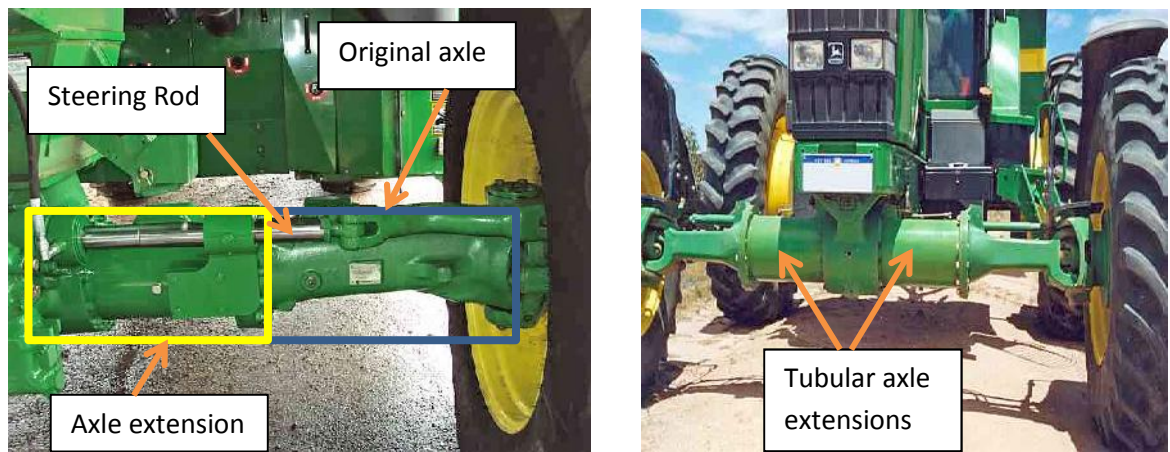


Figure 3.1: John Deere round bail cotton picker extension. (Source: C and C Machining)

In the left photo of Figure 3.1, the original axle enclosed in the blue box has been moved out to accommodate the extension on the left. The axle is a bit complicated than the one shown in the right photo. A provision for the steering rod in the extension creates some manufacturing challenges. Both axles shown in Figure 3.2 result in large moment arms which ultimately put high level stress on the parts joined to the tractor axle or the mounting parts on the wheel end. C and C Machining on their website stated that tubular sections have proved to increase stress on the kingpins on the front axle which may ultimately leads to failure.

Tractors are a huge investment for farmers costing several hundred hundreds of thousands of dollars and conversion costs to controlled traffic farming which may be prohibitive, breakdowns resulting in downtime and added costs is the least of things the farmers have to worry about. This affects the uptake of controlled traffic farming by the farmers for this creates uncertainties around the performance of the modified axle extensions. The traditional method of building a prototype and performing field tests to measure the performance and structural integrity of a design is becoming outdated and it's not something the farmers want to rely on. Analysis of modified extensions using the now powerful FEA software that has been tested and results validated over the years could boost the confidence of farmers on these modifications. The older tractors without front suspension had to be equipped with a tubular section due to the configuration of the driver train and the suspension. More types of axle extensions are shown below.



Figure 3.2: Axle extensions. Source: Larocque, S, 2012 Nuffield Report.

These tractor types shown above do not have a front wheel suspension such as the one incorporated into the JD8530 which enables the front wheels to move up and down in response to the terrain while maintaining the whole tractor level and stable. Detailed discussion of the JD8530 modified axle is in the next chapter.

## 4.0 Tractor Specifications

John Deere 8530 tractor was manufactured out of United States of America by one of the biggest tractor manufacturers John Deere. It was manufactured from 2006 to 2009.



Figure 4.1: JD8530 tractor. Source (Chris Snook)

Tractor Information or data is in Appendix D. The tractor cost around AU\$200 000 to buy second hand and is a huge investment for farmers. Any modification to such equipment has to be of very high standard. The modifications to the front axle of this tractor were complex because of the independent front suspension rams, drive line and the steering rod all of which had to be considered in the axle design. And because of the incorporation of the independent suspension, the tractor is capable of high speeds reaching up to 50 km/h without compromising the comfort of the ride.



Figure 4.2: Independent-Link Suspension Source (John Deere & Chris Snook)

The proximity sensor indicated in Figure 4.2 senses the position in space of pin coupled to the top wishbone and communicates to the control unit which ultimately adjust the wishbones up or down through the hydraulic ram thereby maintaining the level of the tractor. Modifications to the front axle should not compromise such functionalities and its accessories.

#### 4.1 General dimensions and weight.

The Figure 4.3 below shows the overall dimensions of the tractor and the measure that was worth taking note was the operating weight of the tractor. This measure was used in the determination of loads on the tractor axle.

Operating Weight	12156 kg
Wheelbase (D)	3020 mm
Length (A)	5560 mm
Height (C)	3120 mm

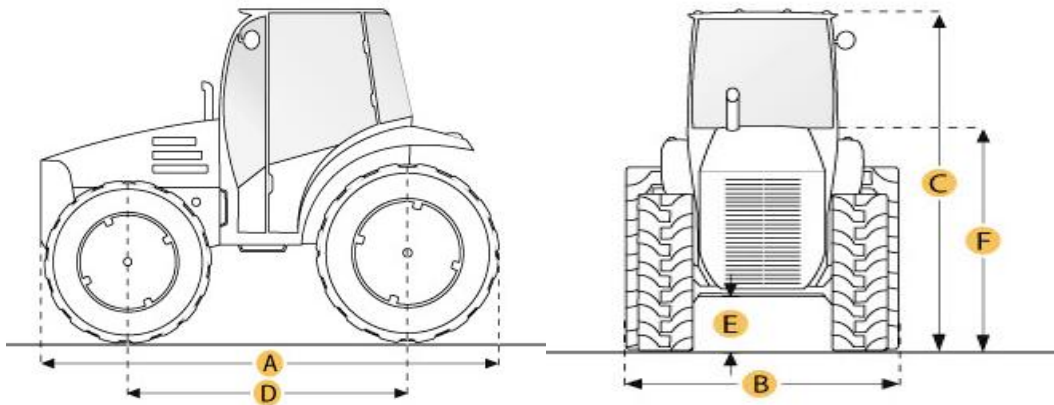


Figure 4.3: Tractor dimension and weight Source (Tractordata.com)

## 4.2 Original front axle configuration

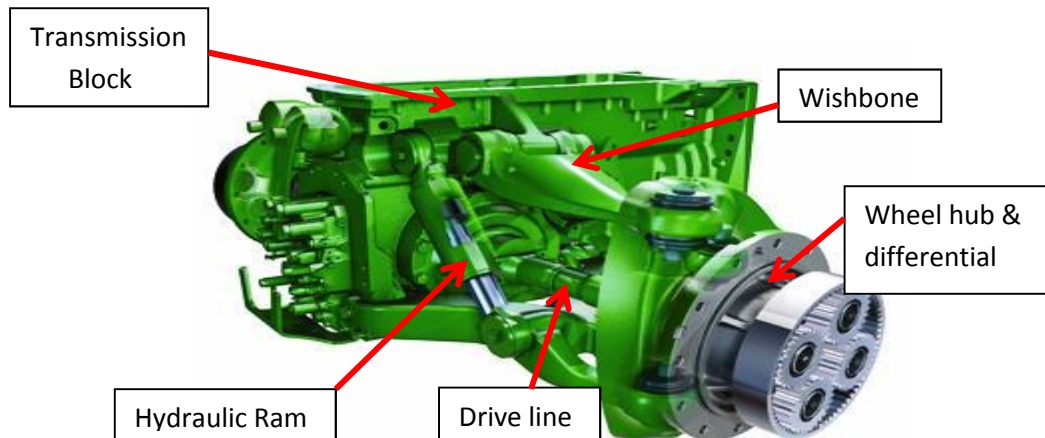


Figure 4.4: Original John Deere 8530 Tractor axle. (Source- John Deere)

The original axle of John Deere 8530 is shown in Figure 4.4 above. The wishbones were basically used to link the block and the wheel hub differential assembly. A hydraulic ram also fixed to the block on one end is attached to the bottom wishbone and can therefore move the block up and down relative to the wheel position.

## 4.3 Modified Axle overview and configuration



Figure 4.5: John Deere 8530 with front modified axle. (Source-Chris Snook)

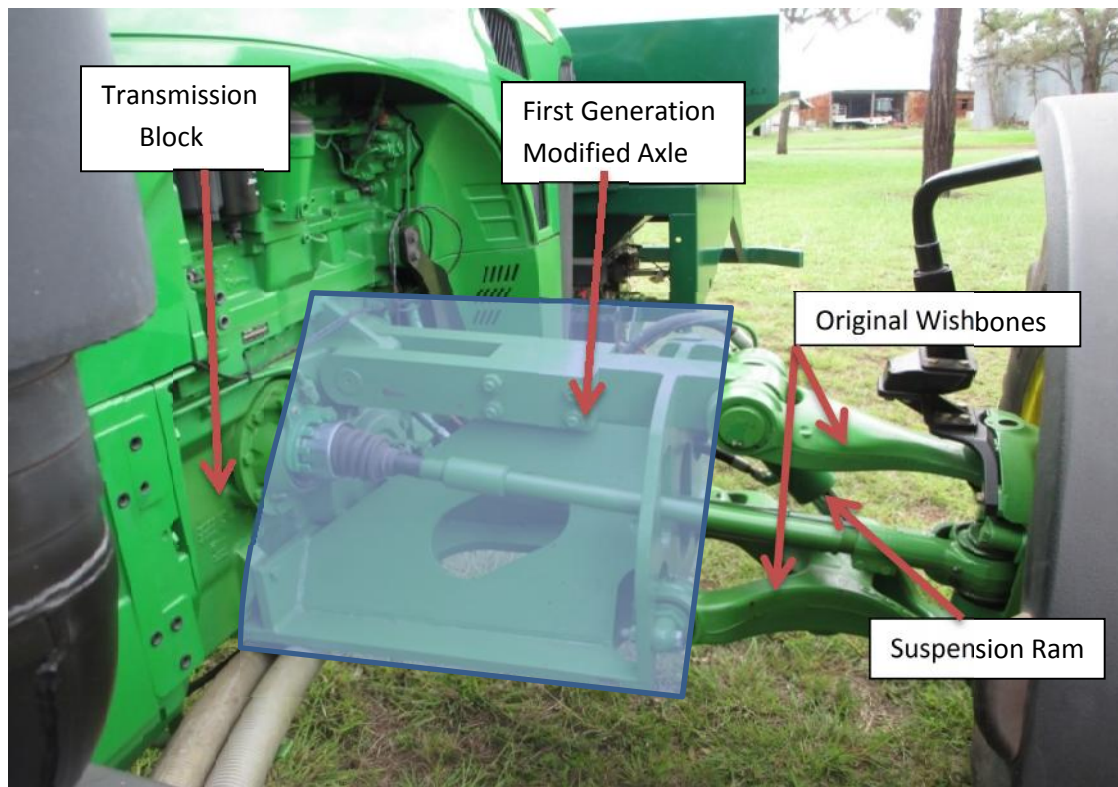


Figure 4.6: Modified John Deere 8350 Tractor axle at close range.

The modified axle is basically a welded and bolted steel block that has been inserted in between the tractor gearbox or transmission block and the wishbones as shown in the figure above. This increases the wheel span of the front axle and increases the performance of the tractor. The new axle is attached to the block using the existing anchor points to which the wishbones were previously attached. The wishbones were moved further out to the new anchoring points on the new axle while still connected to the old existing ones on the wheel side. The axle component parts are discussed in more detail in section 5.

#### 4.3.1 Difference between the two (MK I) and MK II Axles designs

The first generation axle which will be referred to as MK I design in the report is the shown on the left side in Figure 4.7 below has been in use for past seven years. It has

proved to be a success because it has not failed in operation. It however had some few disadvantages which prompted redesigning or modification. The overall length of the MK I modified axle was a bit longer than required. This resulted in the wheel span being over three metres which was not suitable for the most common controlled traffic farming span. The MK II had to be shortened to resolve this problem. Handling of the first generation (MK I) modified axle is difficult especially when fitting or dismounting onto and off the tractor block. It is a one long block and obviously fitting onto the block poses some challenges. The MK2 is a modification of this first generation axle to rectify any challenges posed MK I. MK I has been basically divided into manageable sections of MK II which can be easily assembled by bolting. A model of the MK II is also shown in Figure 4.7.

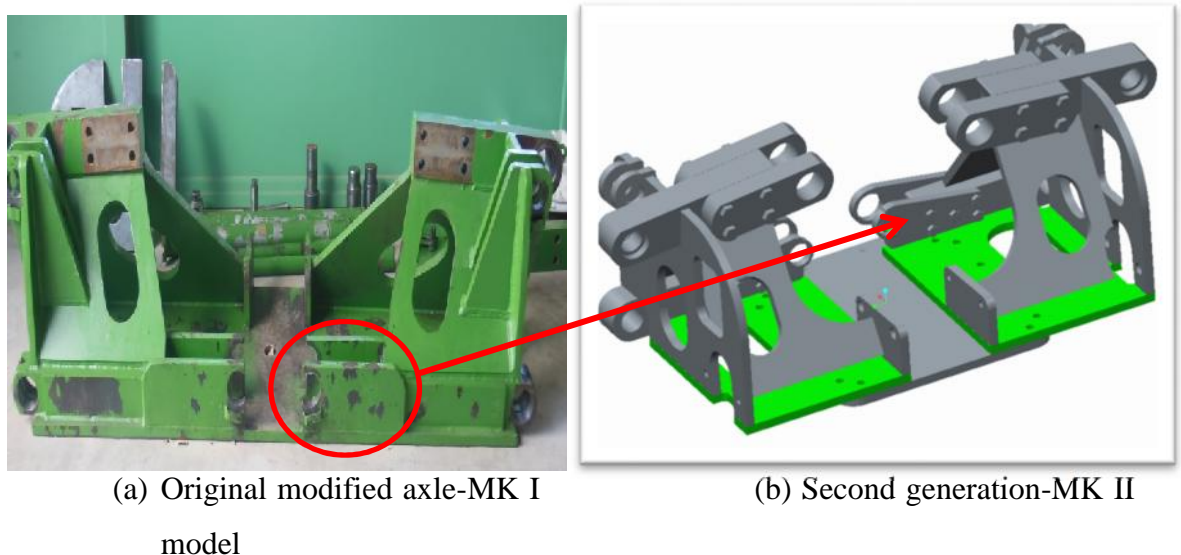


Figure 4.7: Generation I (MK I) and MK II Axles

Some other crucial modifications have been done which will facilitate easy and quick replacement of parts if for some reason they do fail or get worn out. The parts circled in red in (a) have been modified by drilling bolt holes in them so that they can be bolted onto the main piece instead of being welded.

#### 4.3.2 Material Properties

The components of the modified axle are to be manufactured from the same steel that has been used to fabricate the first generation modified axle. The steel is SAE 1020 steel

and a summary of the mechanical properties of the material are shown IN Table 4.1 below. The more detailed list of the material's properties is in Appendix J.

Component	Material	Density( $\frac{m^3}{\rho}$ )	Yield Strength ( $\sigma_y$ )	Tensional Strength ( $\sigma_t$ )	Modulus of elasticity (E)	Poisson's Ratio ( $\nu$ )
STEEL PLATES	SAE 1020	7800kg/m <sup>3</sup>	350.00 MPa	420.00 MPa	205,000 N/mm <sup>2</sup>	0.3

Table 4.1: SAE 1020 steel Mechanical Properties of Steel

1020 steel has some advantages which make it suitable for use in manufacture of the modified axle and these include welding ability, machinability, heat treatment and low cost. The ability of the steel to be machined is high and it is a requirement for the axle components because most of them have to be machined in some way. The mating surfaces of some components had to be machined to improve the contact area and some had holes for pins bored out and drilled out holes for the bolts.

As can be seen from the first generation modified axle there was some substantial welding done to join most of the components. The SAE 1020 steel used offers high ability for welding which ultimately affect the overall structural integrity or strength of the axle. Convectional or traditional methods of welding can be used in the joining of the SAE 1020 steel parts. This means basic workshop welding equipment which does not need a highly skilled labour can be used in the manufacture of the modified axle. This effectively influences and lowers the cost of manufacturing the axle.

#### 4.3.2.1 Material Failure modes

SAE 1020 is a ductile material and it is likely to show signs of yielding before fracture can take place. If the stress is maintained below the yield stress( $\sigma_y$ ), the steel is in a position to retain to original shape if the load causing the stress is removed. This phenomenon happens in the elastic region shown in the Figure 4.8 where there is a linear relationship between the stress and strain. Continual application of stress equal or above the yield stress will cause plastic deformation of components which result in permanent structural deformity. Further increase in stress will result in necking or reduction of the components area which may cause fracturing. The component on the

left in Figure 4.8 shows the effects of sustained stress above the ultimate stress of the material.

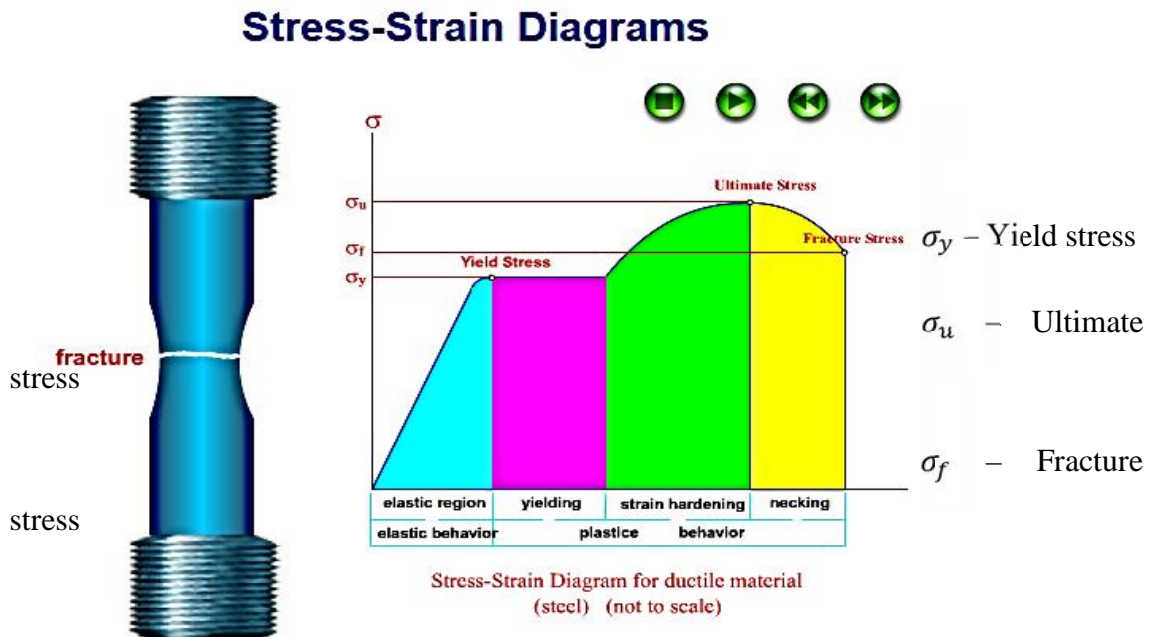


Figure 4.8: Stress-Strain graph Source (Pennsylvania State University)

The modified axle model will be tested against yield stress which is 350 MPa for the material defined for the model. Stress below this will be deemed to be safe for the model. And stress above the yield stress will be considered unsafe. This although does not result in instant damage but constant exposure to those high stresses cause material fatigue which may ultimately result in failure. Yielding is a probably a good sign of overloading and may prompt replacement or redesign of component.

#### 4.3.2.2 Factor of Safety Calculations

To guard the designed components from failure a factor of safety is normally incorporated in the design and this effectively reduces the maximum safe loadings on a component. A guide on how to determine the factor of safety of a component is in Appendix G. Contribution of material, stress, geometry, failure analysis and reliability are considered when determining appropriate factor of safety. Ullman, D. G (2010) suggested that each element mentioned above should be determined separately and then multiplied to get the overall factor of safety of the component. An example of how a factor of safety for material is determined as suggested by Ullman, D. G (2010) is shown below.

$FS_{\text{material}} = 1.0$  If the properties for the material are well known, if they have been experimentally obtained from tests on a specimen known to be identical to the component being designed and  $v$  tests representing the loading to be applied

$FS_{\text{material}} = 1.1$  If the material properties are known from a handbook or a manufacturer's values

$FS_{\text{material}} = 1.2-1.4$ . If the material properties are not well known

Once all contributions are established, the overall factor of safety is calculated as follows:

$$F.S = FS_{\text{MATERIAL}} \times FS_{\text{STRESS}} \times FS_{\text{GEOMETRY}} \times FS_{\text{FAILURETHEORY}} \times FS_{\text{RELIABILITY}}$$

The parameters on the right hand side of the equation are estimated using factor of safety guide in Appendix D. If the parameters are well known or defined the factor of safety can be theoretically close to unity but there is always an element of error in areas like workmanship and material. Calculated factor of safety for the modified axle model was calculated as follows.

$FS_{\text{MATERIAL}} = 1.1$	If the material properties are known from a handbook or a manufacturer's values
$FS_{\text{STRESS}} = 1.1$	The load is well defined as static or fluctuating
$FS_{\text{GEOMETRY}} = 1.0$	Manufacturing tolerances are average
$FS_{\text{FAILURETHEORY}} = 1.0$	Failure analysis to be used is derived for the state of stress,
$FS_{\text{RELIABILITY}} = 1.2$	The reliability is an average of 92–98%

Table 4.2: Factor of Safety Contributions

Therefore  $F.S_{\text{MODEL}} = 1.1 \times 1.1 \times 1.0 \times 1.0 \times 1.2 = 1.5$

#### 4.4 Related Standards and Certification Tests

A search for specific standards governing the design and testing of tractor axle did not yield results. John Foley, the designer and manufacturer of the JD 8530 front axle extension confirmed that no industry related standards were being used or referred to. Previous studies by Mahanty, D, K Manohar, V, Khomane, B, S, Nayak (2002) on the structural and dynamic analysis of a tractor's Front Axle however used some test conditions which they called certification tests. Drop test is one of the certification tests and is discussed in more detail under section 4.4.1. A crucial assumption that has been made to facilitate the analysis of the modified axle is that the reactions of the ground to the wheels are acting directly to the axle. The effects of the suspension and the wishbones are beyond the scope of this analysis.

#### 4.4.1 Drop Test

In this test the tractor is driven over a pit which is 762mm deep, 610mm wide and 1500 mm long which is dug on a very hard ground. The maximum dynamic loading component is determined by driving the tractor over the pit at maximum speed of 50km/h. One of the wheels is dropped into the hole and the figure below shows the simplified representation of the scenario at the point when the wheel is in the hole. The tractor is driven from maximum speed to zero speed. The standard distance used for the purposes of these calculations is 1.5 metres.

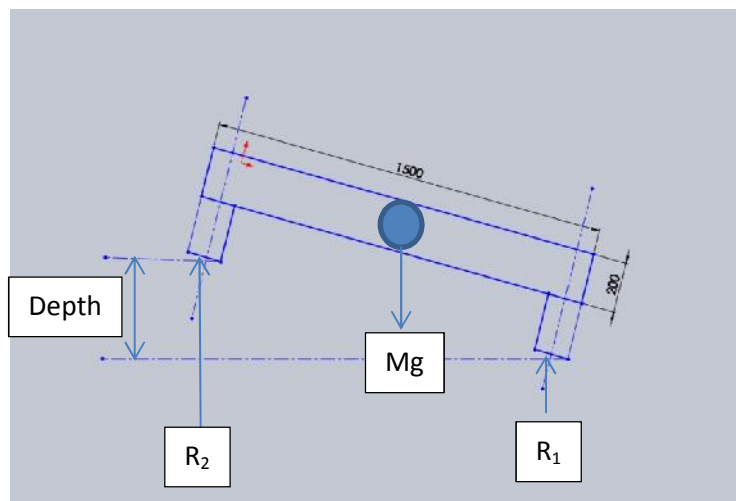


Figure 4.9: Drop Test Graphical Representation

Calculations of forces to be used in the dynamic analysis for this scenario are as follows

Velocity of the tractor = 50km/h = 13.9 m/s

Acceleration =  $-\frac{U^2}{2S}$  where U = initial velocity, S is the distance covered.

$$= - \frac{13.9^2}{2 \times 1.5} = - 64.4 \text{ m/s}$$

Using  $F = \text{mass} \times \text{acceleration}$

$$= 631 \text{ kg} \times 64.4 \text{ m/s}$$

$$= 40.687 \text{ kN force on the front of the axle due to velocity of tractor.}$$

Mass on the front axle is 45% of the total weight of the tractor of 12000 kg = 5400kg.

$$\text{Reactions } R_1 \text{ and } R_2 \text{ are equal} = (5400/2 \times 9.81) = 26.487 \text{ kN}$$

The other certification tests which include Torture Test, '8' shaped track test, impact test, pit test and worst load test follow a similar setup as the drop test described above. The difference is in the scenarios which include differing velocity applied and orientation of the axle relative to the field.

#### 4.4.2 VSB 14 Tests

Other studies though have used a different approach to the one adopted by Mahanty, D, K Manohar, V, Khomane, B, S, Nayak (2002) described above. Koyuncu, A & Gökler, M, I & Balkan, T, (2010) in their strength and fatigue analysis for agricultural tractors, they simply used 3g and 2g loading cases to simulate the dynamic loads induced by rugged terrain of the field. VSB14 loading cases used by Krank Engineering are similar to the ones used by Koyuncu, A & Gökler, M, I & Balkan, T, 2010. These are however more detailed and there is some loading cases similarity with those used by Mahanty, D, K Manohar, V, Khomane, B, S, Nayak (2002). Brett Longhurst in his analysis of the front axle of A Holden also used the VBS 14 loading cases. They basically used three loading cases which are specified in Vehicle Standards Bulletin 14, a bulletin produced by department of infrastructure and regional development. The cases though cover vehicles covered by legislation and off road vehicles are not covered in Australian government legislation that is according to the department website. The three loading cases were classified as follows:

##### 1. Loading Case 1: Normal Reaction Loads

Normal weight reaction loads are applied to the ends of the model to simulate the normal static situation. Governing mode of failure in this analysis is by yielding.

2. Loading Case 2: Bump loads: 4g vertical

This simulates the scenario where the vehicle has to drive over a pothole. This test is similar to the drop loading case used by Mahanty, D, K Manohar, V, Khomane, B, S, Nayak (2002) except that the force in this particular case is already defined as 4g vertical. In addition to the calculated reactional forces on the axle due to the weight of the vehicle a vertical force equivalent to four times the weight of the axle also acts in the same direction as the reaction forces. The additional 4g force is applied to one end of the axle. In this loading case the materials ultimate tensile strength is used as the upper limit for this test on the assumption that the critical parameter in this particular test is fracture. The axle in this analysis is allowed to deform due to yielding but not exceeding the fracture limits.

3. Loading Case 3: Overturning loads: 2g vertical with 2.5g side load

Overturning can result in some substantial dynamic loads being imposed on the axle and to simulate such loads the code recommends that 2g vertical and 2.5g side or lateral loads be applied. The governing failure mode in this analysis is by yielding.

4. Loading Case 4: Skid loads: 2g vertical with 1.2g longitudinal

Skid loads or braking loads are applied as combined loadings of 2g vertical with 1.2g longitudinal.

5. Loading Case 5: Worst Case Loading

The highest loads in the above four tests are identified for all directions to create a worst case scenario. These are applied that vertical, lateral and horizontally.

The VSB14 tests were adopted for the analysis of the modified axle because the tests give higher testing loads. The model is exposed to worst case scenarios in these tests. These tests are also covered by legislation and this gives some credibility to the tests. They have been formulated based on wide ranging studies. The certification tests have not been used anywhere else except by Mahanty, D, K Manohar, V, Khomane, B, S, Nayak (2002). The VSB14 detailed loading cases are under section 7.1.7.

## 5.0 Review of the e-drawings of the modified axle

The client provided an e drawing of the modified axle. The drawings were initially drawn in AutoCAD. E drawings can be viewed using e drawings model viewer in Solidworks and measurements of the components can easily be determined from the drawing using the measure tool in the software. The Figure below shows the some drawings of the component as supplied displayed in the Solidworks e-Drawing Viewer. The drawings could not be modified in the Solidworks e-Drawing Viewer software. Options were considered as to how to import the drawings into Creo 2.0. Redrawing the components one by one using Pro Engineer or Creo Parametric was one option but was deemed to be time consuming. The other alternative considered was using the CAD software and in this case AutoCAD 2014 was used to open the drawing file (DWG).

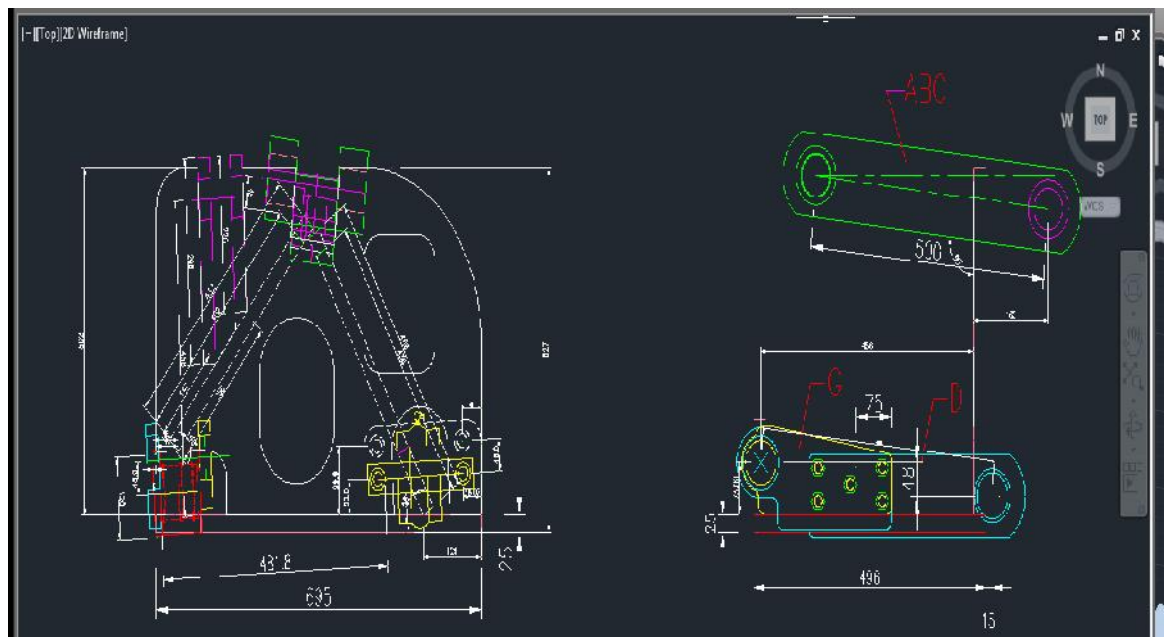


Figure 5.1: Part of Original drawings in e-drawing model viewer.

### 5.1 Make 2D drawings of the axle components

The following procedure was used in producing individual drawings for the individual components. The original drawing provided was opened using the AutoCAD 2014 and the individual component drawing is then selected and highlighted. Once highlighted, it is then copied onto the clipboard and another window or new drawing window is

opened onto which the highlighted drawing is then pasted. The new drawing is then saved as a DXF file (Drawing eXchange Format). This format enables the files to be opened in other programs other than the AutoCAD. In processing these files into 3D models, they are imported into Creo 2.0 Parametric.

In Creo Parametric, a new 3D part is opened, select the sketch mode and choose a drawing plane. Import the DXF file through the file system under the model toolbar. Under the status (Processing interface data) right click to select the vertex or Csys and accept by clicking the green button. Creo's default units are English and they were changed to Metric (SI) units before importing the DXF file since the original files were in metric units.

## 5.2 Issues with drawings and software.

The minimum computer system requirements for running Creo 2.0 on a Windows 7 64-bit operating system are main memory which is normally known as RAM should be at least 4 GB. The memory should be at 3 GB for the Windows 7 32-bit. Installation of academic version of Creo 2.0 was unsuccessful on this system due to PTC registration limitations. Ended up with a student version which has a lot of limitations as far as simulation and structural analysis is concerned. 2D and 3D drawings were however completed using this version of the software.

Recommended system requirements for running the same software on a Windows XP 64-bit and 32-bit is a minimum of 3GB of RAM. Software has been installed on personal computer running on a 2GB memory and has been successfully used in computational mechanics course. The drawings supplied were sufficient and detail was also sufficient. Holes in the base plate did not initially line up and had to change the centre distance on one of the plate to match the holes in the other plate. The slots in the upright 25mm plate had to be altered as their positioning was not the same as the original drawings.

## 6.0 3D model of the modified axle

Creo 2.0 Parametric was used to create the 3D model of the modified axle. Some of the modified axle's 3D components are in Appendix C. The procedure to create an assembly in Creo 2.0 Parametric involves the following steps. The new assembly part is opened and the main part is inserted in the assembly area. The constraints for the main part or the first part to be inserted in the assembly are default constraints. The selected main part for the model was the base plate sub assembly shown in the Figure 6.1 below. The placement or constraint options include coincident, normal, offset angle, parallel and distance. Coincident was used to constrain components with edges, surface, curves and axis which coincide. In the sub assembly in Figure 6.1 the holes axis was used to align and constrain the holes in the plates. To complete the placement and mate the plates, the surfaces were constrained using coincident option. All other components were then inserted and constrained appropriately.

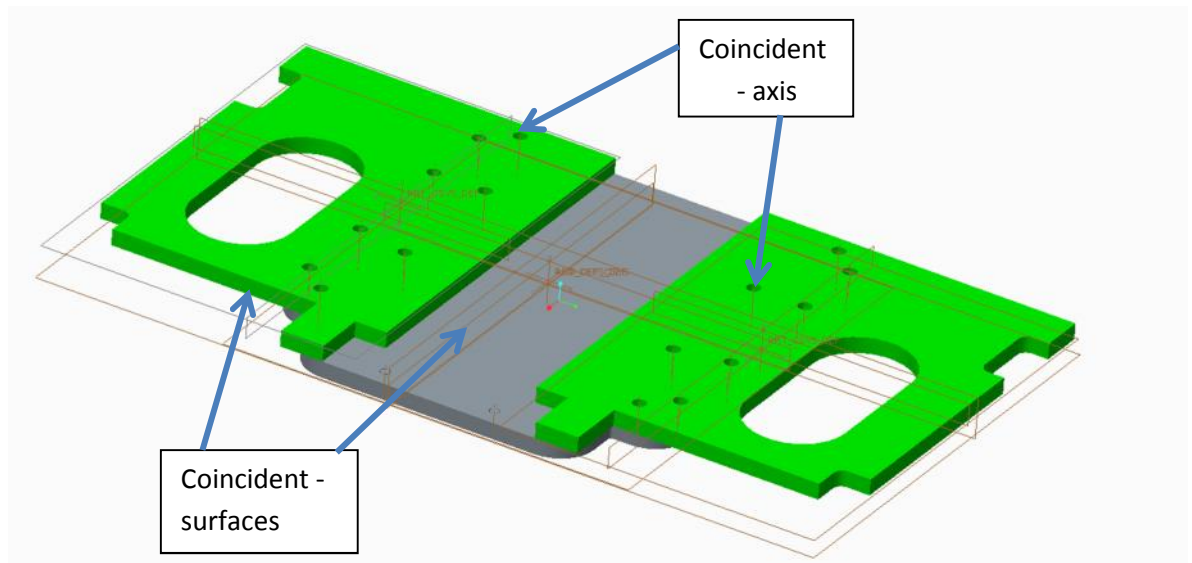


Figure 6.1: Solid Model of Modified Axle sub assembly

The Figure 6.2 shows the exploded view of Modified Axle components included in the assembly. The names of the components are included in the bill of materials in Appendix L.

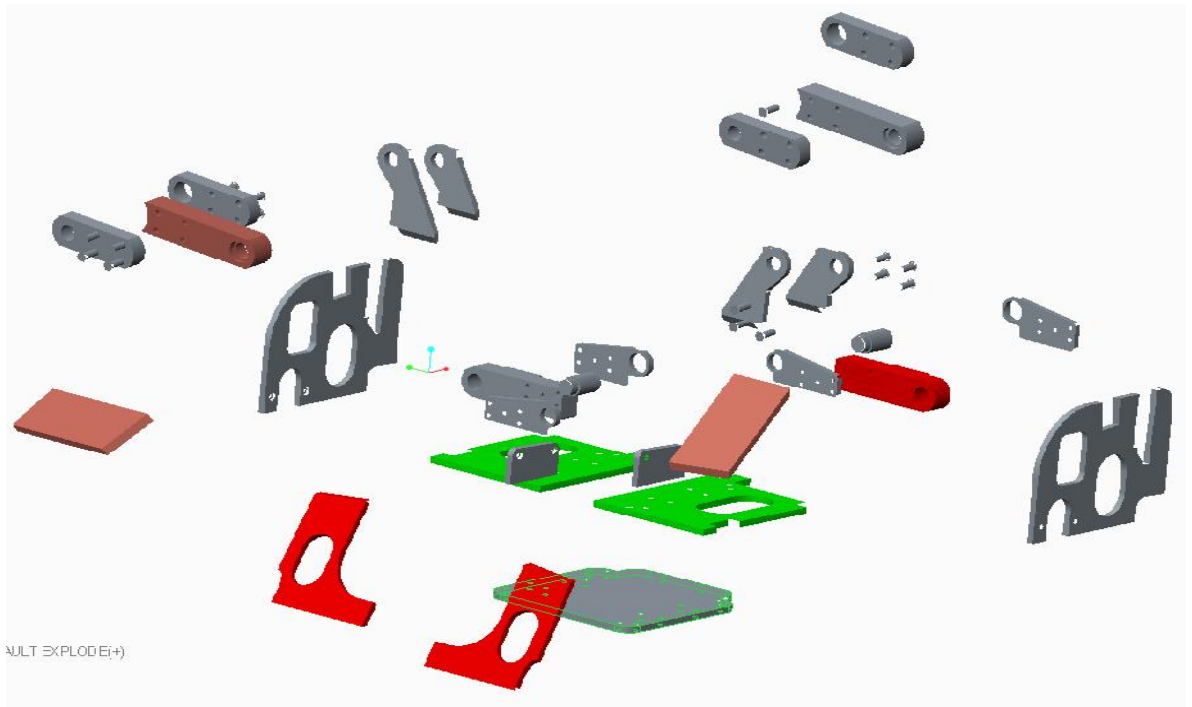
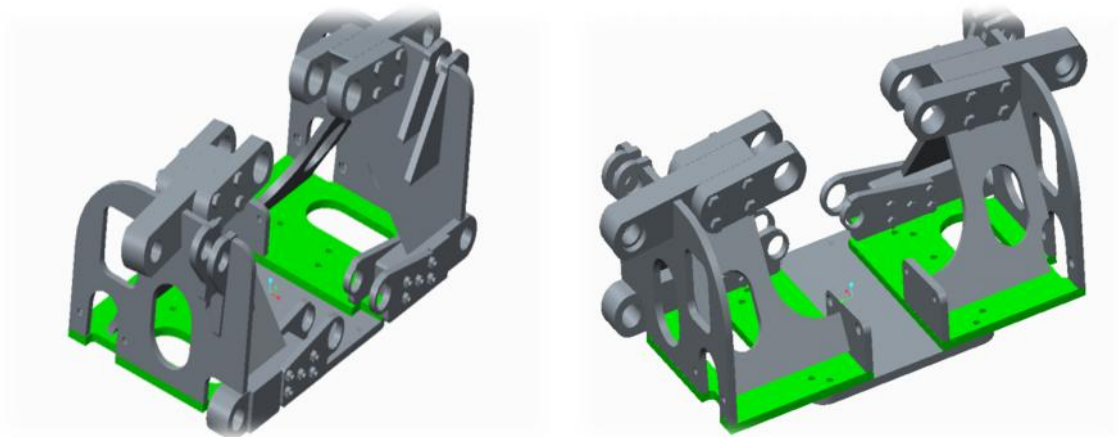


Figure 6.2: Exploded view of Modified Axle components.



(a) Front view

(b) Rear view

Figure 6.3: Solid Model of Modified Axle

The model shown in Figure 6.3 is based on the drawings provided by the manufacturer of the axle and on the assembly procedure outlined above. The rear view of the same model is shown in Figure 6.4.

## 7.0 FE Analysis- Static Structural Analysis

As previously stated, the major assumption made for this analysis was that the effect of tyres and hydraulic suspension ram were not considered in the analysis. There are three stages or processes involved in the static and structural analysis of the component. These are namely pre-processing, processing and post processing. In pre-processing the axle model is set up for analysis by converting it into a finite element model by adding and defining some or all of the following finite element model characteristics. The characteristics defined for the model include the geometry of the model, material used in the model and its properties, type of elements, meshing, boundary conditions or constraints and the loads applied. Once the setting up or pre-processing was completed the model was then subjected to a static and structural analysis and this stage of analysis is known as processing. In processing, convergence and outputs are set and these are discussed in more detail in subsection 7.2.--. Post processing was the final stage of analysis where the results of the analysis were analysed, factor of safety calculated and plots of different loading cases and deformed axle model were created.

### 7.1 Pre-processing

In pre-processing the axle model is set up for analysis by converting it into a finite element model by adding and defining some or all of the following finite element model characteristics. The characteristics which defined the model including the geometry of the model, material used in the model and its properties, type of elements, meshing, boundary conditions or constraints and the loads applied bare discussed in more detail in the subsections below.

#### 7.1.1 Geometry

The 3D solid geometry of the modified axle was created in Creo 2.0 Parametric as shown in the previous chapter. Once imported into Creo Simulate the geometry had to be checked and confirmed.

#### 7.1.2 Element/Model type

In Creo 2.0 Simulate under the home page, model setup icon was chosen and Advanced tab was selected for the model setup window. Confirmed that 3D option was checked and the bonded default interface is also selected.

### 7.1.3 Material properties of the model.

The material assigned to the model has been discussed in section 4.3.2 Material Properties and the material properties have been included here in Table 7.1 for convenience.

Component	Material	Density( $\rho$ )	Yield Strength ( $\sigma_y$ )	Tensional Strength ( $\sigma_t$ )	Modulus of elasticity (E)	Poisson's Ratio ( $\nu$ )
PLATES	SAE 1020	7800kg/m <sup>3</sup>	350.00 MPa	420.00 MPa	205,000 N/mm <sup>2</sup>	0.3

Table 7.1: SAE1020 steel Mechanical Properties of Steel.

And the following Creo window in Figure 7.1 shows how the material properties in the above table were defined for the model.

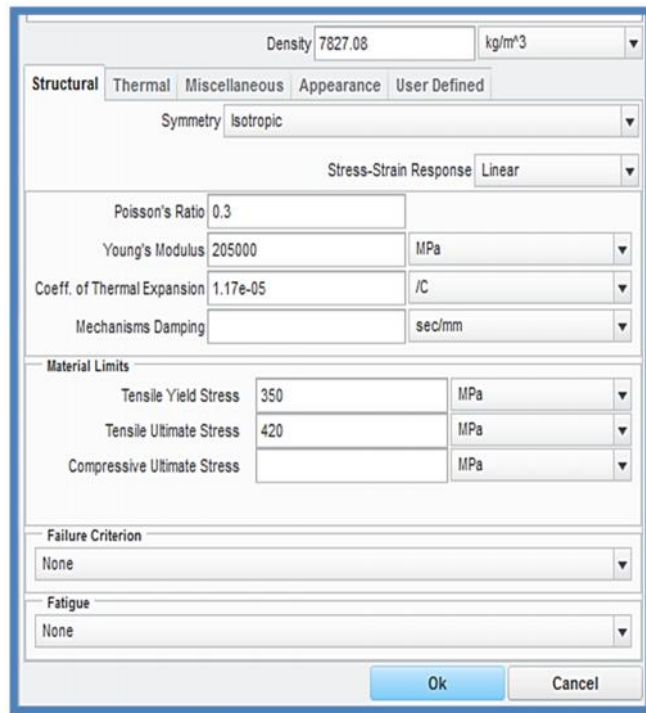


Figure 7.1: Material Definition in Creo 2.0

### 7.1.4 Element connectivity/Mesh the model

The model's elements were connected or meshed using meshing for solids known as tetrahedral elements. The mesh was also automatically generated in the running mode. The difference between a fine meshed and a coarse meshed component is shown in the Figure 7.2 below. Toogood, R (2012) noted that the density of the mesh in Creo does not have a large effect on the final solution of an analysis. The running time of the analysis though can be hugely affected.

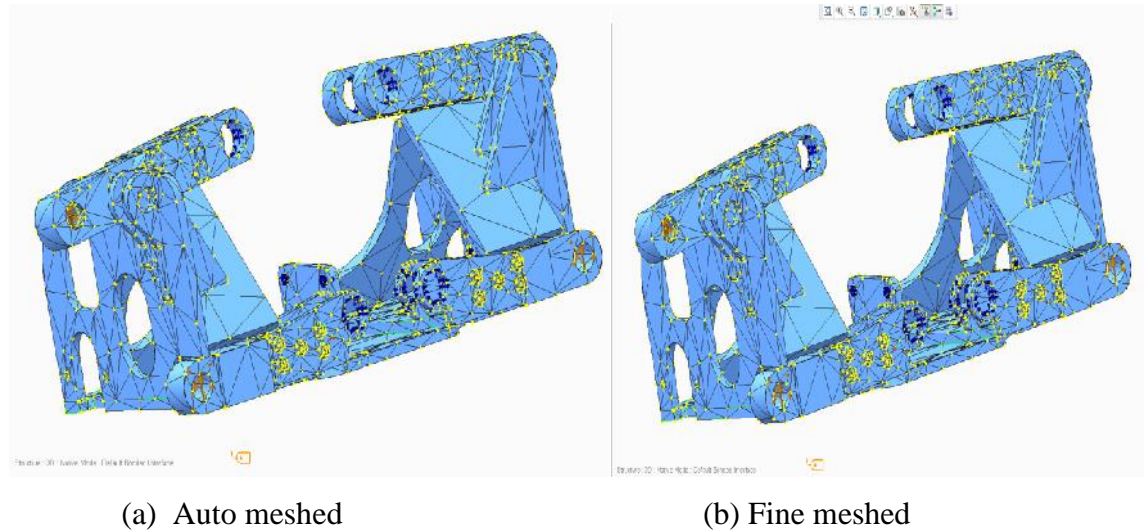


Figure 7.2: Finite Element Model of modified Axle

#### 7.1.5 Boundary conditions

The details of the loads applied on the model were calculated and given in the next section and in Appendix-A. A typical model showing loads and boundary conditions is given in Figure 7.3 below. The fixed constraint was applied to the inner mounting points of the model which are used to mount the modified axle to the tractor block or chassis. There should be no movement between these two parts and all movement especially of the wishbones and the hydraulic ram should be restricted to the outer mounting ends of the axle. That is the reason bearing loadings were applied on these outer mounting points to cater for such movement.

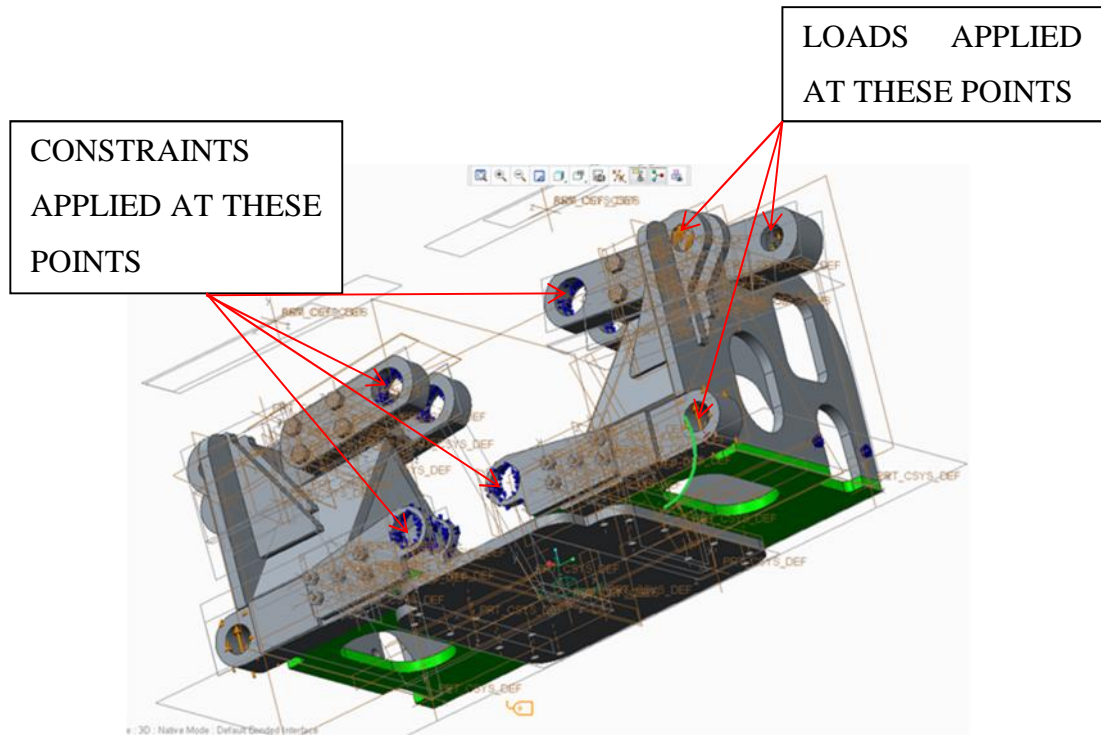


Figure 7.3: FE Model of Modified tractor Axle showing constraints and loadings

#### 7.1.6 Overview of Tests and Loading conditions.

Distribution of weight distribution between the front and rear wheels of the tractor had to be considered in evaluation of the actual loadings on the modified front axle. A Canadian government department of Agriculture and development developed a guide on how to evaluate the weight distribution between the front and the rear wheel. The weight distribution depends on type of the tractor especially the type of drive. The table below shows the weight distribution as a percentage for the different types of tractors. These were considered using total ballasted weight or the working weight of the tractors.

Tractor drive type	Front Axle	Rear Axle
2WD	30%	70%
4WD	55%	45%
FWA	40%	60%

Table 7.2: Tractor axle weight distribution

John Deere 8530 type of drive is specified as MFWA in the tractor's data sheet in Appendix 4. The manufacturers sought to differentiate this front wheel drive tractor from one of their previous products which used hydraulics to drive the front wheels. On John Deere 8530 tractor the drive is all mechanical through a gearbox hence the addition of mechanical in Front Wheel Drive. The operating weight of the tractor determined from the information sheet is 12156 kg. Using the 40% to 60% ratio for the FWA drive as a guide for weight distribution for the front axle, the mass acting on the front axle is 4862.4 kg. It has been assumed that the weight due this mass is acting at the centre of the axle as graphically shown in Figure 7.4 below.

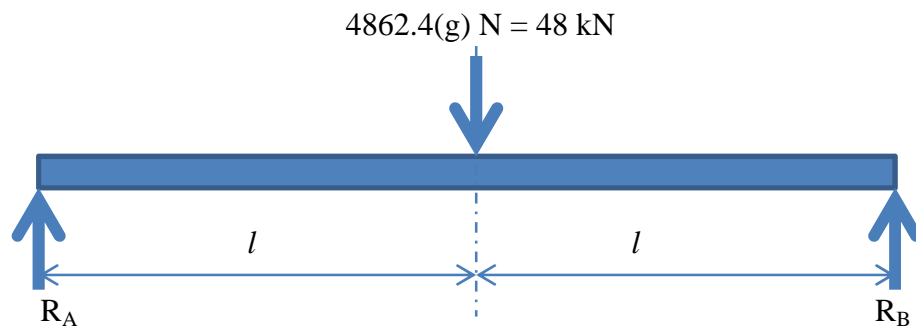


Figure 7.4: Weight distribution on front axle.

The acceleration due to gravity ( $g$ ) was assumed to be  $9.81\text{m/s}^2$ . The reaction  $R_A$  and  $R_B$  are equidistant from the centre of the axle. The reactions acting on the wheels are therefore equal and are half the weight applied at the centre which was 24 kN. The self-weight of the axle was also included in the analysis and using the inspect tool the volume of the model was determined to be  $0.081\text{m}^3$ .

$$\text{Using Density} = \frac{\text{Mass}}{\text{Volume}}$$

$$\text{Mass} = 7800\text{kg/m}^3 \times 0.081 \text{ m}^3 = 631,8\text{kg}.$$

$$\text{Weight of the modified axle} = 631,8\text{kg} \times 9.81\text{m/s}^2 = 6.2 \text{ kN}$$

Therefore the total working weight on the front wheels was  $(48 + 6.2) = 54.2 \text{ kN}$  which translated to  $27.1 \text{ kN}$  reaction at each end of the axle.

Application of loads and constraints in Creo 2.0 Simulate was performed as follows. On the Creo 2.0 Simulate home screen, bearing load under the Loads section was selected which brought an input window. Inputs such as the surface to be loaded and the magnitude of the force including its direction were defined in the window. The Figure 7.5 shows the loads and constraints and where they have been applied on the model. For the modified axle analysis the central section of the axle which is fixed to the tractor gearbox or transmission block was considered fixed and therefore translations in all directions were restrained. The bearing loads were applied to the outer mounting points of the axle where the wishbones and the hydraulic ram would otherwise be mounted.

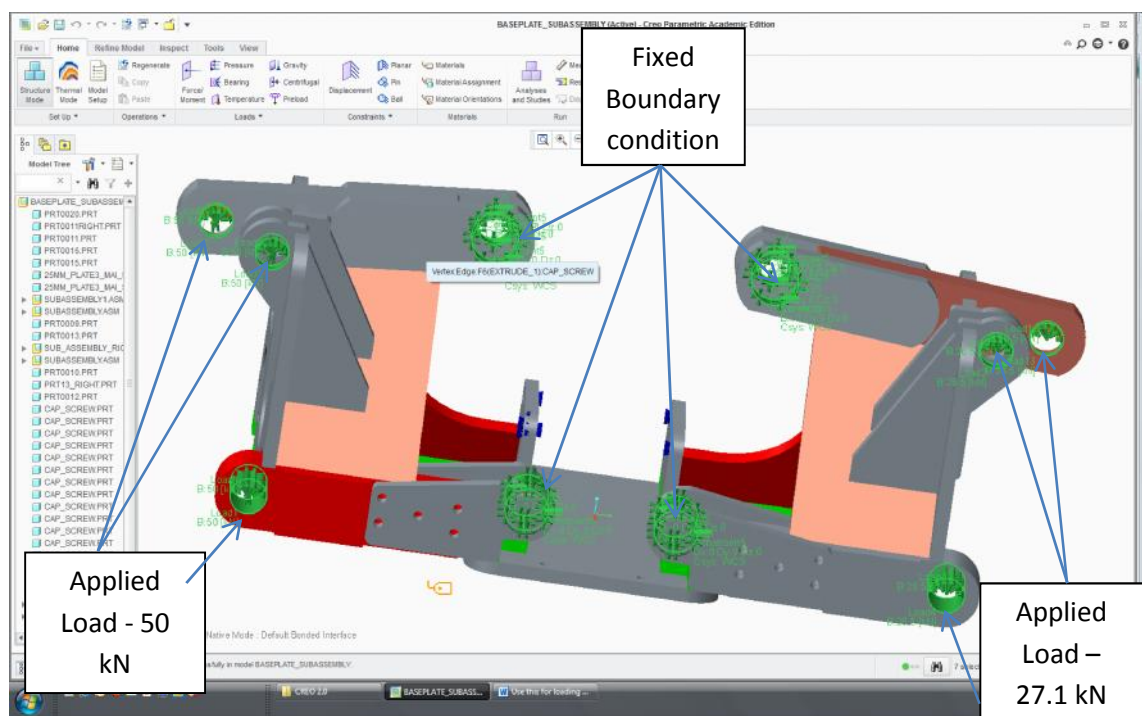


Figure 7.5: Loading Conditions and boundary constraints

As discussed in section 4.4, the VSB14 loading cases were adopted for static and structural analysis of the modified axle. The Figure below graphically shows how the loads were applied to the ends of the axle. This represents the first test case where the axle was subjected to reactions only at the end due the weight of tractor and modified axle. The 27.1 kN force was applied to each individual mounting point. This was done deliberately so as to create a worst case scenario for the mounting points. A safety

feature is thus created and in case the other two mounting points fails then the remaining mount would be capable of safely holding the load.

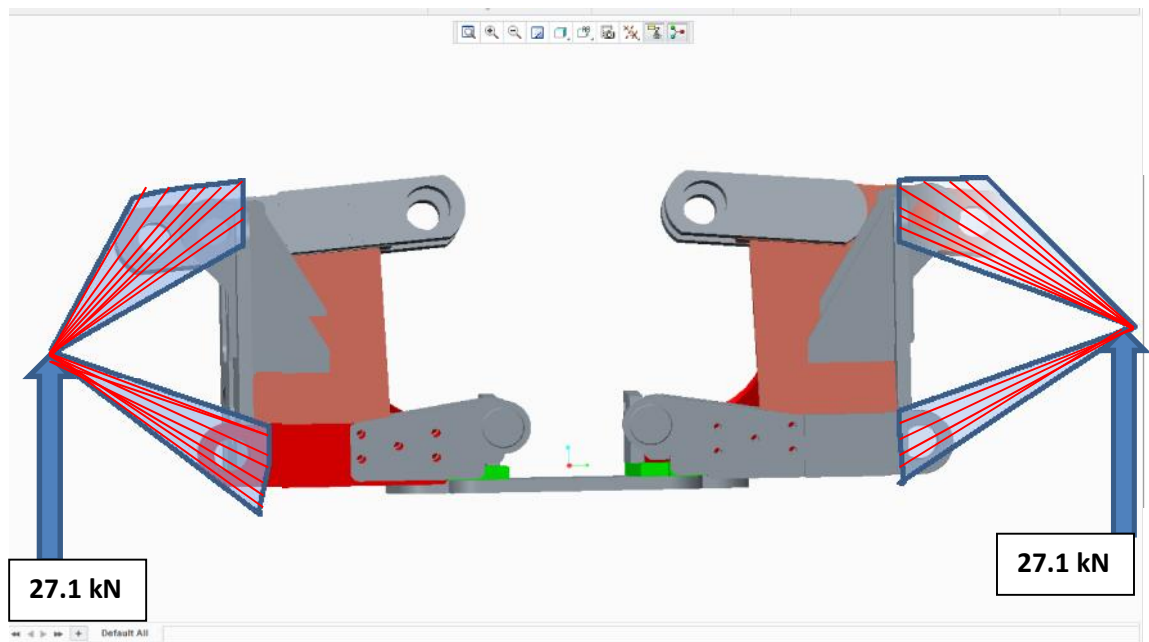


Figure 7.6: Loading Case 1: Equal reaction loads

Loading Case/Test	Mounting/Wheel A Loads (kN)			Mounting/Wheel B Loads (kN)		
	$F_x$	$F_y$	$F_z$	$F_x$	$F_y$	$F_z$
Test 1	0	27.1	0	0	27.1	0
Test 2	0	27.1	0	0	50.0	0
Test 3	15.5	27.1	0	15.5	38.9	0
Test 4	0	38.9	7.5	0	38.9	7.5
Test 5 (Worst case)	15.5	38.9	7.5	15.5	38.9	7.5

Table 7.3: Loading Scenarios.

The other four loading cases are shown in the table above. The force directions used in the table above are based on the global coordinate system used in Creo which is shown below.

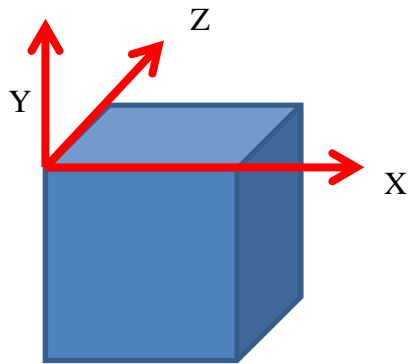


Figure 7.7: Coordinate System

## 7.2 Processing

In the processing stage, the axle model is committed to an analysis by defining the type of analysis, convergence and output file directory in Creo 2.0 Simulate. A new Static and Structural analysis was selected from the file drop down menu and the Static Analysis window came up where constraints and load already applied in the pre-processing stage are selected. Under the convergence tab, the Quick Check method was initially chosen to basically check if there are any errors in the model which may render the analysis insolvable. This initial analysis failed because meshing of some components could not be completed. Closer inspection revealed that there was some interference of some component. The other problem identified was the geometry of some components which resulted in the supposedly mating components not completely coinciding. The components of the model which created some analysis problems are shown below.

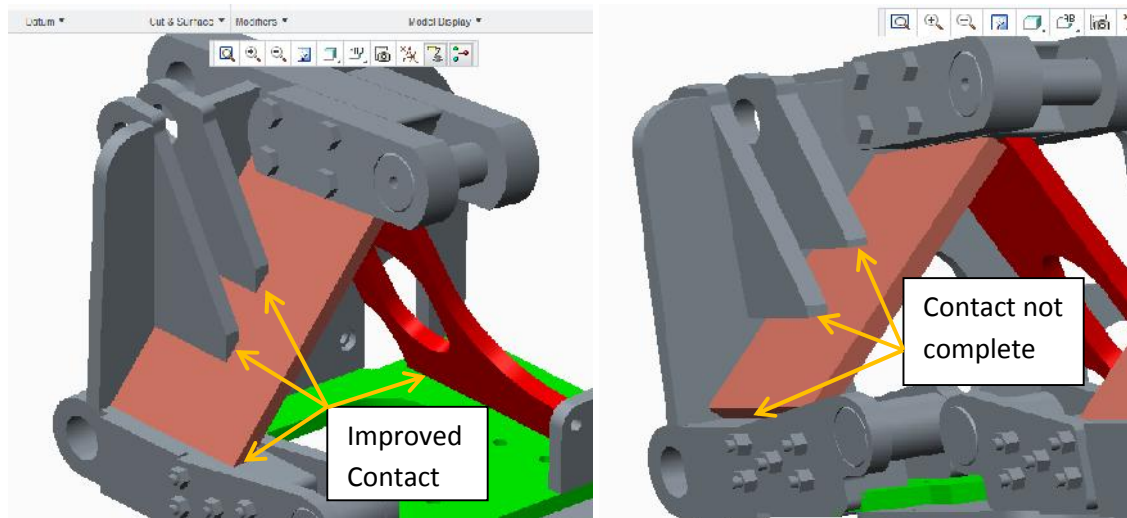


Figure 7.8: Components Contact issues

The areas on the components that did not have full contact and bondage were modified by introducing bevelled edges as shown in the left section of Figure 7.7. Once the Quick Check analysis was successfully completed the model was subjected to Single-Pass Adaptive method of analysis which is more reliable. An analysis for different loading cases was then run and completed successfully.

### 7.3 Post Processing/Results

Post processing is the final stage in the analysis where the results obtained from the processing stage are critically analysed evaluated. Creo as some of the post processing software on the market is capable of analysing the results and producing color-coded Stress von Mises plots. It is also capable of sorting, printing, and plotting selected results from a finite element analysis. Some of the routines that can be performed in post processing are sorting element resultant stresses and displacements in order of magnitude, calculation of factor of safety, creating convergence graphs and creation of plots ad graphs

One of the crucial capabilities of post processing software is ability to animate the deformed structural shape of a component. This allows a judgement to be made on whether the model was constrained properly. The modified axle model was constrained at the inner mounting points and loads applied at the outer points. The expected

behaviour of the model was the outer sections of the model to move in the upward or vertical direction in response to the applied loads. The following plot in Figure 7.9 shows the deformed model of the axle. The deformation has been exaggerated for visual clarity. The results of animation clearly show that the model was correctly constrained.

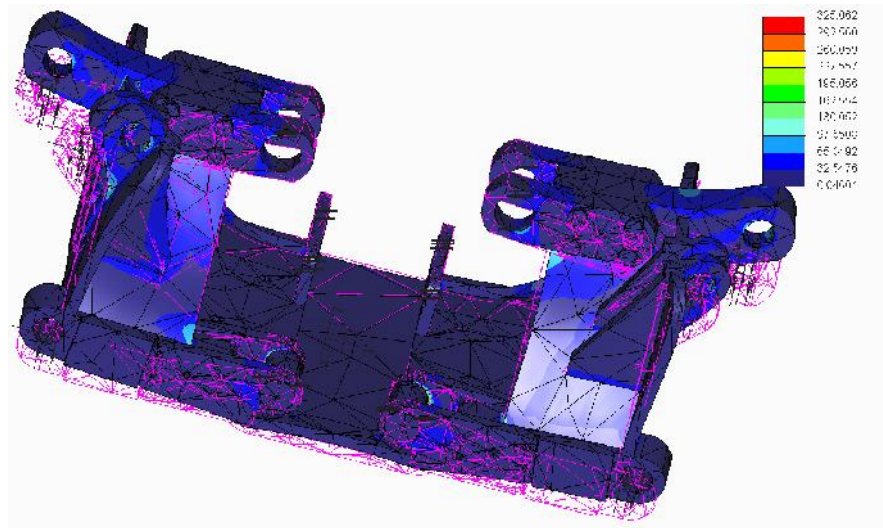


Figure 7.9: Deformed modified axle model

After running the analysis, the results of the analysis were viewed and processed by opening the Review results of a design Study or Finite Element Analysis which brought up the Results Window definition. In this window, display type, quantity, display location and display options were defined. Fringe display type was selected for most of the analysis in this study and stress and displacement were also defined as quantities of measure. The results obtained for different loading cases are discussed under section 7.1.7 are shown and discussed in the next chapter.

## 8.0 Results and Discussions

Results of analysis of different loading cases were analysed for high stress levels and displacements. The results are discussed below for each separate case.

### 8.1 Loading case 1

In this analysis the following loads shown in table below were applied as discussed under section 7.1 Pre-processing. Vertical loads of 27.1 kN were applied at the outer edges of modified axle.

Loading Case/Test	Mounting/Wheel A Loads (kN)			Mounting/Wheel B Loads (kN)		
	$F_x$	$F_y$	$F_z$	$F_x$	$F_y$	$F_z$
Test 1	0	27.1	0	0	27.1	0

Table 8.1: Loading case 1.

The Figure 8.1 below shows the plots of the stress distribution in the model due to the above applied loading. The two plots basically show the different view angles of the stress distribution. The maximum stress under these loading conditions is 220 MPa.

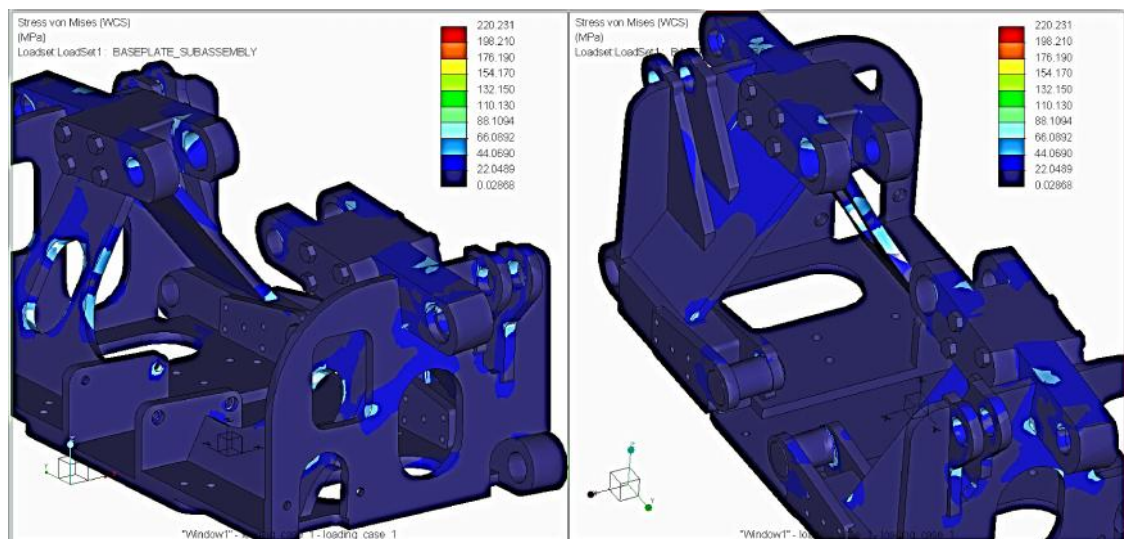


Figure 8.1: Loading case 1 Von Mises Stress plot.

The area of high stress was identified to be the section on the underside of the model at the contact area between the baseplate component 0011RIGHT and component 26R. This localised area of high stress could be a result of some interference of the components which has not been picked up in the quick check analysis due to its small size or nature. In the Simulation diagnostics there was a warning that one or more measures were evaluated at (or close to) results singularities and the results may be inaccurate. This area was ignored as it did not pose any failure and the high stress in this localised area is below the yield stress anyway. Other than this localised area of high stress all other sections of the model have a maximum stress level of around 88 MPa which was way below the yield strength of the material. For this analysis the yield strength had been determined to be the critical parameter. The magnification of the area is shown in Figure 8.2 below.

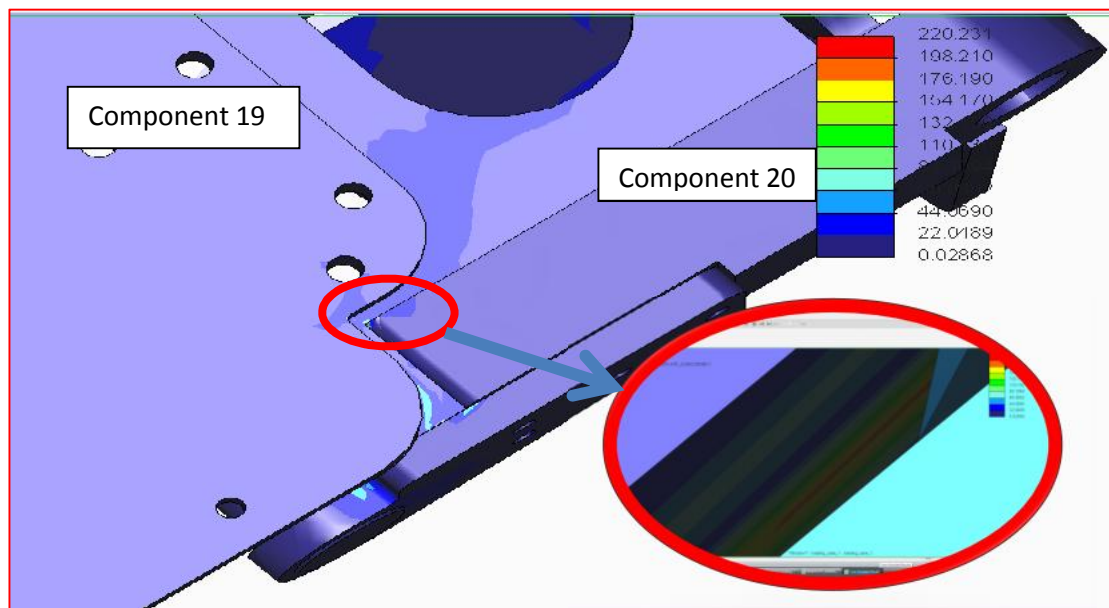


Figure 8.2: Identified area of high stress

Factor of safety against yield for this analysis was determined as

$$\frac{\text{Yield Stress}}{\text{Actual Stress}} = \frac{\sigma_y}{\sigma_a} = \frac{350}{88} = 4.0$$

Factor of safety against fracture for this analysis was determined as

$$\frac{\text{Ultimate Stress}}{\text{Actual Stress}} = \frac{\sigma_u}{\sigma_a} = \frac{420}{88} = 4.7$$

Displacement results showed a maximum displacement of 0.33mm at the areas colour coded red Displacement plot in Figure 8.3 below. The graphs in Figure 8.4 show the actual areas that were subjected to maximum displacements.

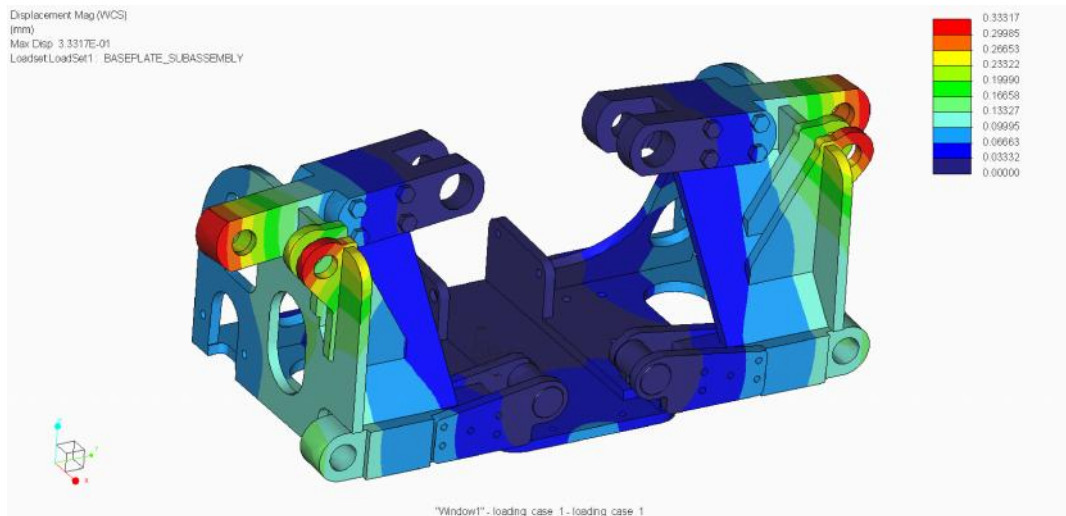


Figure 8.3: Displacement plot for loading case 1.

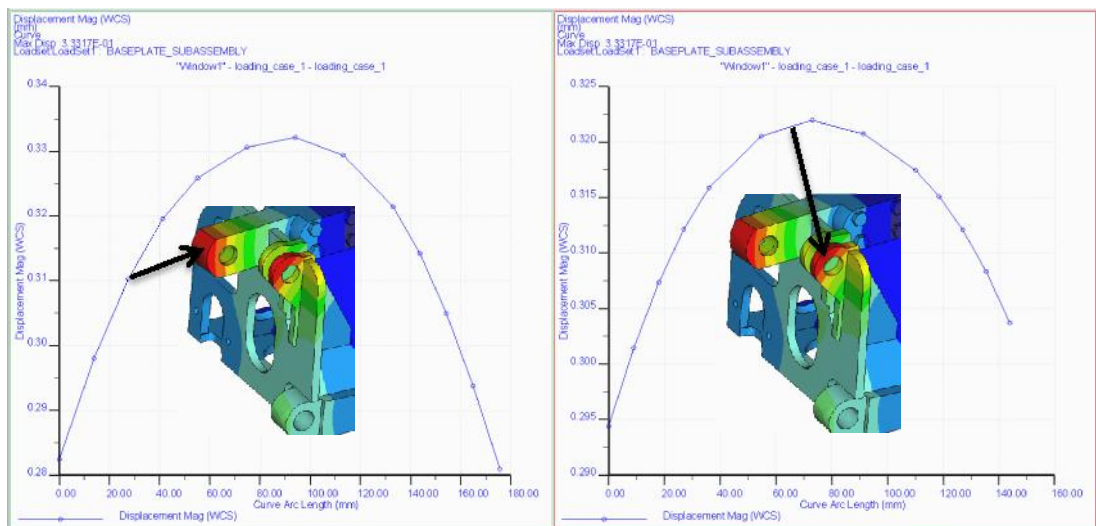


Figure 8.4: Displacement graph for loading case 1.

The graphs in Figure 8.4 show the maximum displacement for the sections indicated by the respective arrows.

### Summary of Analysis

Memory and Disk Usage:	
Machine Type:	Windows Vista Service Pack 2
RAM Allocation for Solver (megabytes):	512.0
Total Elapsed Time (seconds):	734.99
Total CPU Time (seconds):	357.80
Maximum Memory Usage (kilobytes):	1168864
Working Directory Disk Usage (kilobytes):	14707712
Results Directory Size (kilobytes):	455043 .\Analysis7 1801216

Table 8.2: Computer Memory and Disk Usage

## 8.2 Loading case 2

In this analysis the following loads shown in table below were applied as discussed under section 7.1 Pre-processing. A vertical load of 27.1 kN was applied at one end of modified axle model and another vertical load of 50 kN was applied to the other end to simulate the tractor driving over a hump.

	Mounting/Wheel A Loads			Mounting/Wheel B Loads		
	(kN)			(kN)		
Loading Case/Test	F <sub>x</sub>	F <sub>y</sub>	F <sub>z</sub>	F <sub>x</sub>	F <sub>y</sub>	F <sub>z</sub>
Test 2	0	27.1	0	0	50.0	0

Table 8.2: Loading case 2.

The Figure 8.5 below shows the plots of the stress distribution in the model due to the above applied loading. Different view angles are represented in the stress distribution plots. The maximum stress under these loading conditions was found to be 302 MPa. The controlling mode of failure for this analysis was fracture mode as discussed under section 4.4.

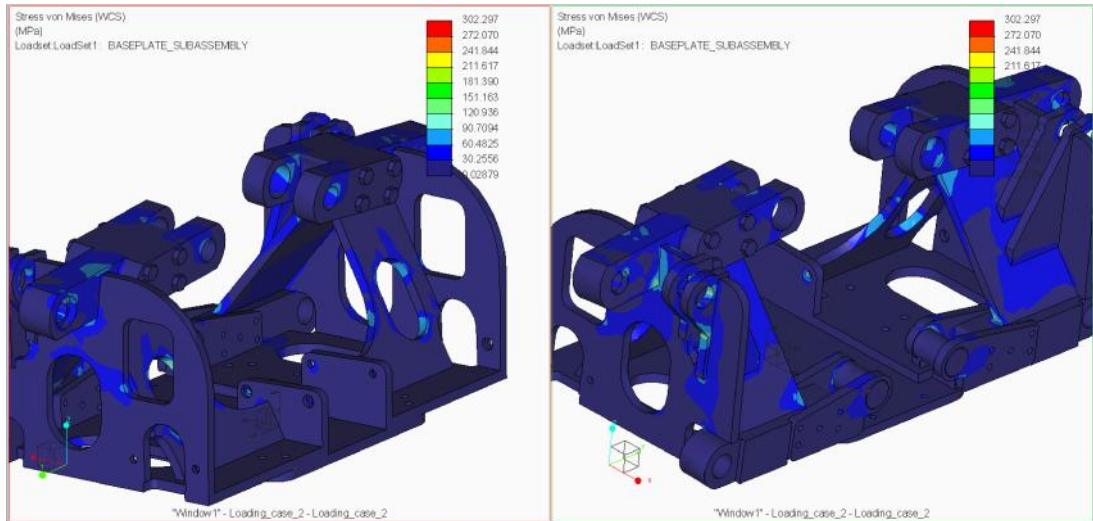


Figure 8.5: Loading case 2 Von Mises Stress plot.

There was a localised area of this high stress on the edge of the hole in component 12. The high stress was due to high loading conditions and geometry of the component. The high stress was on the end where a load of 50 kN was applied. Other than this localised area of high stress all other sections of the model have a maximum stress level of around 185 MPa which was way below the yield and ultimate strength of the material. For this analysis the ultimate strength had been determined to be the critical parameter. The magnification of the area of high stress is shown in Figure 8.6 below.

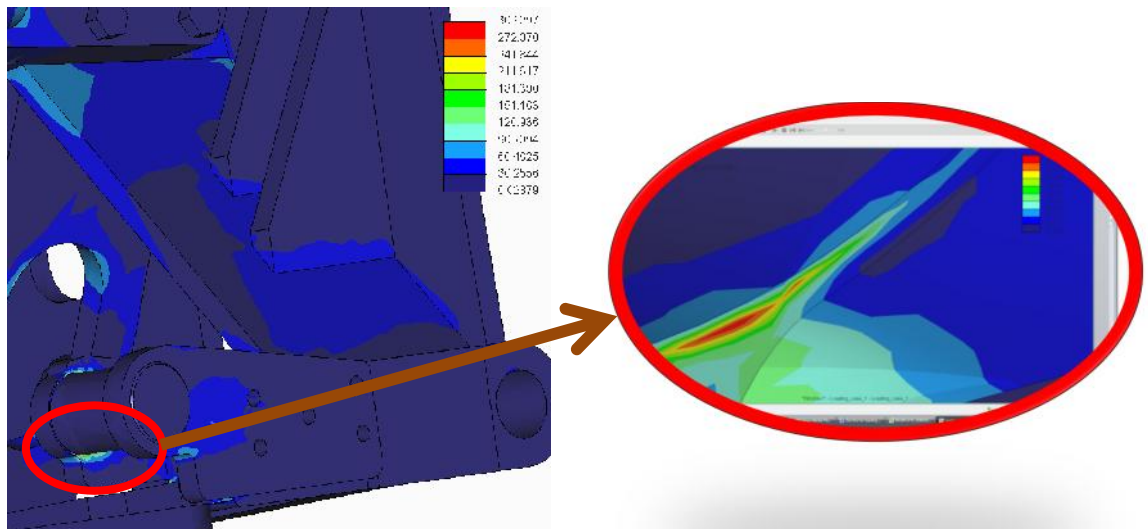


Figure 8.6: Identified area of high stress

Factor of safety against yield for this analysis was determined as

$$\frac{\text{Yield Stress}}{\text{Actual Stress}} = \frac{\sigma_y}{\sigma_a} = \frac{350}{302} = 1.16$$

Factor of safety against fracture for this analysis was determined as

$$\frac{\text{Ultimate Stress}}{\text{Actual Stress}} = \frac{\sigma_u}{\sigma_a} = \frac{420}{302} = 1.4$$

Displacement results showed a maximum displacement of 0.597mm at the area colour coded red in the displacement plot in Figure 8.7 below. The graph in Figure 8.8 shows the graph and the actual areas that were subjected to maximum displacements.

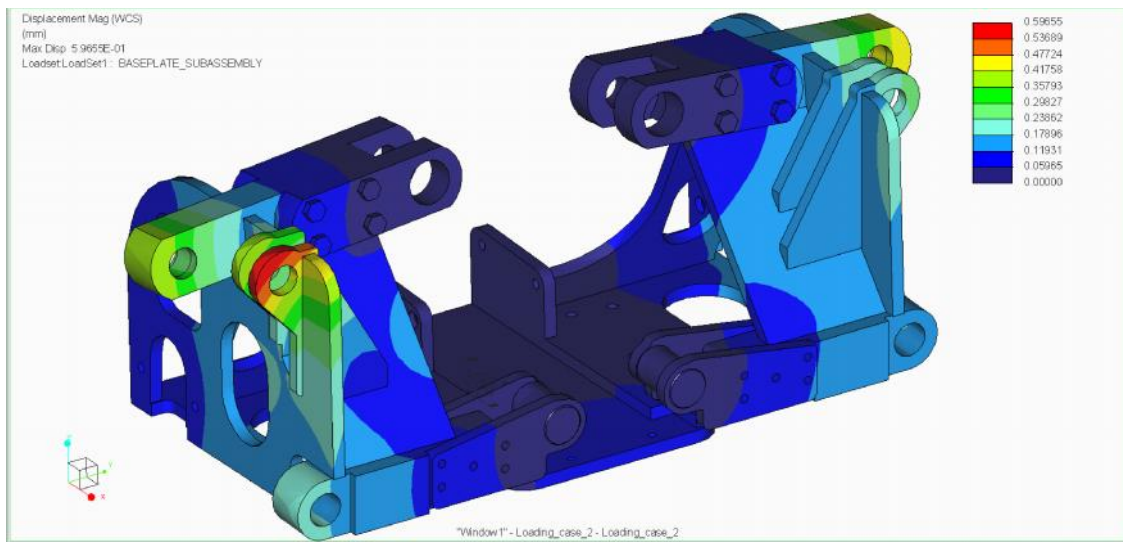


Figure 8.7: Displacement plot for loading case 2.

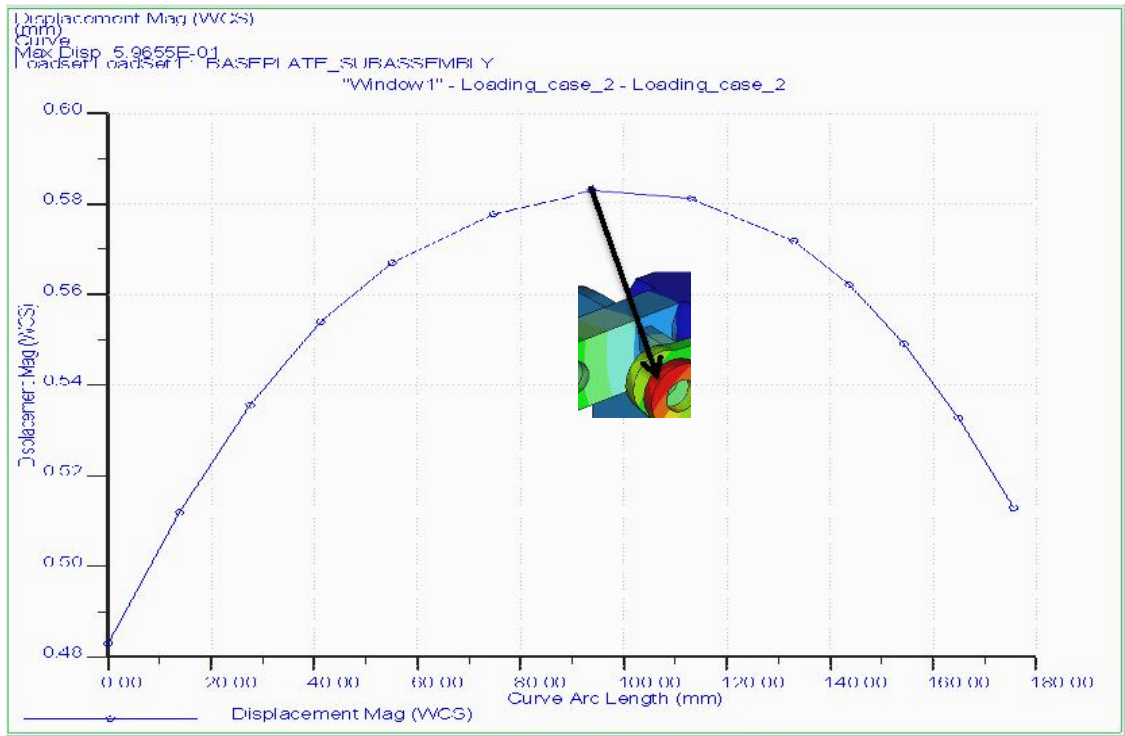


Figure 8.8: Displacement graph for loading case 1.

### 8.3 Loading case 3

In this analysis the following loads shown in table below were applied as discussed under section 7.1 Pre-processing. A vertical load of 27.1 kN was applied at one end of the model and 38.9 kN on the other end. A lateral or side load of 15.5 kN was also applied on both ends but in the same direction.

	Mounting/Wheel A Loads			Mounting/Wheel B Loads		
	(kN)			(kN)		
Loading Case/Test	F <sub>x</sub>	F <sub>y</sub>	F <sub>z</sub>	F <sub>x</sub>	F <sub>y</sub>	F <sub>z</sub>
Test 3	15.5	27.1	0	15.5	38.9	0

Table 8.3: Loading case 3.

The Figure 8.9 below shows the plots of the stress distribution in the model due to the above applied loading conditions. The two plots basically show the different view angles of the stress distribution. The maximum stress under these loading conditions was found to be 332 MPa.

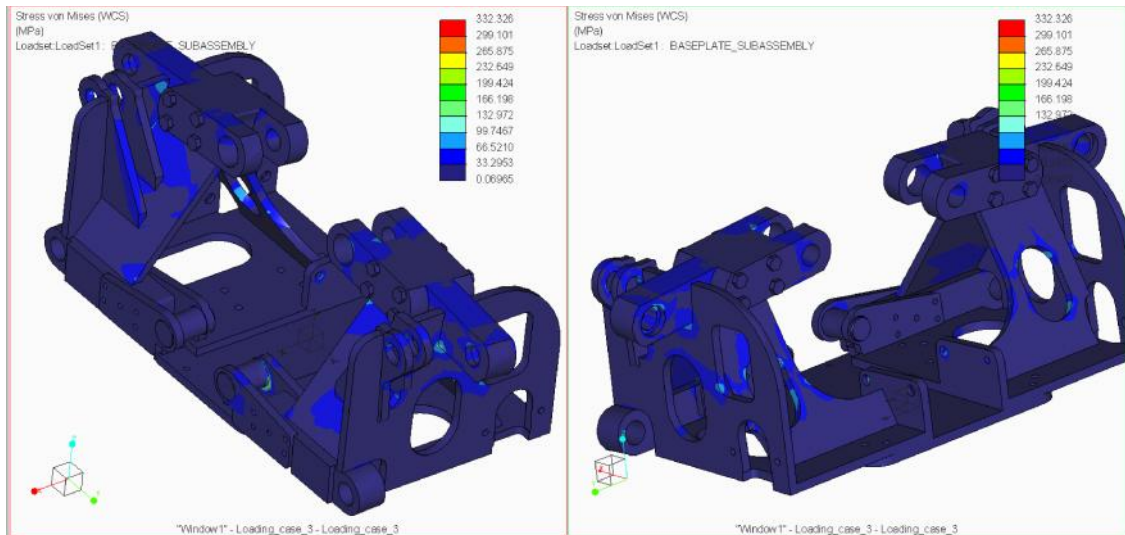


Figure 8.9: Loading case 3 Von Mises Stress plot

There was a localised area of this high stress on the edge of the hole in component 12. The same area showed high stress as in loading case 2. The high stress was due to high loading conditions and geometry of the component. The high stress was on the end where a load of 38.9 kN was applied. The increase in stress levels were also attributed to additional lateral loading that was applied to the model. Other than this localised area of high stress all other sections of the model have a maximum stress level of around 200 MPa which was below the yield and ultimate strength of the material. For this analysis the yield strength was determined to be the critical parameter.

Figure 8.10 shows the magnified area of high stress.

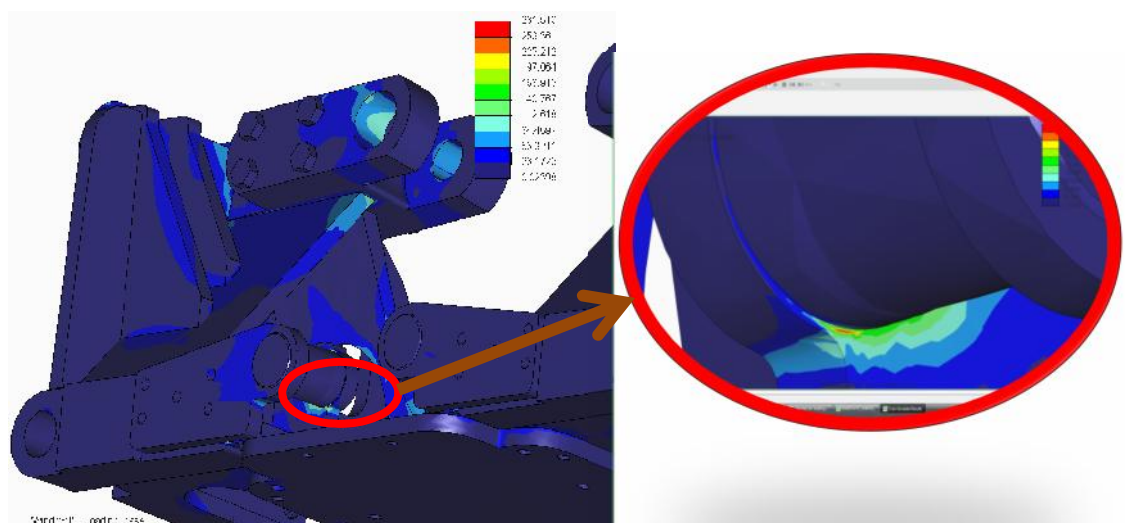


Figure 8.10: Identified area of high stress

Factor of safety against yield for this analysis was determined as

$$\frac{\text{Yield Stress}}{\text{Actual Stress}} = \frac{\sigma_y}{\sigma_a} = \frac{350}{332} = 1.05$$

Factor of safety against fracture for this analysis was determined as

$$\frac{\text{Ultimate Stress}}{\text{Actual Stress}} = \frac{\sigma_u}{\sigma_a} = \frac{420}{332} = 1.27$$

Displacement results showed a maximum displacement of 0.56 mm at the areas colour coded red. Displacement plot and graphs are represented in Figure 8.11 and Figure 8.12 below. The graphs in Figure 8.11 also indicate the actual areas that were subjected to maximum displacements.

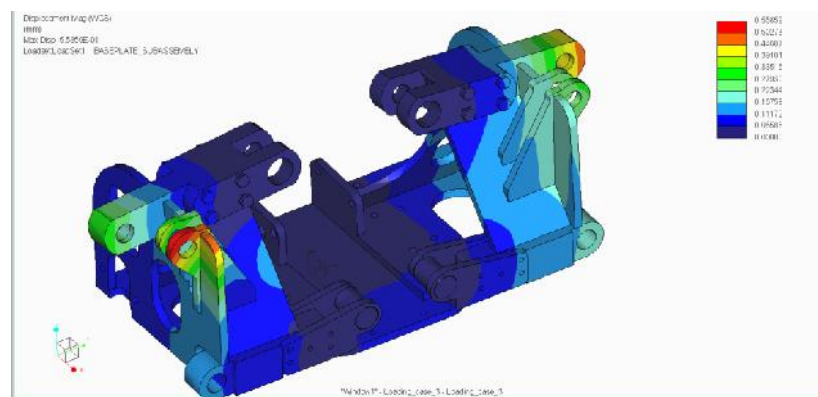


Figure 8.11: Displacement plot for loading case 3.

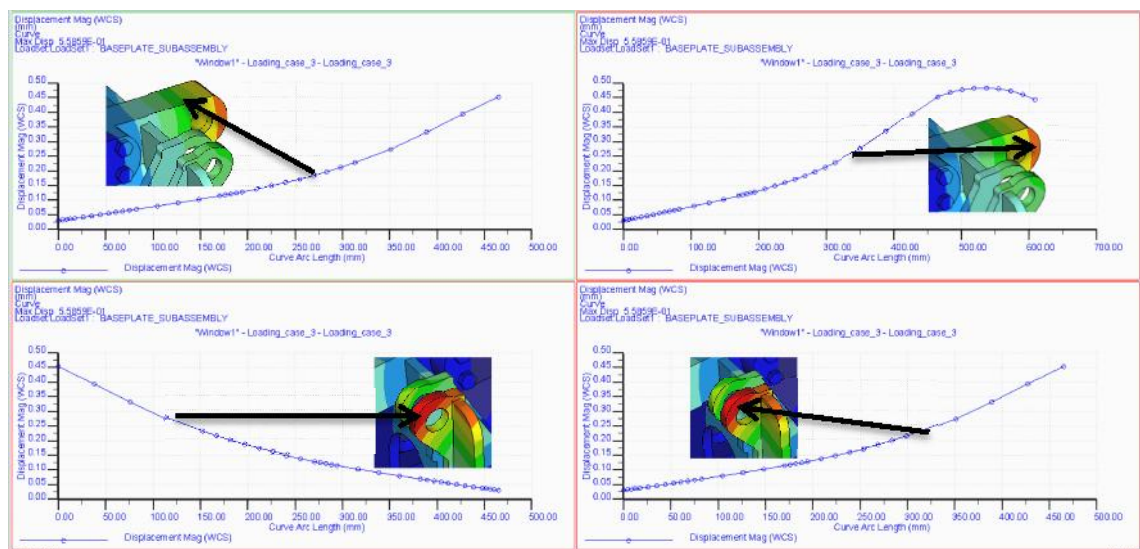


Figure 8.12: Displacement plot for loading case 3.

## 8.4 Loading case 4

In this fourth analysis the following loads shown in Table 8.4 below were applied as discussed under section 7.1 Pre-processing. Vertical load of 38.9 kN and a horizontal load of 7.5 kN were applied on both ends of the axle model.

Loading Case/Test	Mounting/Wheel A Loads			Mounting/Wheel B Loads		
	(kN)			(kN)		
	$F_x$	$F_y$	$F_z$	$F_x$	$F_y$	$F_z$
Test 4	0	38.9	7.5	0	38.9	7.5

Table 8.4: Loading case 4.

The Figure 8.13 below shows the plots of the stress distribution in the model due to the above applied loading. The two plots as in the previous discussions basically show the different view angles of the stress distribution. The maximum stress under these loading conditions is 307 MPa.

There was a localised area of this high stress in the same area as in loading case 1. The localised high stress area was on the boundaries of the interface where components 18 and 20 are bonded. Other than this localised area of high stress all other sections of the model have a maximum stress level of around 200 MPa which was below the yield and ultimate strength of the material. This maximum was located around the periphery of hole in component 11. For this analysis the yield strength was determined to be the critical parameter.

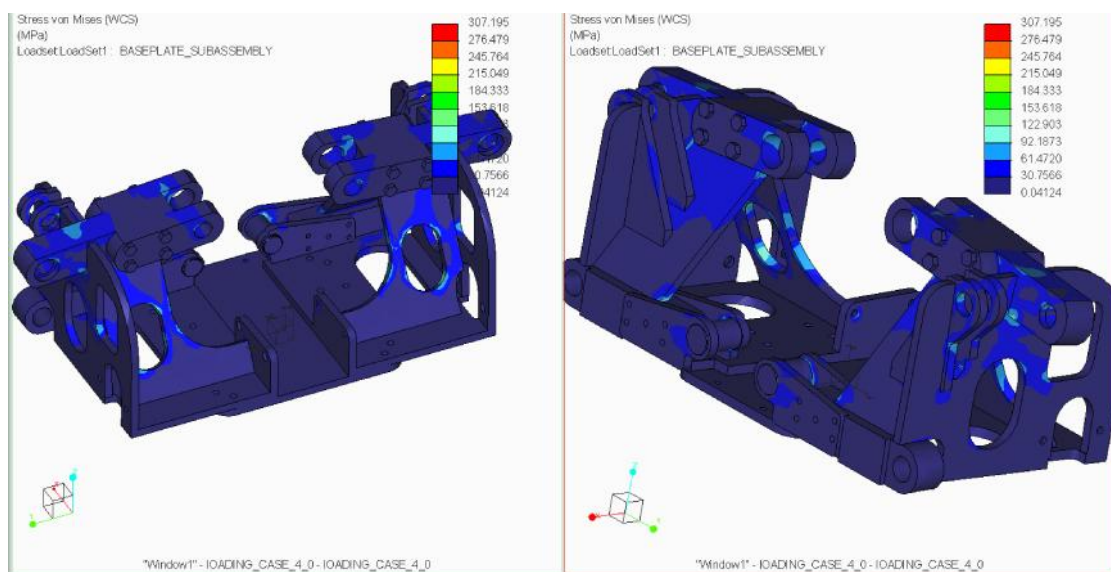


Figure 8.13: Loading case 4 Von Mises Stress plot.

The localised high stress of 307 MPa could be a result of some interference of the components which has not been picked up in the quick check analysis due to its small size or nature. The magnification of the high stress area is shown in Figure 8.14 below. For calculations of factor of safety stress of 200 MPa was used.

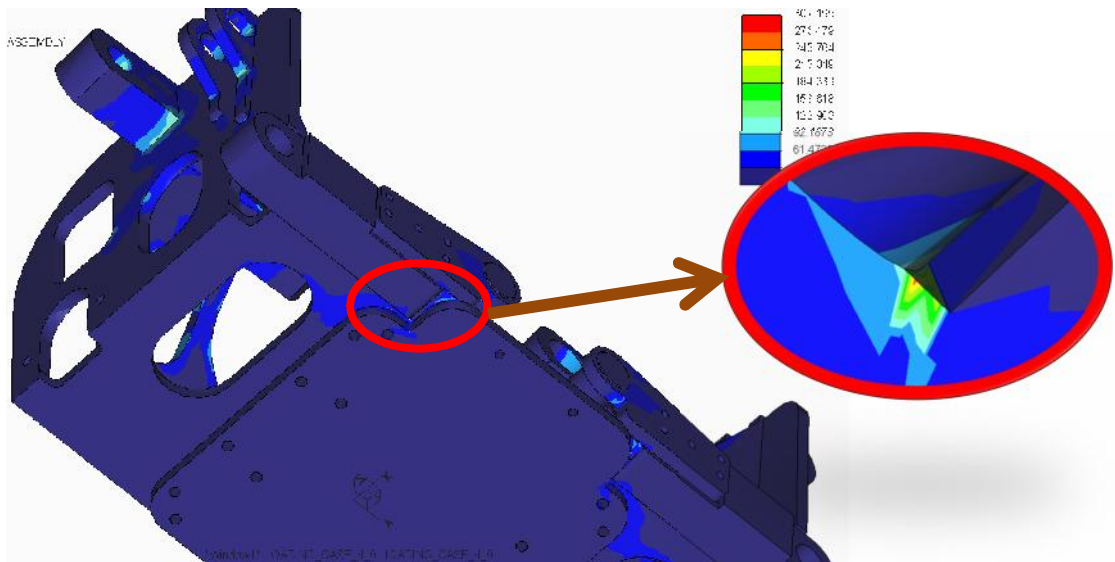


Figure 8.14: Identified area of high stress

Factor of safety against yield for this analysis was determined as

$$\frac{\text{Yield Stress}}{\text{Actual Stress}} = \frac{\sigma_y}{\sigma_a} = \frac{350}{307} = 1.14$$

Factor of safety against fracture for this analysis was determined as

$$\frac{\text{Ultimate Stress}}{\text{Actual Stress}} = \frac{\sigma_u}{\sigma_a} = \frac{420}{307} = 1.37$$

Displacement results showed a maximum displacement of 0.47 mm at the areas colour coded red in the displacement plot in Figure 8.15 below.

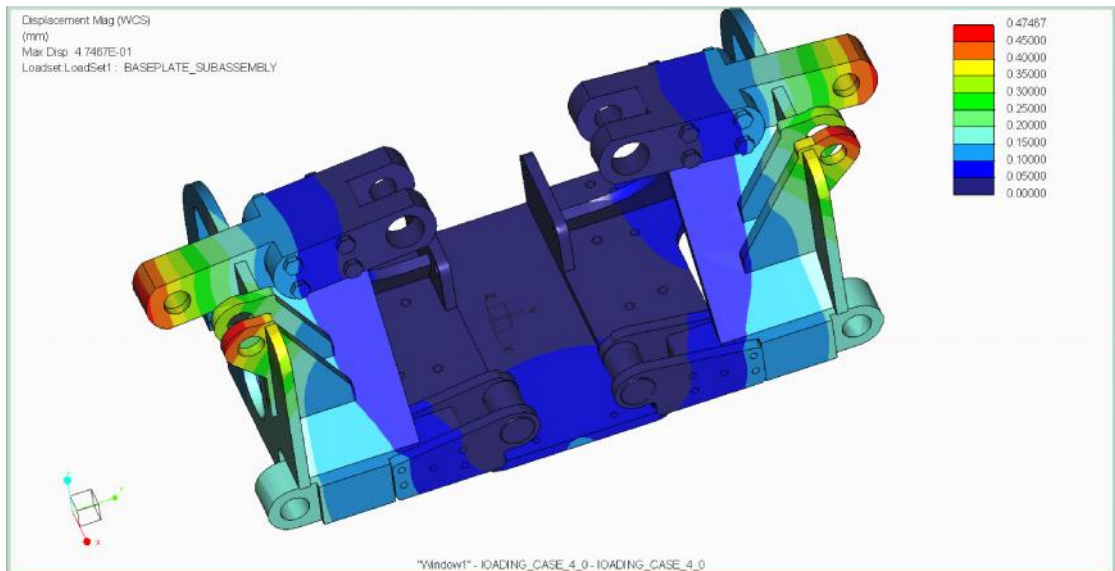


Figure 8.15: Displacement plot for loading case 4.

The graph in Figure 8.16 shows the actual area that was subjected to maximum displacement.

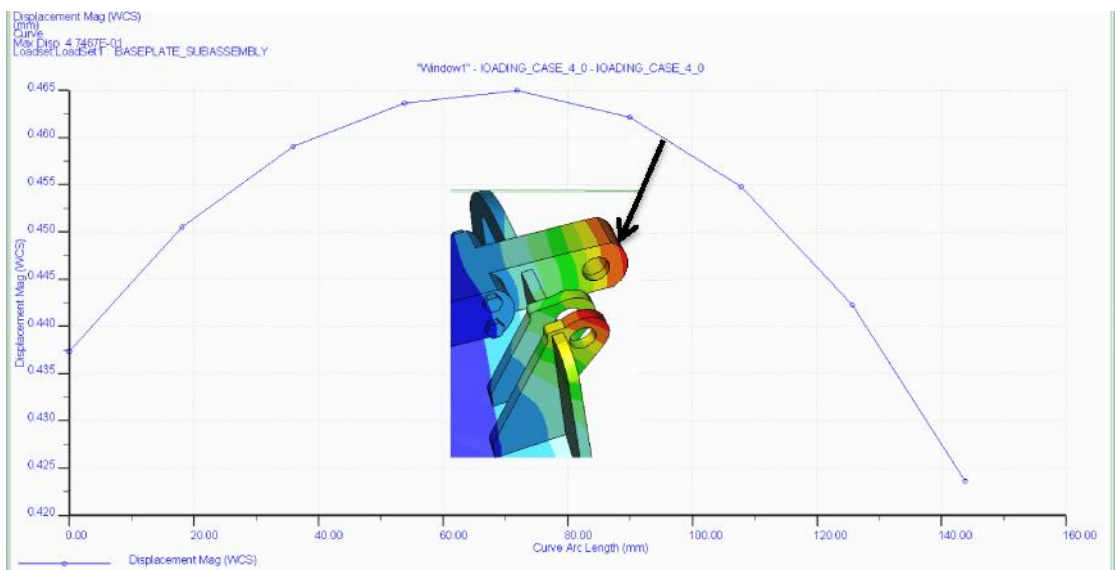


Figure 8.16: Displacement graph for loading case 4.

## 8.5 Worst case loading-case 5

In the final worst case loading analysis the following loads shown in Table 8.5 below were applied as discussed under section 7.1 Pre-processing. The maximum loads

applied in the previous analysis were combined to give a worst case scenario. Vertical load of 38.9 kN, horizontal load of 7.5 kN and a lateral load of 15.5 kN were applied on both ends of the axle model.

	Mounting/Wheel A Loads (kN)			Mounting/Wheel B Loads (kN)		
Loading Case/Test	F <sub>x</sub>	F <sub>y</sub>	F <sub>z</sub>	F <sub>x</sub>	F <sub>y</sub>	F <sub>z</sub>
Test 5 (Worst case)	15.5	38.9	7.5	15.5	38.9	7.5

Table 8.5: Loading case 5.

The Figure 8.17 below shows the plots of the stress distribution in the model due to the above applied loading. The two plots basically show the different view angles of the stress distribution. The maximum stress under these loading conditions was determined to be 302 MPa.

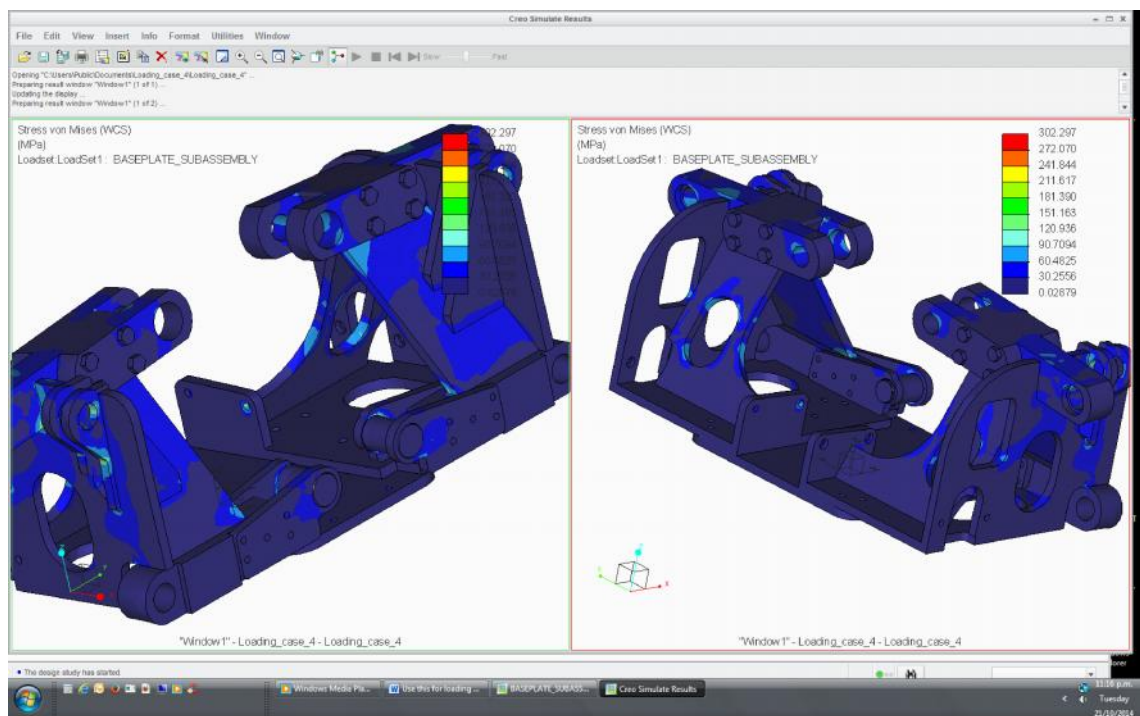


Figure 8.17: Loading case 5 Von Mises Stress plot.

There was a localised area of this high stress on the edge of the hole in component 12 as in loading case 2. The high stress was due to high loading conditions and geometry of the component. The increase in stress levels are was also attributed to additional lateral and horizontal loadings applied to the model. Other than this localised area of high

stress all other sections of the model have a maximum stress level of around 168 MPa which was below the yield and ultimate strength of the material. For this analysis the yield strength was determined to be the critical parameter. This magnification of the area of high stress is shown in Figure 8.18 below.

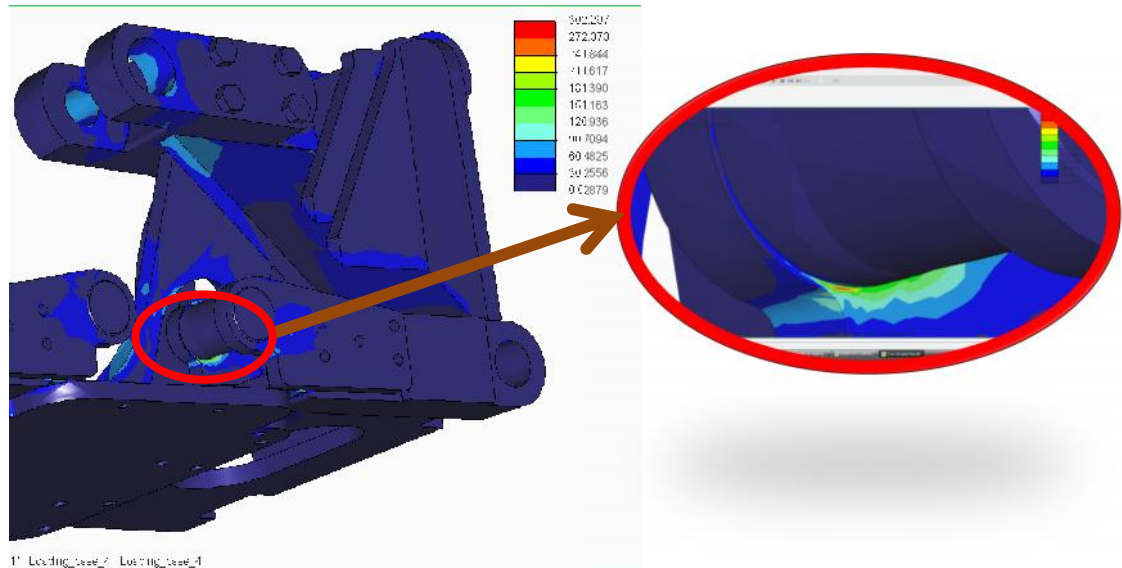


Figure 8.18: Identified area of high stress

Factor of safety against yield for this analysis was determined as

$$\frac{\text{Yield Stress}}{\text{Actual Stress}} = \frac{\sigma_y}{\sigma_a} = \frac{350}{302} = 1.16$$

Factor of safety against fracture for this analysis was determined as

$$\frac{\text{Ultimate Stress}}{\text{Actual Stress}} = \frac{\sigma_u}{\sigma_a} = \frac{420}{302} = 1.4$$

Displacement results showed a maximum displacement of 0.597 mm at the areas colour coded red Displacement plot in Figure 8.3 below. The graphs in Figure 8.4 show the actual areas that were subjected to maximum displacements.

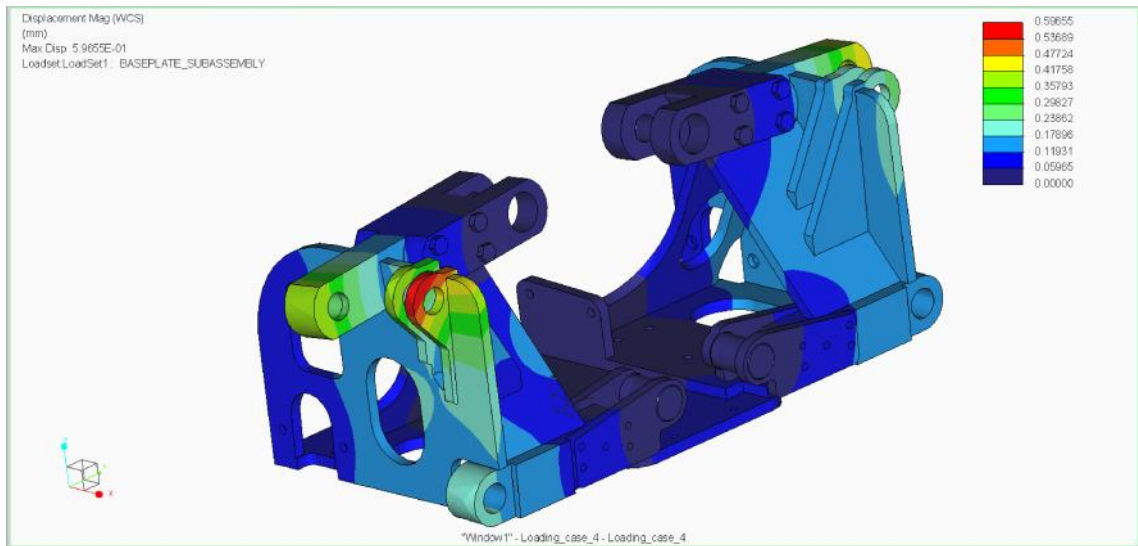


Figure 8.19: Displacement plot for loading case 5.

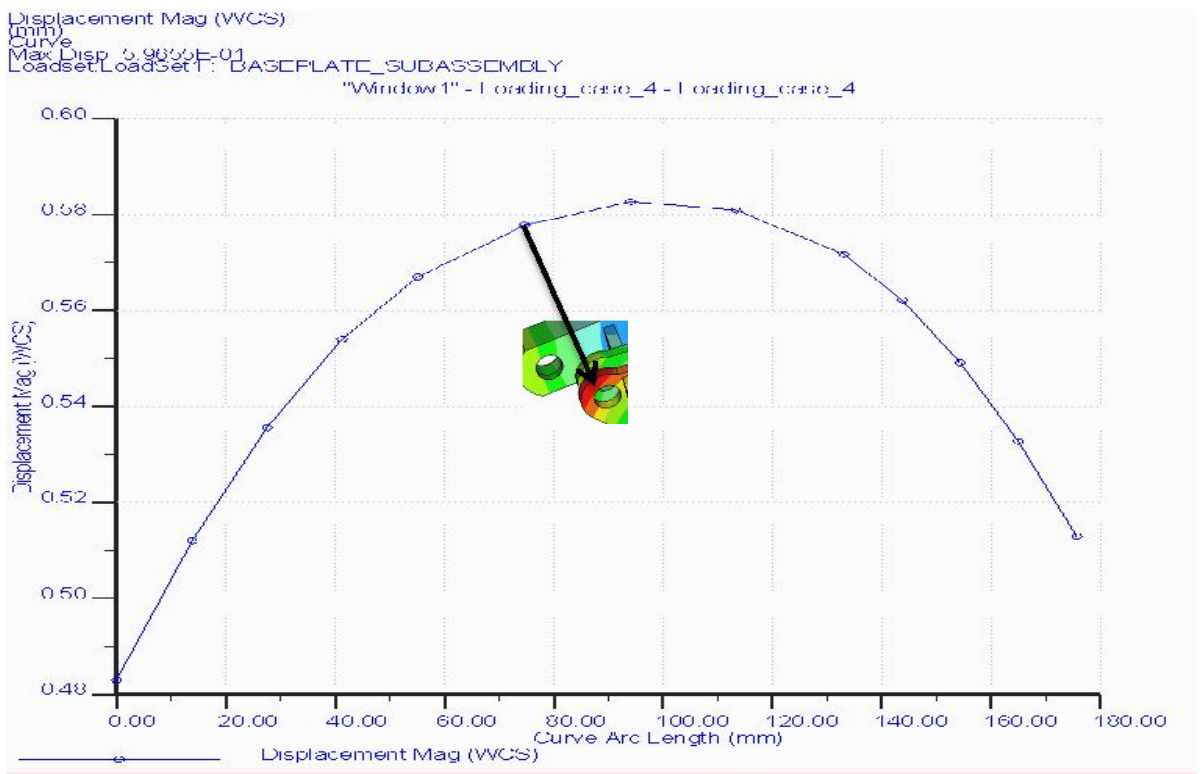


Figure 8.20: Displacement graph for loading case 5.

## 8.6 Convergence of results

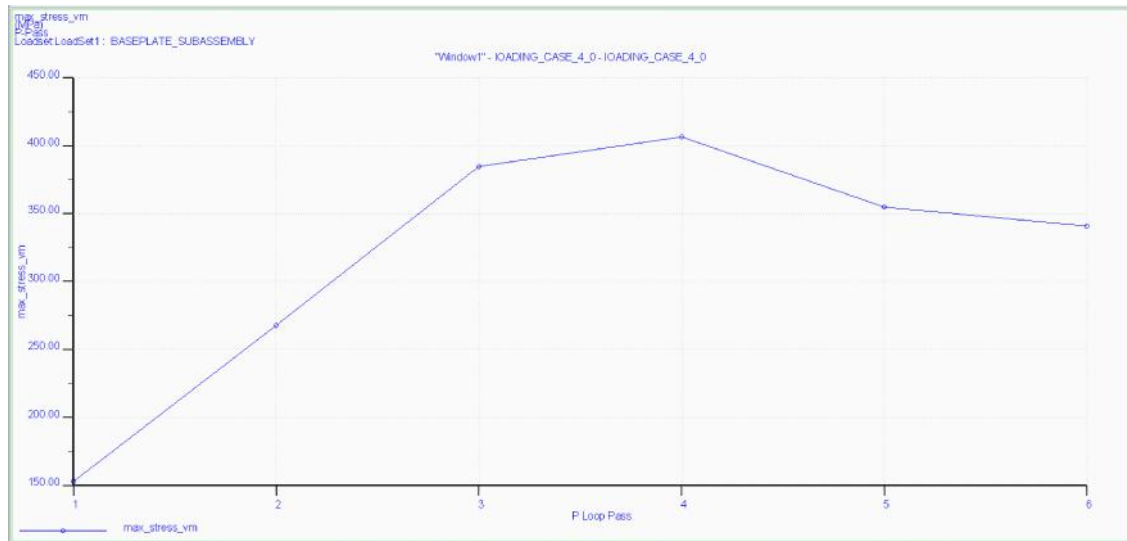


Figure 8.21: Convergence graph

The convergence for the analysis was set at 5% and the polynomial order was set at maximum of 9. The graph in Figure 8.21 shows that the result of this particular analysis converged at the sixth pass and the results can certainly be relied on.

## 9.0 Conclusions and suggestions for future work

Conclusions were drawn based on the results outline in Chapter 8 and a summary of results and loads applied is shown in the table below.

	Mounting/Wheel A Loads			Mounting/Wheel B Loads		
	(kN)			(kN)		
Loading Case/Test	F <sub>x</sub>	F <sub>y</sub>	F <sub>z</sub>	F <sub>x</sub>	F <sub>y</sub>	F <sub>z</sub>
Test 1	0	27.1	0	0	27.1	0
Test 2	0	27.1	0	0	50.0	0
Test 3	15.5	27.1	0	15.5	38.9	0
Test 4	0	38.9	7.5	0	38.9	7.5
Test 5 (Worst case)	15.5	38.9	7.5	15.5	38.9	7.5

Loading Case/Test	Max Von Mises Stress (MPa)	Maximum Displacement (mm)	FOS (Yield)	FOS (Fracture)
Test 1	220.2	0.33	4	4.7
Test 2	302	0.597	1.16	1.4
Test 3	332	0.56	1.05	1.27
Test 4	307	0.47	1.16	1.37
Test 5 (Worst case)	302	0.597	1.16	1.4

Table 8.1: Summary of Von Mises stress, displacements and factor of safety

- Loading case 1 – Loading conditions for this case are safe as the factor of safety is more than twice the nominal factor of safety calculated for the model. The factor of safety calculated for the model using the guide in Appendix G was 1.5.

- Loading case 2 – Due to high loading of 50 kN on one end of the axle, the model just clears the yield threshold. The factor of safety is below the expectation of 1.5. The maximum stress though is still under the yield stress.
- Loading case 3 – The model just like in loading case 2 the factor of safety is below the expectation of 1.5. The maximum stress is just under the material's yield stress of 350 MPa.
- Loading case 4 – For this loading case, the model again just clears the yield threshold. The factor of safety is below the expectation of 1.5. The maximum stress though is still under the yield stress.
- Loading case 5 – the model just clears the yield threshold. The factor of safety is below the expectation of 1.5. The maximum stress though is still under the yield stress.

## 9.1 Conclusions

Generally results for loading cases 2 to 5 were in the same range and they point to some particular problem on the model. Close inspection of results indicated that part of component 12 shown in Figure 9.1 below is likely to fail in cases of extreme overloading.

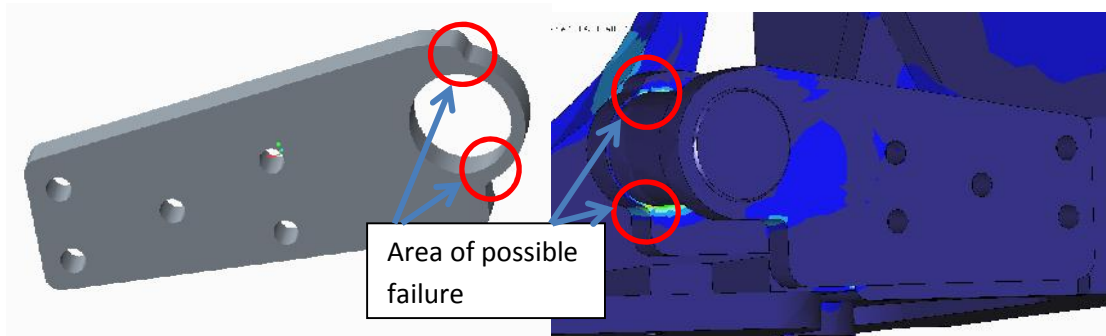


Figure 9.1: Bracket sections susceptible to failure

The area circled in red in Figure 9.1 shows the area that is likely to fail on the modified axle. The overall stress on most parts of the model is reasonably low, generally around 200 MPa and failure is not a possible outcome for these.

The conclusion drawn from these results and the overall analysis of the modified tractor axle was that the chances or likelihood of failure under the loading conditions discussed and applied in this project are low including the bracket identified above to be at risk. The loads used in the analysis are worst case scenario loads and the actual working loads would be much lower. Therefore the loads applied in the analysis are considered to be safe for the modified axle. The working or operating weight of the tractor should not be exceeded and should be used as a guide for safe loading level for the axle.

## 9.2 Recommendations

The general conclusion was that the axle is safe and would not fail under the loading conditions applied in this particular analysis but application of the tractors and where they are used tends to hugely vary. And to guard against any possible failure of component 12 identified due to the unforeseen circumstances it is recommended that the thickness of the plate be increased.

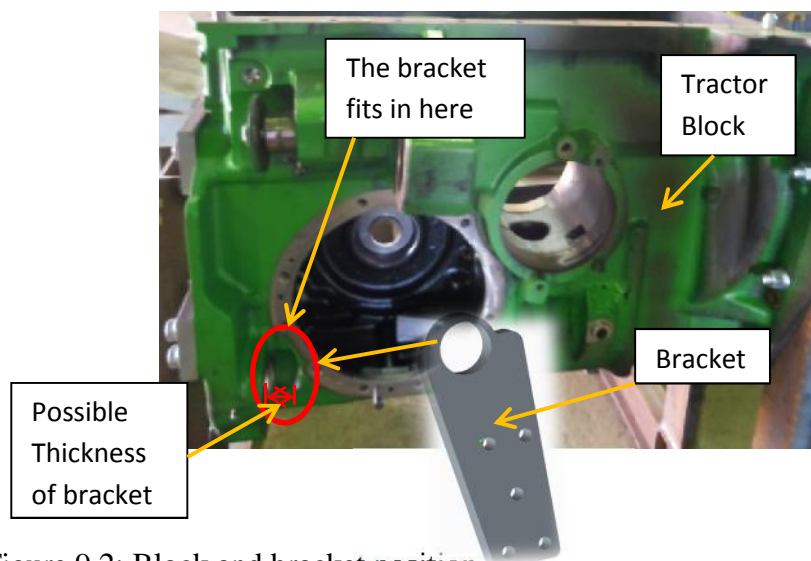


Figure 9.2: Block and bracket position

It has been noted that the profile of the section of the bracket that fits into the area indicated on the block has been made that way with little material because of space limitations. The possible maximum thickness of the bracket is also shown in Figure 9.2 below. The increase in thickness should be done such that it does not interfere or complicate the assembly and disassembly of axle parts.

The second recommendation is on geometry of some of the axle's components. There are few components which by design have to be at a particular angle and contact of those components with those adjacent is minimal. This inadequate contact created meshing problems in the analysis of the model and the solution to that problem can certainly be used to improve the manufacture of the axle. This can ultimately reduce the manufacturing cost and possibly simplify the fabrication process. Recommended geometrical changes of some components are shown in Figure 9.3. The amount of welding that will be required to join the components because of bevels introduced in the components. This will save on welding consumables required and time spent welding the components.

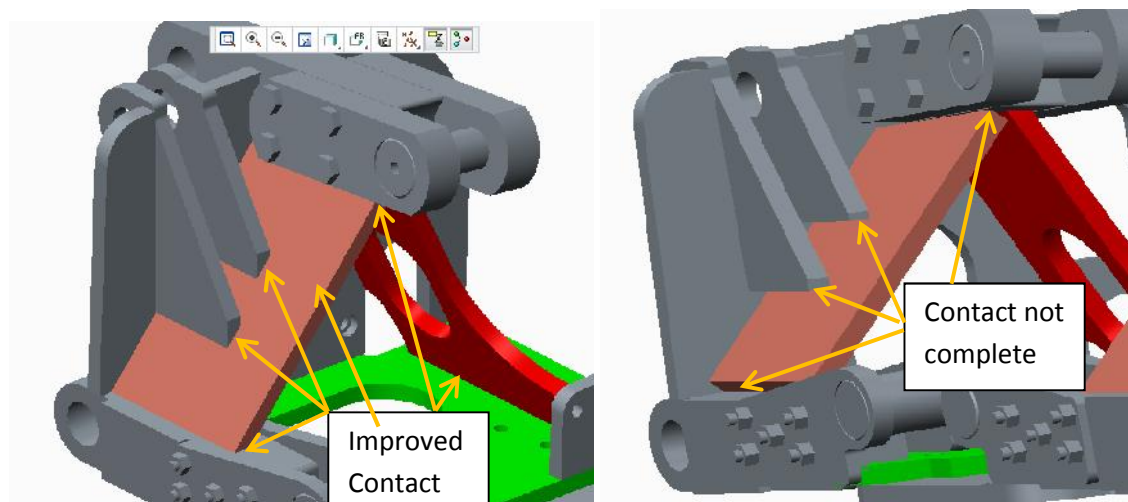


Figure 9.3: Potential component geometry changes

Given the capabilities of modern Laser cutting machines creation or incorporation of bevel edges on the components can be easily accomplished and the models of components created for this research project can be adopted for manufacture.

### 9.3 Future Work

Suggestions for future include creation of a parametric model of the modified axle to suit any similar tractor that might be used for controlled traffic farming. The research would involve identifying the tractors and verifying the axle's configuration to determine if the current model's parameters could be altered to create a parametric model.

The effects of the tractor's independent suspension, linkages such as the wishbones and the tyres were ignored for the purposes of this research project. Complete analysis of the axle including these effects of the tyres and independent suspension on the modified axle is hereby put forward as an area that need further research.

## 10.0 REFERENCES

Adams, V. *Do FEA Tools Give The Same Answers? A Comparison of Finite Element Analysis Software* [ONLINE]. Available at:

[https://www.clear.rice.edu/mech403/FEA/Compare\\_FEA\\_Codes.pdf](https://www.clear.rice.edu/mech403/FEA/Compare_FEA_Codes.pdf) [Accessed 04 May 2014].

AFGRI Equipment South Africa 2014, AFGRI Equipment, Highveld, Centurion, viewed 31 July 2014. <<http://afgri.johndeeredealer.co.za/John-Deere/Agriculture2/Tractors/Row-Crop-Tractors/8R-8RT-Series/8285R-Tractor>>.

Aloni, S & Khedkar, S 2012, 'Comparative Evaluation of Tractor Trolley Axle by Using Finite Element Analysis Approach', *International Journal of Engineering Science and Technology (IJEST)*, Vol. 4 No.04, p. 1351.

AZO Materials United Kingdom 2014, AZO Materials, Macclesfield, Cheshire, viewed 30 July 2014. <http://www.azom.com/article.aspx?ArticleID=6114>

*Ballasting Your Tractor for Performance by Alberta Agriculture & Rural Development* 2013, A practical guide to proper weighting of your tractor, viewed 04 May 2014, <[http://www1.agric.gov.ab.ca/\\$Department/deptdocs.nsf/all/eng5240](http://www1.agric.gov.ab.ca/$Department/deptdocs.nsf/all/eng5240)>.

Bowman, K 2008 'Economic and Environmental Analysis of Converting to Controlled Traffic Farming', *Proceedings of the sixth Australian Controlled Traffic Farming Conference*, Dubbo, New South Wales, pp. 61-68.

*Buyer's guide for FEA software Tips to help you select an FEA solution*, Siemens Software, viewed 20 April 2014, <<http://www.mayahtt.com/wpcontent/uploads/2013/04/Buyers-Guide-for-FEA-Software.pdf>>.

EMCH213D Design in Strength of Materials: Tutorial/Instructional Resources 2014, Pennsylvania State University, Pennsylvania, viewed 17 October 2014, <<http://www.esm.psu.edu>>.

ENG4111 Project Reference Book 2014, University of Southern Queensland,  
Toowoomba.

*Implementing a controlled traffic farming system by Grains Research & Development Corporation* 2013, Controlled traffic farming factsheet, viewed 04 May 2014,  
<<http://www.grdc.com.au/~media/B1422ABEE81649E2BB3895D2D198099F.pdf>>

Jensen, H, G. Jacobsen, L, Pedersen, S, M, Tavella, E 2012, 'Socioeconomic impact of widespread adoption of precision farming and controlled traffic systems in Denmark', *Journal of Precision Agriculture*, vol. 13, no. 6, pp. 661-677.

Koyuncu, A, Gökler, M, & Balkan, T, 2012, 'Development of a design verification methodology including strength and fatigue life prediction for agricultural tractors', *International Journal of Advanced Manufacturing Technology*, vol. 60, no. 5-8, pp. 777-785.

Larocque, S, 2012 *Controlled Traffic Farming*. Canada: Office for Official Publications of the Nuffield Canada.

León, O, N, Martínez, P, Orta C, P. & Adaya 2000, *Reducing the weight of a frontal truck axle beam using experimental test procedures to fine tune FEA*. 2nd Worldwide MSC Automotive Conference. Dearborn, Michigan; October 9-11, 2000 viewed 04 May 2014, <<http://web.mssoftware.com/support/library/conf/auto00/p04300.pdf>>.

Logan, D, L 2007, *The First Course in the Finite Element Method*, Thomson Learning, United States.

Longhurst, B, 2010 *FX-HR Holden Front End Stress Analysis & Geometry Assessment*, Australia: Official Publications of Bremar Automotion Pty Ltd.

Mahanty, D, K Manohar, V, Khomane & B, S, Nayak. S 2002, *Analysis and Weight Reduction of a Tractor's Front Axle*, viewed 04 May 2014,  
<<http://www.ansys.com/staticassets/ANSYS/staticassets/resourcelibrary/confpaper/2002-Int-ANSYS-Conf-106.PDF>>.

Maisuria, M & Patel, D, A 2014 'FE Analysis Of Runner Blade For Small Bulb Turbine', *IOSR Journal of Mechanical and Civil Engineering (IOSR-JMCE)* vol. 11, no. 2, version vii, pp. 73-77.

Neale, T, 2010, *The Cost of Grain Harvester Compaction*, viewed 10 May 2014, <[www.precisionagriculture.com.au/display.php?file=19](http://www.precisionagriculture.com.au/display.php?file=19)>.

Tarighi, J, Mohtasebi, S, S & Alimardani, R 2011, 'Static and dynamic analysis of front axle housing of tractor using finite element methods', *Australian Journal of Agricultural Engineering* vol. 2, no. 2, pp. 45-49.

Toogood, R 2012, *Creo Simulate Tutorial Releases 1.0 & 2.0*, Schroff Development Corporation, Alberta.

Ullman, D, G 2010, *The Mechanical Design Process*, 4th edn, McGraw-Hill, New York, viewed 23 August 2014, <<http://www.scribd.com/doc/116799665/The-Mechanical-Design-Process-David-G-Ullman-4-Edition>>.

# APPENDICES

## APPENDIX A: Project Specification

University of Southern Queensland

ENGINEERING AND BUILT UP ENVIRONMENT

ENG4111/4112 Research Project

### PROJECT SPECIFICATION

FOR: Richard Sambamo.

TOPIC: FEA Analysis of tractor axle modification.

SUPERVISOR: Chris Snook.

SPONSORSHIP: Tractor axle Manufacturer.

PROJECT AIM: To take existing manufacturer's CAD data of a modified tractor axle and perform some robust analysis of the axle under a wider range of load conditions than are feasible through normal field testing. This project seeks to determine maximum safe loading capacities by performing some structural and dynamic analysis through FEA. The analysis will also involve the component under-going interaction with the live suspension system.

PROGRAMME: (Issue A, 12 March 2014)

Review literature on FEA, Dynamic and structural analysis. Also review the literature on previous research work on tractor axle.

Review modified axle Cad files and related standards covering the manufacture of tractor axles.

Create the parametric models of the axle – parameters of the model should be able to be altered to suit different conditions.

Perform static and modal analysis.

Perform a structural and a dynamic analysis.

Critically review the results of the FEA, structural and dynamic analysis.

Recommendations, conclusions and any further work to be undertaken.

AGREED

\_\_\_\_\_ (Student Name) \_\_\_\_\_ (Supervisor Name)

\_\_\_\_\_ (Signature) \_\_\_\_\_ (Signature)

\_\_\_\_ / \_\_\_\_ / \_\_\_\_ (Date)      \_\_\_\_ / \_\_\_\_ / \_\_\_\_ (Date)

## APPENDIX B: Project Timelines

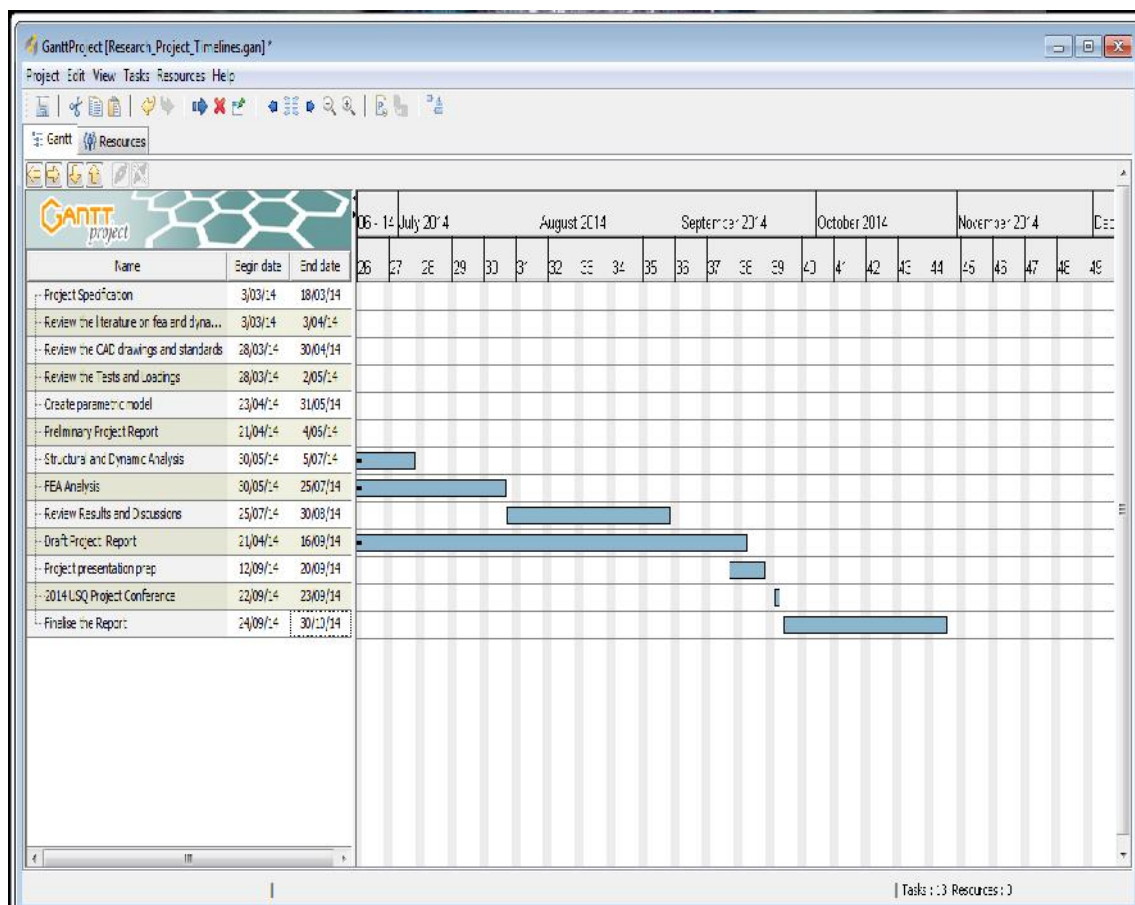
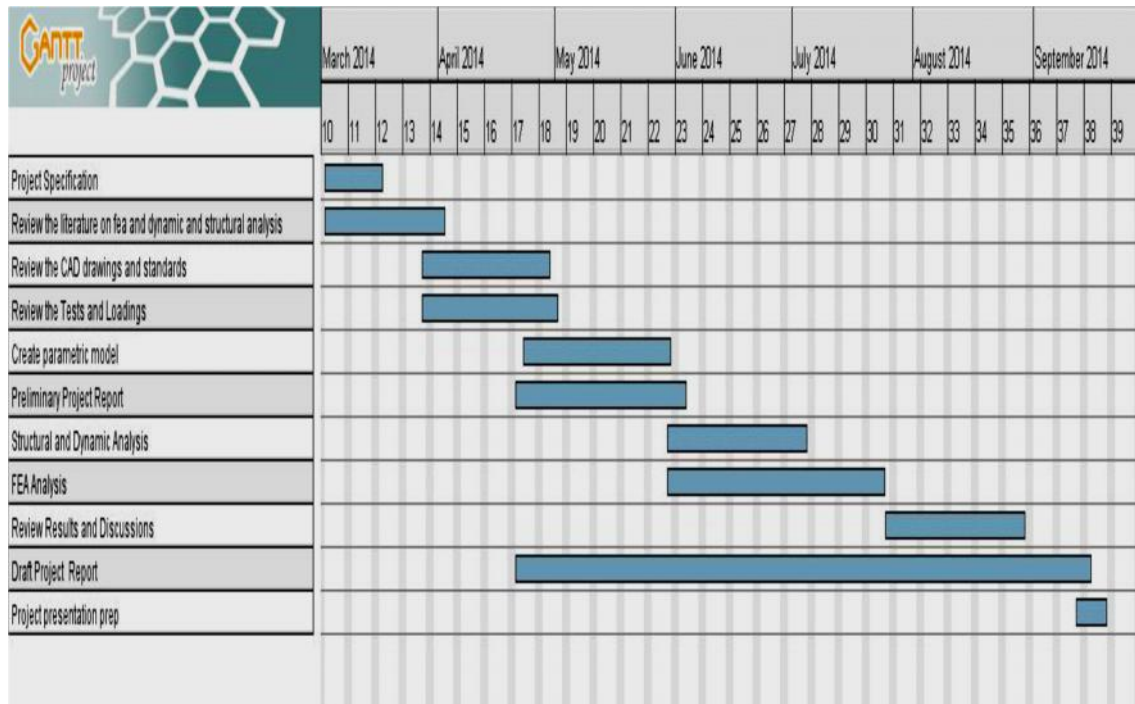
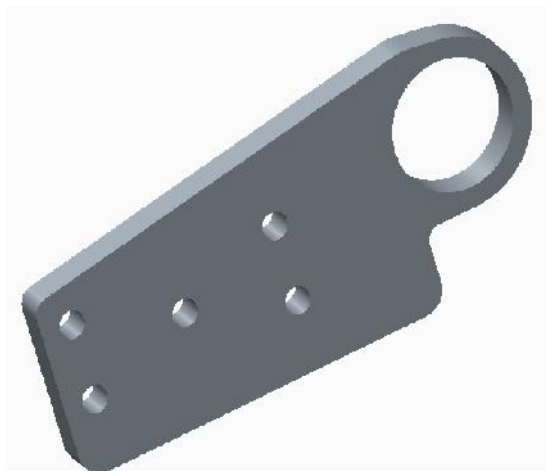
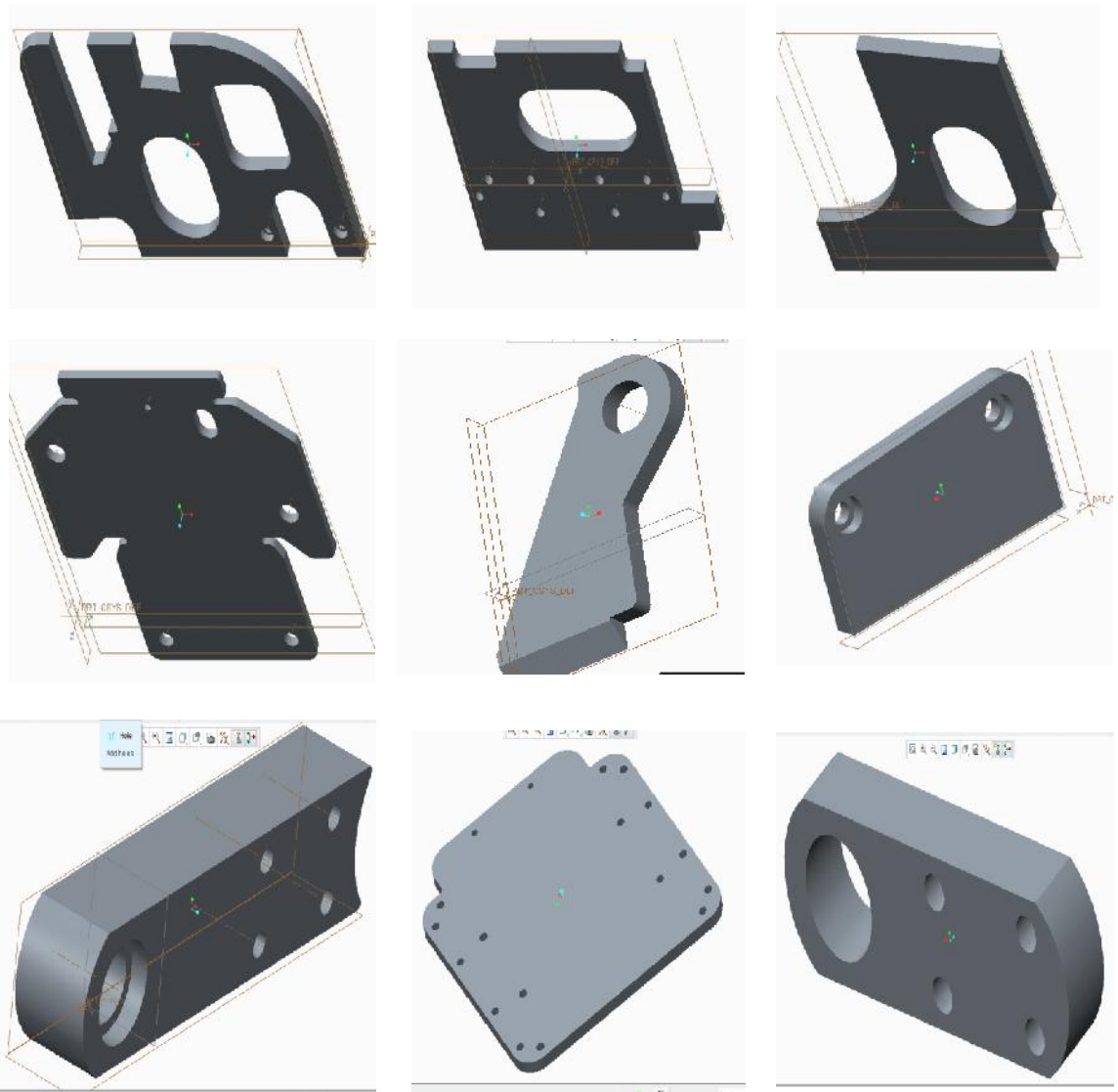


Figure B1: Project Timelines.

**APPENDIX C: 2D DRAWINGS, 3D PART AND ASSEMBLY MODELS**



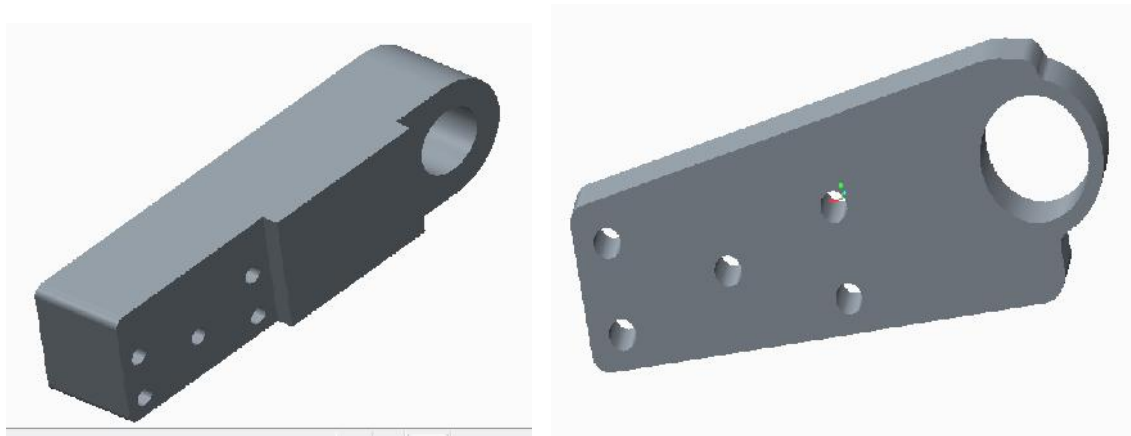


Figure C1: Some examples of modified Axle's components.

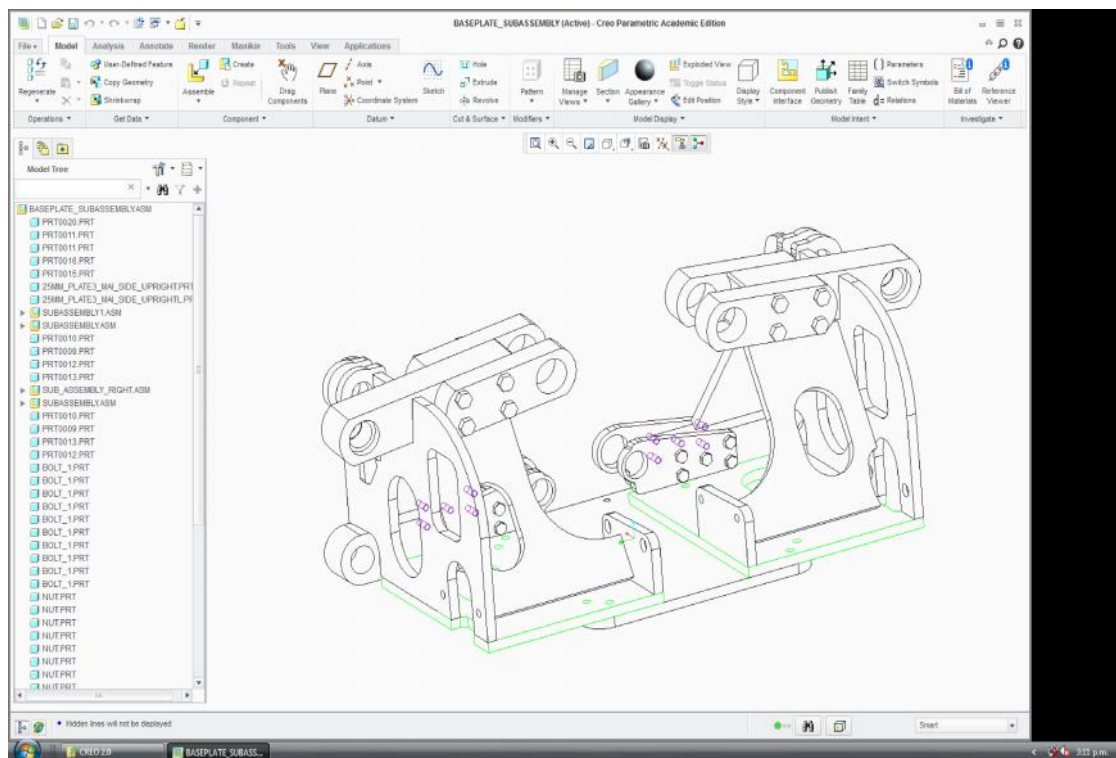


Figure C2: Wireframe model of the modified Axle.

## APPENDIX D: John Deere Tractor Dimensions and Specifications

### John Deere 8530



2006 - 2009 8030 Series

Row-Crop tractor

Previous model: [John Deere 8520](#)

Next model: [John Deere 8345R](#)

Smaller: [John Deere 8430](#)

---

Overview
Engine
Transmission
Dimensions
Photos
Tests

**Production:**

Manufacturer: John Deere

Factory: Waterloo, Iowa, USA

---

**John Deere 8530 Engine:**

John Deere 9.0L 6-cyl diesel

[full engine details ...](#)

---

**Capacity:**

Fuel: 180 gal [681.3 L]

Hydraulic system: 9.5 gal [36.0 L]

14.5 gal [54.9 L] (with aux reservoir)

---

**3-Point Hitch:**

Rear Type: IVN/III

Rear lift (at 24"/610mm): 18,326 lbs [8312 kg]

---

**Power Take-off (PTO):**

Rear PTO: independent

Rear RPM: 1000

540/1000 (optional)

Engine RPM: 540@1817

1000@2000

---

**Dimensions & Tires:**

Wheelbase: 118.9 inches [302 cm]

Weight: 26,800 lbs [12156 kg]

[full dimensions and tires ...](#)

---

**8530 Serial Numbers:**

Location: Rear of tractor

[photo of 8530 serial number](#)

2006: 1001

2007: 10005

2008: 20007

2009: 40000

[how to read serial numbers...](#)

---

**John Deere 8530 Power:**

Engine (gross): 330 hp [246.1 kW]

Engine (max): 360 hp [268.5 kW]

PTO (claimed): 275 hp [205.1 kW]

Drawbar (tested): 240.35 hp [179.2 kW]

PTO (tested): 312.73 hp [233.2 kW]

[power test details ...](#)

---

**Mechanical:**

Chassis: 4x4 Independent Link Suspension (ILS) MFWD 4WD

Steering: hydrostatic power

Brakes: hydraulic wet disc

Cab: CommandView cab standard.

---

**Hydraulics:**

Type: closed center pressure-flow compensating PFC

Capacity: 9.5 gal [36.0 L]

14.5 gal [54.9 L] (with aux reservoir)

Pressure: 2990 psi [206.2 bar]

Valves: 3 to 5

Pump flow: 31.7 gpm [120.0 lpm]

Total flow: 60 gpm [227.1 lpm]

---

**Electrical:**

Ground: negative

Charging: alternator

Figure D.1: John Deere 8530 Tractor information Source(<http://www.tractordata.com>)

## APPENDIX E: Loadings and Constraints

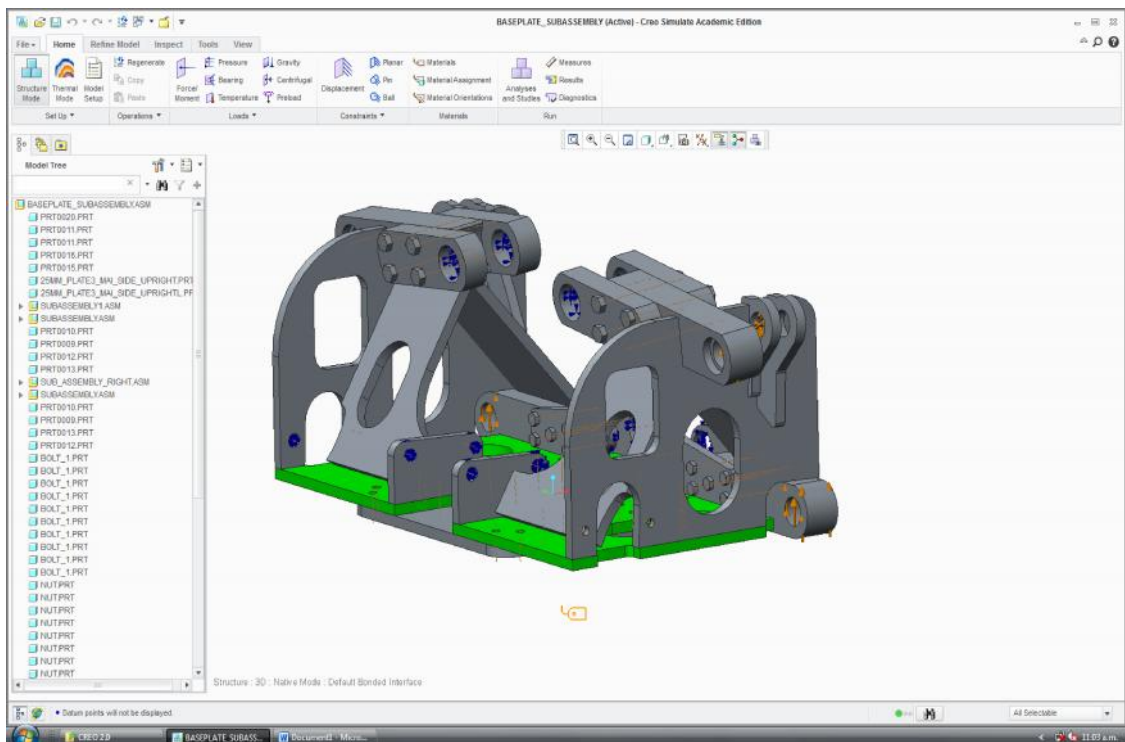
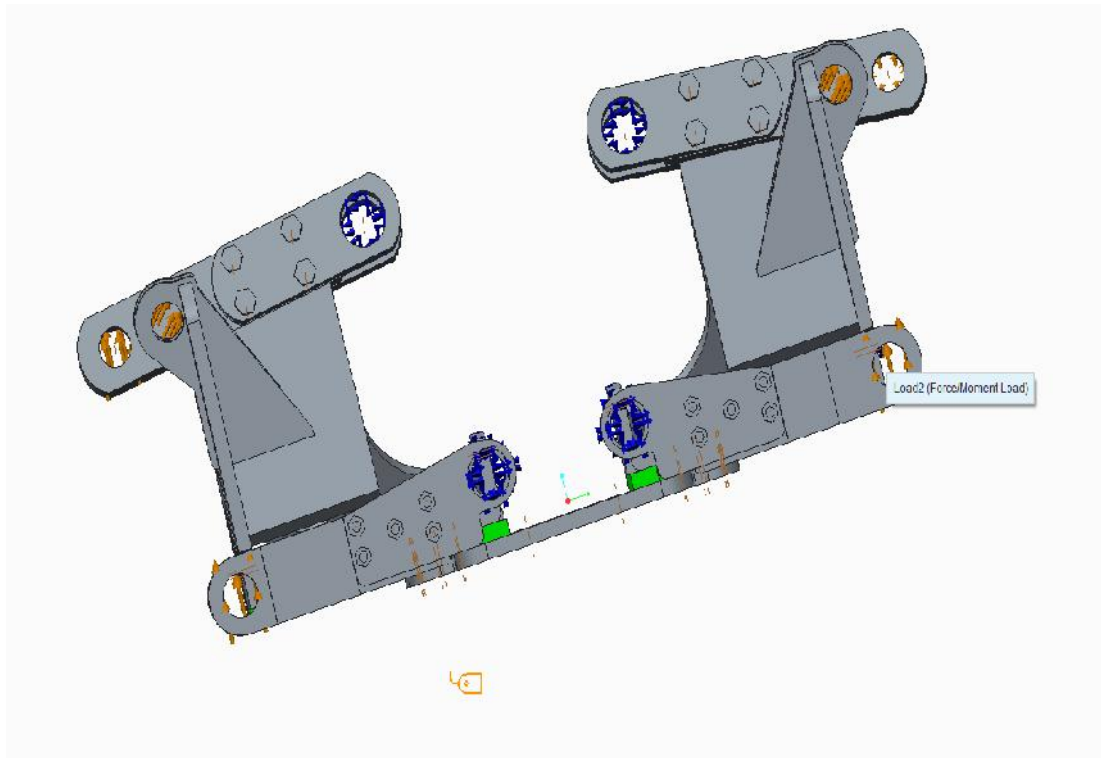


Figure E1: Loadings and constraints on model.

## APPENDIX F: Risk Assessment

### Risk Matrix

The following risk matrix was used for assessing and evaluating the risks and hazards associated with the implementation of this research project. The table F1 below show the ratings of consequences and likelihood of hazard. This is known as a risk matrix and is used extensively in industry and there are several variations of risk matrix that can be found in the literature. It does not matter which matrix you use as long as you consistently use the same matrix.

	CONSEQUENCE				
LIKELIHOOD	Insignificant (1)	Minor (2)	Moderate (3)	Major (4)	Extreme (5)
Rare (1)	Low	Low	Low	Low	Low
Unlikely (2)	Low	Low	Low	Medium	Medium
Possible (3)	Low	Low	Medium	Medium	Medium
Likely (4)	Low	Medium	Medium	High	High
Almost certain (5)	Low	Medium	Medium	High	Extreme

Table F1: Risk Matrix

<b>Hazard / Risk</b>	<b>Harm/Injury resulting from hazard/risk identified.</b>	<b>Risk Score</b>	<b>Remedial/Control Measures</b>	<b>Final Risk Score</b>
Poor working environment	Fatigue		No obstructions under desks.	
Which may include Poor Lighting, High temperatures (Typical of Mt Isa) insufficient working area,	Stress		Adequate work space provided-Converted Rumpus into Study room.	
	Upper limb disorders		Keep hydrated – drink lots of water.	
	muscular skeletal injury		Adequate lighting with blinds provided on windows to reduce glare and reflection.	
	Headaches Eye strain		Room temperature is controlled by the air conditioner Lighting tubes in good working condition.	
<b>Use of electrical equipment</b>	Electrical shock Burns		Check cable for any damages, cuts and bruises	
	Risk of electrical fire		Electrical equipment should be inspected and tested.	
	Power leads present a tripping hazard.		Provide sufficient outlets/adapters for the computer, laptop and printers. Avoid use of extension leads if possible.	
<b>Uncomfortable working position</b>	Upper limb disorders		Position, height and layout of the workstation assessed and appropriate for the work	
	muscular skeletal injury		Posture on the seat should be comfortable and not put strain on back.	
	Eye strain		Adjust the screen resolution to something comfortable for the eye.	
<b>Carrying out a task for a long period of time</b>	Upper limb disorders		Work periods involving a lot of repetition broken up with short breaks.	

	muscular skeletal injury		Short, frequent pauses allowed for very intensive work.	
	Headaches Eye strain		Keep hydrated by drinking lots of fluids.	
<b>Laptop use</b>	Upper limb disorders Muscular skeletal Injury Headaches Eye strain		Docking station / separate keyboard and mouse provided using a laptop for a prolonged period of time. Regular breaks e.g. 5 – 10 minutes every 50 – 60 minutes. Carry out a work station assessment. Suitable furniture provided.	

Table F2: Project Risk Assessment

The risk of injury due to hazards posed by implementation of this project was deemed to range from low to medium. Reasonable steps were taken to reduce the likelihood of any high potential hazards occurring. The project was successfully completed without any issues worth mentioning.

## APPENDIX G: Factor of Safety Calculations

### C.2 THE CLASSICAL RULE-OF-THUMB FACTOR OF SAFETY

The factor of safety can be quickly estimated on the basis of estimated variations of the five measures previously discussed: material properties, stress, geometry, failure analysis, and desired reliability. The better known the material properties and stress, the tighter the tolerances, the more accurate and applicable the failure theory, and the lower the required reliability, the closer the factor of safety should be to 1. The less known about the material, stress, failure analysis, and geometry and the higher the required reliability, the larger the factor of safety. The simplest way to present this technique is to associate a value greater than 1 with each of the measures and define the factor of safety as the product of these five values:

$$FS = FS_{\text{material}} \cdot FS_{\text{stress}} \cdot FS_{\text{geometry}} \cdot FS_{\text{failure analysis}} \cdot FS_{\text{reliability}}$$

Details on how to estimate these five values are given next. These values have been developed by breaking down the rules given in textbooks and handbooks into the five measures and cross-checking the values with those from the statistical method described in Section C.3.

#### Estimating the Contribution for the Material

$FS_{\text{material}} = 1.0$  If the properties for the material are well known, if they have been experimentally obtained from tests on a specimen known to be identical to the component being designed and  $v$  tests representing the loading to be applied  
 $FS_{\text{material}} = 1.1$  If the material properties are known from a handbook or a manufacturer's values  
 $FS_{\text{material}} = 1.2-1.4$ . If the material properties are not well known

#### Estimating the Contribution for the Load Stress

$FS_{\text{stress}} = 1.0-1.1$  If the load is well defined as static or fluctuating, if there are no anticipated overloads or shock loads, and if an accurate method of analysing the stress has been used

$FS_{\text{stress}} = 1.2-1.3$  If the nature of the load is defined in an average manner, with overloads of 20–50%, and the stress analysis method may result in errors less than 50%

FSstress=1.4–1.7 If the load is not well known or the stress analysis method is of doubtful accuracy

Estimating the Contribution for Geometry (Unit-to-Unit)

FSgeometry=1.0 If the manufacturing tolerances are tight and held well

FSgeometry=1.0 If the manufacturing tolerances are average

FSgeometry=1.1–1.2 If the dimensions are not closely held

Estimating the Contribution for Failure Analysis

FSfailure theory = 1.0–1.1 If the failure analysis to be used is derived for the state of stress, as for uniaxial or multi axial static stresses, or fully reversed uniaxial fatigue stresses

FSfailure theory = 1.2 If the failure analysis to be used is a simple extension of the preceding theories, such as for multi axial, fully reversed fatigue stresses or uniaxial nonzero mean fatigue stresses

FSfailure theory = 1.3–1.5 If the failure analysis is not well developed, as with cumulative damage or multi axial nonzero mean fatigue stresses

Estimating the Contribution for Reliability

FSreliability = 1.1 If the reliability for the part need not be high, for in-stance, less than 90%

FSreliability = 1.2–1.3 If the reliability is an average of 92–98%

FSreliability = 1.4–1.6 If the reliability must be high, say, greater than 99%

These values are, at best, estimates based on a verbalization of the factors affecting the design combined and on experience with how these factors affect the design. The stress on a part is fairly insensitive to tolerance variances unless they are abnormally large. This insensitivity will be more evident in the development of the statistical factor of safety.

Source: The Mechanical Design Process, David G. Ullman, 4 Edition.

## Appendix H: Loading Scenarios

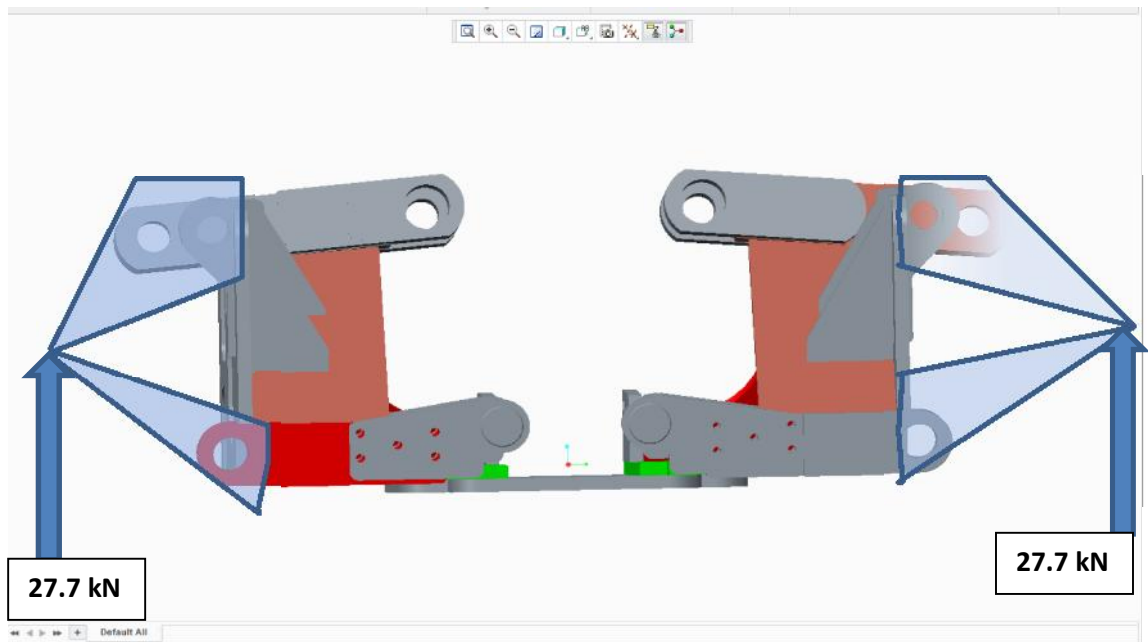


Figure H1: Loading Case 1- Normal Reaction loads

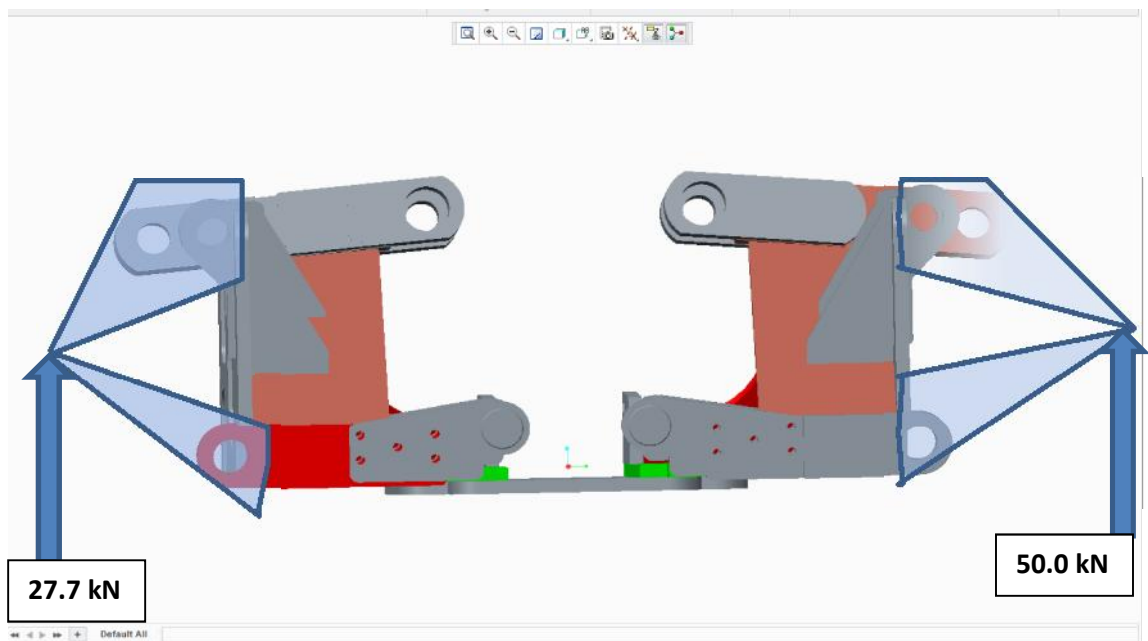


Figure H2: Loading Case 2 - Bump loads: 4g vertical

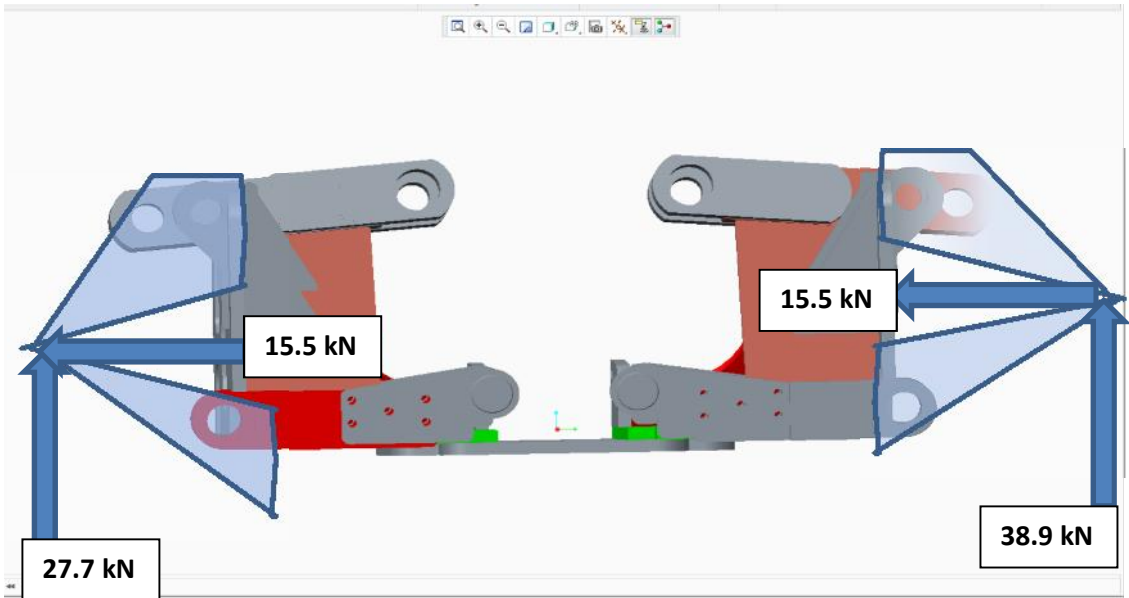


Figure H3: Loading Case 3 – Overturning loads: 4g vertical with 2.5 g side load

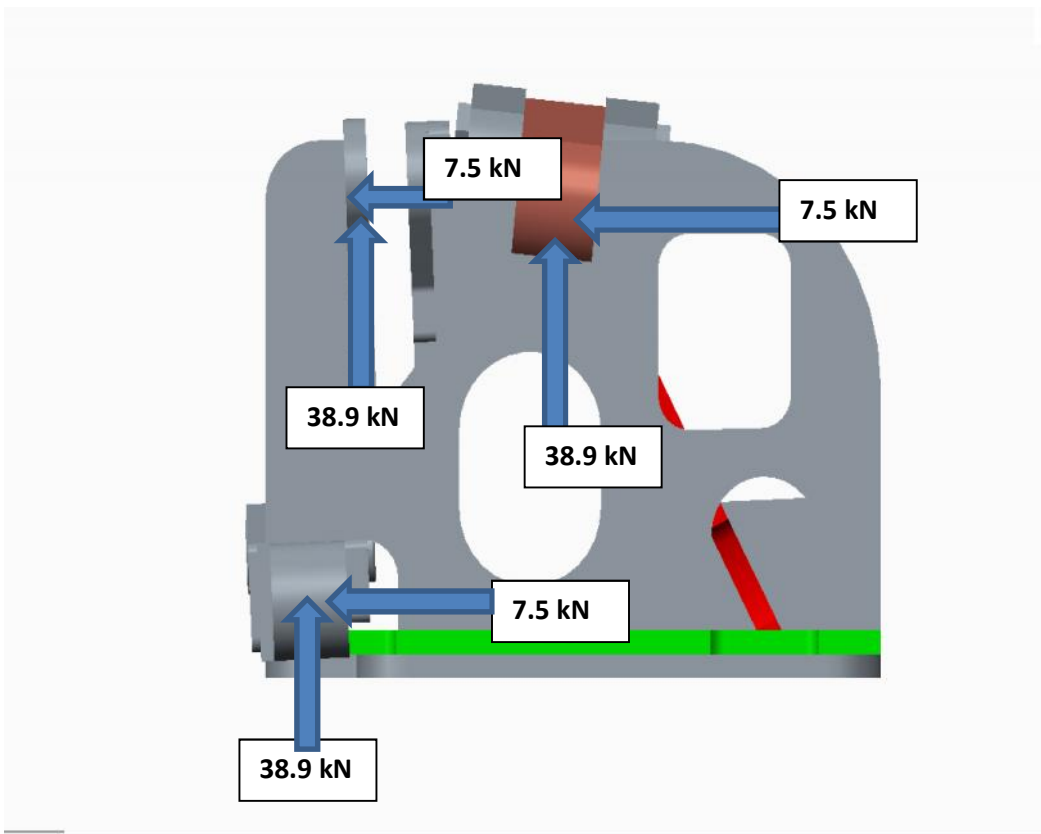


Figure H4: Loading Case 4 - Skid loads: 2g vertical and 1.2g longitudinal

## APPENDIX I: AISI 1020 Steel Mechanical Properties (Research more on this)

The following table shows mechanical properties of cold rolled AISI 1020 carbon steel

Properties	Metric	Imperial
Tensile strength	420 MPa	60900 psi
Yield strength	350 MPa	50800 psi
Modulus of elasticity	205 GPa	29700 ksi
Shear modulus (typical for steel)	80 GPa	11600 ksi
Poisson's ratio	0.3	0.3
Elongation at break (in 50 mm)	15%	15%
Hardness, Brinell	121	121
Hardness, Knoop	140	140
Hardness, Rockwell B	68	68
Hardness, Vickers	126	126
Machinability	65	65

Source - Strategic Research Institute

### Chemical Composition

The chemical composition of AISI 1020 steel is:

Element	Content
Carbon, C	0.17 - 0.230 %
Iron, Fe	99.08 - 99.53 %
Manganese, Mn	0.30 - 0.60 %
Phosphorous, P	0.040 %
Sulphur, S	0.050 %

## APPENDIX J: Analysis Summary

Creo Simulate Structure Version P-10-20:spg

Summary for Design Study "loading\_case\_1"

Tue Oct 21, 2014 20:32:12

---

### Run Settings

Memory allocation for block solver: 512.0

### Parallel Processing Status

Parallel task limit for current run: 2

Parallel task limit for current platform: 64

Number of processors detected automatically: 2

Checking the model before creating elements...

These checks take into account the fact that AutoGEM will automatically create elements in volumes with material properties, on surfaces with shell properties, and on curves with beam section properties.

Generate elements automatically.

Checking the model after creating elements...

No errors were found in the model.

### Creo Simulate Structure Model Summary

Principal System of Units: millimeter Newton Second (mmNs)

Length: mm

Force: N

Time: sec

Temperature: C

Model Type: Three Dimensional

Points: 7989

Edges: 41264

Faces: 59337

Springs: 0

Masses: 0  
Beams: 0  
Shells: 0  
Solids: 26117  
Elements: 26117

-----  
Standard Design Study

Static Analysis "loading\_case\_1":

Convergence Method: Single-Pass Adaptive

Plotting Grid: 4

Convergence Loop Log: (20:32:43)

>> Pass 1 <<

Calculating Element Equations (20:32:44)

Total Number of Equations: 446124

Maximum Edge Order: 3

Solving Equations (20:33:06)

Post-Processing Solution (20:35:22)

Checking Convergence (20:35:44)

Resource Check (20:36:08)

Elapsed Time (sec): 237.23

CPU Time (sec): 158.64

Memory Usage (kb): 1113286

Wrk Dir Dsk Usage (kb): 1568768

>> Pass 2 <<

Calculating Element Equations (20:36:09)

Total Number of Equations: 492681

Maximum Edge Order: 7

Solving Equations (20:37:45)  
Post-Processing Solution (20:40:43)  
Checking Convergence (20:41:19)  
Calculating Disp and Stress Results (20:41:39)

RMS Stress Error Estimates:

Load Set	Stress Error	% of Max Prin Str
-----	-----	-----
LoadSet1	4.33e+00	1.6% of 2.64e+02

Resource Check (20:44:12)

Elapsed Time (sec): 721.47  
CPU Time (sec): 356.51  
Memory Usage (kb): 1157394  
Wrk Dir Dsk Usage (kb): 1801216

Total Mass of Model: 6.340980e-01

Total Cost of Model: 0.000000e+00

Mass Moments of Inertia about WCS Origin:

Ixx: 1.91247e+05  
Ixy: -5.01598e+03 Iyy: 9.59451e+04  
Ixz: -1.91380e+04 Iyz: -9.14701e+03 Izz: 1.62265e+05

Principal MMOI and Principal Axes Relative to WCS Origin:

Max Prin	Mid Prin	Min Prin
2.00763e+05	1.54603e+05	9.40912e+04

WCS X: 8.95835e-01	4.36877e-01	8.13523e-02
WCS Y: -4.09149e-03	-1.74950e-01	9.84569e-01
WCS Z: -4.44368e-01	8.82344e-01	1.54939e-01

Center of Mass Location Relative to WCS Origin:

( 1.29952e+02, 6.08340e+01, 2.37149e+02)

Mass Moments of Inertia about the Center of Mass:

Ixx: 1.53238e+05

Ixy: -3.13808e+00 Iyy: 4.95752e+04

Ixz: 4.03592e+02 Iyz: 9.58060e-01 Izz: 1.49210e+05

Principal MMOI and Principal Axes Relative to COM:

Max Prin	Mid Prin	Min Prin
1.53278e+05	1.49170e+05	4.95752e+04

WCS X: 9.95115e-01	-9.87206e-02	3.03099e-05
WCS Y: -2.92004e-05	1.26831e-05	1.00000e+00
WCS Z: 9.87206e-02	9.95115e-01	-9.73848e-06

Constraint Set: ConstraintSet1: BASEPLATE\_SUBASSEMBLY

Load Set: LoadSet1: BASEPLATE\_SUBASSEMBLY

Resultant Load on Model:

in global X direction: -8.844842e+03

in global Y direction: -2.067449e+00

in global Z direction: 3.232497e+05

Measures:

max\_beam\_bending: 0.000000e+00

max\_beam\_tensile: 0.000000e+00

max\_beam\_torsion: 0.000000e+00

max\_beam\_total: 0.000000e+00

max\_disp\_mag: 3.331653e-01

max\_disp\_x: 1.603038e-01

max\_disp\_y: 2.069645e-01

max\_disp\_z: 3.231939e-01

max\_prin\_mag\*: -2.635869e+02

max\_rot\_mag: 0.000000e+00

max\_rot\_x: 0.000000e+00

max\_rot\_y: 0.000000e+00

max\_rot\_z: 0.000000e+00

max\_stress\_prin\*: 1.793829e+02

max\_stress\_vm\*: 2.202305e+02

max\_stress\_xx\*: -1.361661e+02

max\_stress\_xy\*: -1.002041e+02

max\_stress\_xz\*: -5.702105e+01

max\_stress\_yy\*: -2.311854e+02

max\_stress\_yz\*: 6.647720e+01

max\_stress\_zz\*: -1.399856e+02  
min\_stress\_prin\*: -2.635869e+02  
strain\_energy: 3.404424e+04

\*\* Warning: The measures marked by an asterisk (\*) were evaluated at (or close to) results singularities. The values of these measures may be inaccurate, and you must use engineering judgment when interpreting them.

Analysis "loading\_case\_1" Completed (20:44:14)

-----

Memory and Disk Usage:

Machine Type: Windows Vista Service Pack 2

RAM Allocation for Solver (megabytes): 512.0

Total Elapsed Time (seconds): 734.99

Total CPU Time (seconds): 357.80

Maximum Memory Usage (kilobytes): 1168864

Working Directory Disk Usage (kilobytes): 1801216

Results Directory Size (kilobytes):

242106 .\loading\_case\_1

Maximum Data Base Working File Sizes (kilobytes):

1048576 .\loadp\_case\_1.tmp\kblk1.bas

161792 .\loading\_case\_1.tmp\kblk2.bas

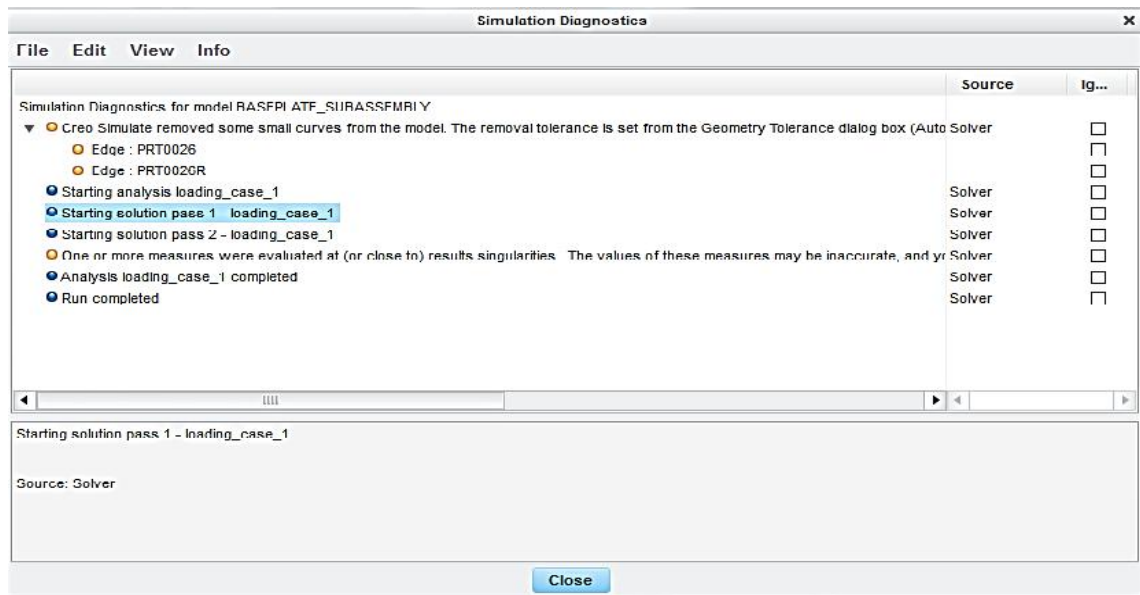
480256 .\loading\_case\_1.tmp\kel1.bas

110592 .\loading\_case\_1.tmp\oel1.bas

-----  
Run Completed

Tue Oct 21, 2014 20:44:26

### Simulation diagnostics summary



Shows the analysis completed successfully

APPENDIX K: Bill of Materials

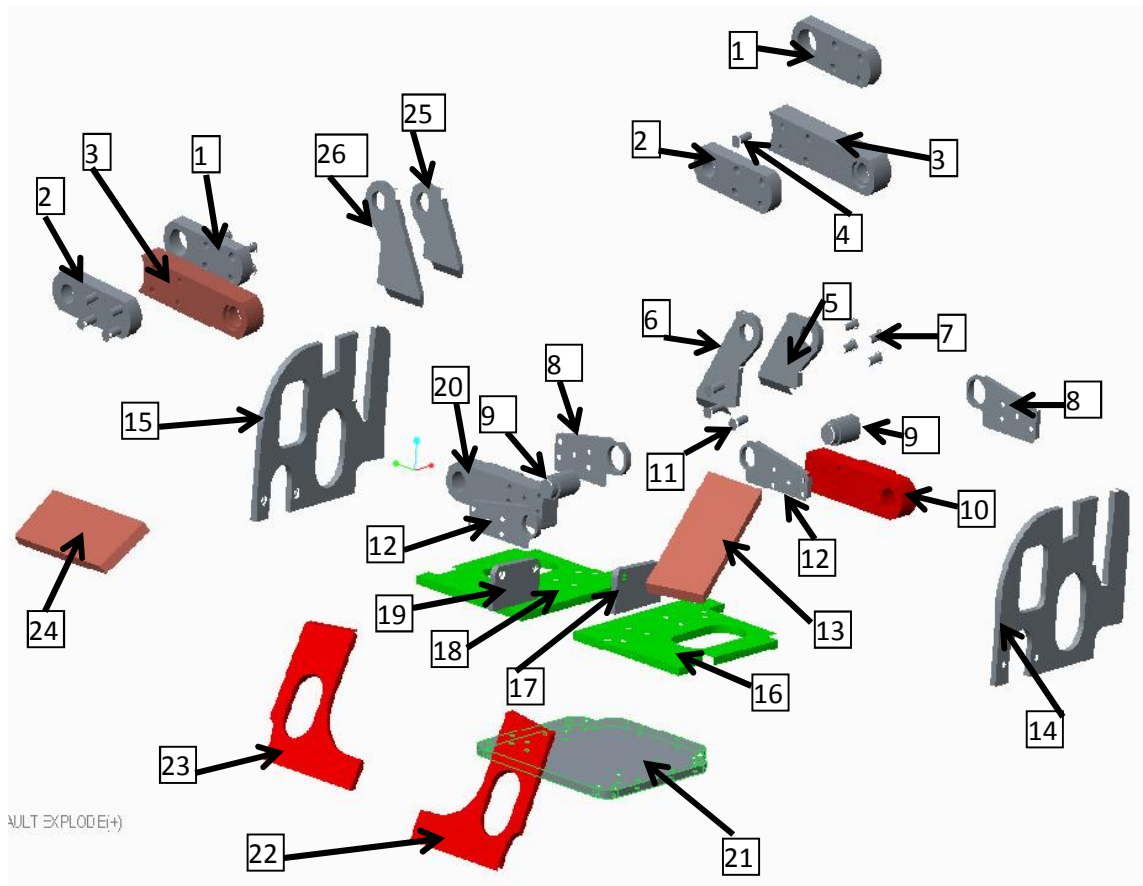


Figure L1: Model exploded view

Part Number	Name in Model	Quantity
1	PRT0021	2
2	PRT0001	2
3	PRT0007	2
4	BOLT	16
5	PRT0013	1
6	PRT0012	1
7	BOLT	10
8	PRT0024	1
9	LOWER_FRONT_PIN	2
10	PRT0026	1
11	BOLT	10
12	PRT0017	1
13	PRT0009	1
14	25MM_PLATE3_MAI_SIDE_UPRIGHT	1
15	25MM_PLATE3_MAI_SIDE_UPRIGHTL	1
16	PRT0011RIGHT	1
17	PRT0016	1
18	PRT0011	1
19	PRT0015	1

20	PRT0026R	1
21	PRT0020	1
22	RIGHT_PLATE	1
23	PRT0010	1
24	RIGHT_FLANGE	1
25	PRT13_RIGHT	1
26	LEFT_LONG_BRACKET	1
27	CAR SCREW	16

Table L1: Bill of Materials

Appendix L: Finite Element Analysis Software Comparison.

2D Frame Analysis Dynamic Edition	Price (\$/U)	Graphical geometry modeler	Graphical manual meshing	CAD Import	UpSolvers	Linear static	Nonlinear	Nonlinear - large displacements	Transient contact	Transient linear	Transient nonlinear	Natural frequency	Linear buckling	Acoustic	Heat transfer	Electric/magnetic	Fluid flow	Fluid structure interaction	Solid elements	Shell elements	Beam/plate	Anisotropic materials	Composites	Hypoclastic/rubber	Plasticity	Viscoplastic/creep
ADINA	no	✓	✓	✓	✓	✓	✓	✓	✓	✓	✓	✓	✓	✓	✓	✓	✓	✓	✓	✓	✓	✓	✓	✓	✓	
AMPS	no	✓	✓	✓	✓	✓	✓	✓	✓	✓	✓	✓	✓	✓	✓	✓	✓	✓	✓	✓	✓	✓	✓	✓	✓	
Analysis for Windows	Free	✗	✗	✓	✓	✓	✗	✗	✗	✗	✗	✗	✗	✗	✗	✗	✗	✗	✗	✗	✗	✗	✗	✗	✗	
ANSYS Mechanical	no	✓	✓	✓	✓	✓	✓	✓	✓	✓	✓	✓	✓	✓	✓	✓	✓	✓	✓	✓	✓	✓	✓	✓	✓	
Autodesk Simulation Mechanical	no	✓	✓	✓	✓	✓	✓	✓	✓	✓	✓	✓	✓	✓	✓	✓	✓	✓	✓	✓	✓	✓	✓	✓	✓	
AutoFEM Analysis	\$1495 - \$4955	✓	✓	✓	✓	✓	✓	✓	✓	✓	✓	✓	✓	✓	✓	✓	✓	✓	✓	✓	✓	✓	✓	✓	✓	
CADRE Pro	\$570	✓	✓	✓	✓	✓	✓	✓	✓	✓	✓	✓	✓	✓	✓	✓	✓	✓	✓	✓	✓	✓	✓	✓	✓	
CAEFEM	no	✓	✗	✓	✓	✓	✓	✓	✓	✓	✓	✓	✓	✓	✓	✓	✓	✓	✓	✓	✓	✓	✓	✓	✓	
CakulEX	Free	✗	✗	✗	✓	✓	✓	✓	✓	✓	✓	✓	✓	✓	✓	✓	✓	✓	✓	✓	✓	✓	✓	✓	✓	
Code_Aster	Free	✓	✓	✓	✓	✓	✓	✓	✓	✓	✓	✓	✓	✓	✓	✓	✓	✓	✓	✓	✓	✓	✓	✓	✓	
COMSOL Multiphysics	no	✓	✓	✓	✓	✓	✓	✓	✓	✓	✓	✓	✓	✓	✓	✓	✓	✓	✓	✓	✓	✓	✓	✓	✓	
Creo Elements/Direct FEA	no	✓	✓	✓	✓	✓	✗	✗	✗	✓	✓	✓	✓	✓	✓	✓	✓	✓	✓	✓	✓	✓	✓	✓	✓	
ED Elas2D	\$110	✗	✓	✗	✓	✓	✓	✓	✓	✓	✓	✓	✓	✓	✓	✓	✓	✓	✓	✓	✓	✓	✓	✓	✓	
Flmer	Free	✗	✗	✓	✓	✓	✓	✓	✓	✓	✓	✓	✓	✓	✓	✓	✓	✓	✓	✓	✓	✓	✓	✓	✓	
EngiLab Beam.2D	\$180	✓	✓	✓	✓	✓	✓	✓	✓	✓	✓	✓	✓	✓	✓	✓	✓	✓	✓	✓	✓	✓	✓	✓	✓	
FEAP	no	✗	✗	✓	✓	✓	✓	✓	✓	✓	✓	✓	✓	✓	✓	✓	✓	✓	✓	✓	✓	✓	✓	✓	✓	
FFATool	no	✓	✓	✓	✓	✓	✓	✓	✓	✓	✓	✓	✓	✓	✓	✓	✓	✓	✓	✓	✓	✓	✓	✓	✓	
FEBio with PreView	Free	✓	✓	✓	✓	✓	✓	✓	✓	✓	✓	✓	✓	✓	✓	✓	✓	✓	✓	✓	✓	✓	✓	✓	✓	
Fedem Mechanical	no	✓	✓	✓	✓	✓	✓	✓	✓	✓	✓	✓	✓	✓	✓	✓	✓	✓	✓	✓	✓	✓	✓	✓	✓	
FELIPE	Free	✗	✓	✓	✓	✓	✓	✓	✓	✓	✓	✓	✓	✓	✓	✓	✓	✓	✓	✓	✓	✓	✓	✓	✓	
FEIt	Free	✗	✗	✗	✓	✓	✓	✓	✓	✓	✓	✓	✓	✓	✓	✓	✓	✓	✓	✓	✓	✓	✓	✓	✓	
FEMdesigner	\$300 - \$900	✗	✓	✓	✓	✓	✓	✓	✓	✓	✓	✓	✓	✓	✓	✓	✓	✓	✓	✓	✓	✓	✓	✓	✓	
FEMIA	Free	✗	✗	✓	✓	✓	✓	✓	✓	✓	✓	✓	✓	✓	✓	✓	✓	✓	✓	✓	✓	✓	✓	✓	✓	
IesaWin	\$15 - \$200	✓	✓	✓	✓	✓	✓	✓	✓	✓	✓	✓	✓	✓	✓	✓	✓	✓	✓	✓	✓	✓	✓	✓	✓	
FlexPDE	\$195 - \$1,995	✓	✓	✓	✓	✓	✓	✓	✓	✓	✓	✓	✓	✓	✓	✓	✓	✓	✓	✓	✓	✓	✓	✓	✓	
FreeFEM	Free	✓	✓	✓	✓	✓	✓	✓	✓	✓	✓	✓	✓	✓	✓	✓	✓	✓	✓	✓	✓	✓	✓	✓	✓	
Grape GBW32	\$190	✗	✓	✓	✓	✓	✓	✓	✓	✓	✓	✓	✓	✓	✓	✓	✓	✓	✓	✓	✓	✓	✓	✓	✓	
Impact	Free	✗	✗	✗	✓	✓	✓	✓	✓	✓	✓	✓	✓	✓	✓	✓	✓	✓	✓	✓	✓	✓	✓	✓	✓	
KeyCreator Analysis	no	✓	✓	✓	✓	✓	✓	✓	✓	✓	✓	✓	✓	✓	✓	✓	✓	✓	✓	✓	✓	✓	✓	✓	✓	
TopFFA	\$69 - \$1,399	✓	✓	✓	✓	✓	✓	✓	✓	✓	✓	✓	✓	✓	✓	✓	✓	✓	✓	✓	✓	✓	✓	✓	✓	

	Price	Graphical assembly modeling	Graphical assembly modeling	CAD Import	Finite stress	Linear static	Nonlinear - large displacements	Nonlinear - contact	Transient linear	Transient nonlinear	Natural frequency	Linear buckling	Acoustic	Heat transfer	Electro-magnetic	Fluid flow	Fluid structure interaction	Shell elements	Beam elements	Adhesive joints	Composites	Hypertensile rubber	Plastics	Viscoplastic/creep
LS-DYNA	no	✓	✓		✓	✓	✓	✓	✓	✓	✓	✓	✓	✓	✓	✓	✓	✓	✓	✓	✓	✓	✓	✓
LUSAS Analyst	no		✓		✓	✓	✓	✓	✓	✓	✓	✓	✓	✓	✓	✓	✓	✓	✓	✓	✓	✓	✓	✓
M3d	Free	✓	✓	✗	✓	✗	✗	✗	✗	✗	✗	✗	✗	✗	✓	✓	✓	✓	✓	✗	✗	✗	✗	✗
MATruss	\$150	✗	✗	✗	✓	✗	✗	✗	✗	✗	✗	✗	✗	✗	✗	✗	✗	✗	✗	✗	✗	✗	✗	✗
MEANS	\$2,000-\$5,000		✓	✗	✓	✓	✗	✗	✓	✓	✓	✓	✓	✓	✓	✓	✓	✓	✓	✓	✗	✗	✗	✗
Mecury	\$100-\$350	✗	✓	✓	✓	✓	✓	✓	✓	✓	✓	✓	✓	✓	✓	✓	✓	✓	✓	✓	✓	✗	✗	✗
midas.NEX	no	✓	✓		✓	✓	✓	✓	✓	✓	✓	✓	✓	✓	✓	✓	✓	✓	✓	✓	✓	✓	✓	✓
MSC Nastran	no				✓	✓	✓	✓	✓	✓	✓	✓	✓	✓	✓	✓	✓	✓	✓	✓	✓	✓	✓	✓
NISA Mechanical	no		✓		✓	✓	✓	✓	✓	✓	✓	✓	✓	✓	✓	✓	✓	✓	✓	✓	✓	✓	✓	✓
PATRC-PE	no				✓	✓	✓	✓	✓	✓	✓	✓	✓	✓	✓	✓	✓	✓	✓	✓	✓	✓	✓	✓
PARC 5	no				✓	✓	✓	✓	✓	✓	✓	✓	✓	✓	✓	✓	✓	✓	✓	✓	✓	✓	✓	✓
PERMAS	no	✗			✓	✓	✓	✓	✓	✓	✓	✓	✓	✓	✓	✓	✓	✓	✓	✓	✓	✓	✓	✓
PZFlex	no	✓	✓				✓					✓		✓				✓	✓	✓	✓	✓	✓	✓
RADIOSS	no				✓	✓	✓	✓	✓	✓	✓	✓	✓	✓	✓	✓	✓	✓	✓	✓	✓	✓	✓	✓
RamSeries	no				✓	✓	✓	✓	✓	✓	✓	✓	✓	✓	✓	✓	✓	✓	✓	✓	✓	✓	✓	✓
Range	\$60-\$500/year	✓	✓		✓							✓	✓	✓	✓	✓	✓	✓	✓	✓	✓	✓	✓	✓
Roshaz FEA	\$595-\$695	✓	✓		✓	✗	✗	✗	✗	✗	✗	✗	✗	✗	✗	✗	✗	✗	✗	✗	✗	✗	✗	✗
SAMCEF	no				✓	✓	✓	✓	✓	✓	✓	✓	✓	✓	✓	✓	✓	✓	✓	✓	✓	✓	✓	✓
Sesam GenE	no	✓	✓		✓		✓											✓	✓					
SimScale	\$3000-\$12000/year	✗	✓		✓	✓	✓	✓	✓	✓	✓	✓	✓	✓	✓	✓	✓				✓	✓		
SimWise FEA	\$3,500-\$5,000		✓		✓	✗	✗	✗	✓	✓	✓	✓	✓	✓	✓	✓	✓	✓	✓	✓	✓	✓	✓	✓
SLFEEA	Free			✗	✓	✓	✗	✗	✗	✗	✗	✗	✗	✓	✓	✓	✓	✓	✓	✓	✓	✓	✓	✓
Solid Edge Simulation	no	✓	✗	✓	✓	✓	✗	✗	✗	✗	✓	✓	✓	✓	✓	✓	✓	✓	✓	✓	✓	✓	✓	✓
SolidWorks Simulation	no	✓	✓		✓	✓	✓	✓	✓	✓	✓	✓	✓	✓	✓	✓	✓	✓	✓	✓	✓	✓	✓	✓
Strand7	\$4,500-\$11,000	✗	✓	✓	✓	✓	✓	✓	✓	✓	✓	✓	✓	✓	✓	✓	✓	✓	✓	✓	✓	✓	✓	✓
StressCheck	no	✓	✓	✓	✓	✓	✓	✓	✓	✓	✓	✓	✓	✓	✓	✓	✓	✓	✓	✓	✓	✓	✓	✓
Tochnog	Free	✗	✗	✗	✓	✓	✓	✓	✓	✓	✓	✓	✓	✓	✓	✓	✓	✓	✓	✓	✓	✓	✓	✓
VisualFEA	\$1,800	✓	✓		✓	✓	✓	✓	✓	✓	✓	✓	✓	✓	✓	✓	✓	✓	✓	✓	✓	✓	✓	✓
W-Trite	Free	✗	✗	✗	✓	✓	✗	✗	✗	✗	✗	✗	✗	✗	✗	✗	✗	✗	✗	✗	✗	✗	✗	✗
Z88 Aurora	Free	✗	✓	✓	✓	✓	✓	✓	✓	✓	✓	✓	✓	✓	✓	✓	✓	✓	✓	✓	✓	✓	✓	✓